1-1-2015

Quantitative Brain Electrical Activity In The Initial Screening Of Mild Traumatic Brain Injuries After Blast

Chengpeng Zhou
Wayne State University,

QUANTITAITVE BRAIN ELECTRICAL ACTIVITY IN THE INITIAL SCREENING OF MILD TRAUMATIC BRAIN INJURIES AFTER BLAST

by

CHENGPENG ZHOU

THESIS

Submitted to the Graduate School

of Wayne State University,

Detroit, Michigan

in partial fulfillment of the requirements

for the degree of

MASTER OF SCIENCE

2015

MAJOR: BIOMEDICAL ENGINEERING

Approved by:

_____

Advisor Date

DEDICATION

I dedicate my work to my family

ACKNOWLEDGEMENTS

First and foremost, I would like to thank God for giving me the strength to go through the Master journey in Biomedical Engineering.

I would like to thank my mother, Mrs. Jurong Chen, for her love and constant support. I can finish my work today, because she was always ready to give everything! Thank you for your selfless love; you give me strength to continue my work and study.

I would like to thank Dr. Chaoyang Chen, my mentor and my advisor, for giving me the chance to work in his lab. Dr. Chen doesn't only teach his students about Neurophysiology, but he also teaches us to work efficiently.

I would like to thank my dissertation committee members: Dr. John Michael Cavanaugh, Dr. Yuchuan Ding and Dr. Weiping Ren for their guidance and their constructive advise to make my research more complete and sharp.

Last but not least, I would like to thank the Spine Lab Research Facility group, faculty, post docs, graduate students and staff for all their help. I would especially like to thank Mr. Srinivas Kallakuri, Mrs. Ke Feng, Mrs. Heena Sultan Purkait, Mr. Alok Desai, Mrs. Karthika Andrew, Mr. Karthik Somasundaram for all their help. I would also like to thank Dr. John Michael Cavanaugh and Chaoyang Chen for proof reading my thesis.

TABLE OF CONTENTS

LIST OF TABLES

LIST OF FIGURES

ABBREVIATION LIST

EEG	Electro EncephaloGram
VTA	Ventral Tegmental Area
MS	Medial Septum
VH	Ventral Hippocampus
REM	Rapid Eye Movement
DG	Dentate Gyrus
CBF	Cerebral Blood Flow
EMG	Electro MyoGraphy
ECG	Electro MyoGraphy
EOG	Electro OculoGraphy
CMRO2	Cerebral Metabolic Rate of Oxygen consumption
AD	Alzheimer's Disease
PNES	Psychogenic Non-Epileptic Seizures
ADHD	Attention Deficit Hyperactivity Disorder
BD	Bipolar Disorder
MBCT	Mindfulness Based Cognitive Therapy
TMS	Transcranial Magnetic Stimulation
NREM	Non-Rapid Eye Movement
PCP	Phenyl Cyclohexyl Piperidine
MTBI	Mild Traumatic Brain Injuries
IEDs	Improvised Explosive Devices
CT	Computed Tomography
MRI	Magnetic Resonance Imaging
QEEG	Quantitative ElectroEncephaloGraphy

PCS	Post Concussion Syndrome
IOP	Incident Over Pressures
PSD	Power Spectral Density
FFT	Fast Fourier Transformation
GLM	General Linear Model
ADR	Alpha-Delta power Ratio
TAR	Theta-Delta power Ratio
RMS	Root Mean Square
SEF-90	Spectral Edge Frequency fc=90%
AP	Ascending Pharyngeal
CC	Common Carotid
ATP	Adenosine TriphosPhate
BBB	Blood Brain Barrier
FM**θ**	Frontal Midline Theta
DCI	Delayed Cerebral Ischemia
SAH	SubArachnoid Hemorrhage
GABA	Gamma AminoButyric Acid
FXS	Fragile X Syndrome
MRAA	Motor-Related Amplitude Asymmetries
ERS	Event-Related Synchronization
ERD	Event-Related Desynchronization

CHAPTER 1 INTRODUCTION

1. Blast-related mild traumatic brain injuries (mTBI) and Quantitative electroencephalography (QEEG)

Bomb explosions are common in war zones, and urban terrorist attacks. These include rocket-propelled grenades, antipersonnel landmines, high-explosive mortars, and improvised explosive devices (IEDs). Improvised explosive devices (IEDs) are reported to account for 78% of injuries, the highest proportion found for any large scale conflict (Owens BD, et al., 2008, Duncan Wallace., 2009).

A survey of over 2500 U.S. Army Infantry soldiers found that 43.9% of soldiers reported loss of consciousness, memory problems (24.6%), concentration problems (31.4%), and irritability (56.8%) (Hoge CW, et al., 2008). The Rand Corporation estimated that 320 000 US military personnel had a TBI, of the 1.64 million deployed to Iraq and Afghanistan in 2001–2008 (www.rand.org). Since 2000, the department of defense report 313,816 soldiers diagnose TBI. Most of the TBI can be diagnosed as mild traumatic brain injury, which is based on clinical criteria, computed tomography (CT) or conventional magnetic resonance imaging (MRI) (Department of Defense worldwide numbers for traumatic brain injury., 2015). Blast-exposed soldiers are categorically different than patients suffering from traditional blunt trauma injuries (Belanger HG, et al., 2009). A victim exposed to a primary blast wave may appear normal at first but can rapidly demonstrate neurological deficits for a period of time following the blast event indicative of sustained neurological alterations (Ciraulo DL, et al., 2006). TBI has become a “signature injury” of contemporary warfare, and there is growing concern that the effects of TBI on health and well-being may linger well beyond the healing of other, more visible wounds. Advanced neuro-diagnostic technology and

devices are required to allow mTBI to be detected and diagnosed early after sustaining an injury. Early diagnosis promotes early intervention and may improve outcomes. It also provides line leaders the opportunity to make better-informed decisions about which servicemembers should return to duty, receive follow-up, or be triaged for further evaluation and care.

Blast-related traumatic brain injuries (b-TBI) comprise four components. Brain injuries are resulted from the over-pressure of the blast wave (primary blast injury), brain injuries are caused by penetration of projectiles (secondary blast injury), brain injuries are resulted from head hit the fixed surfaces after the blast (tertiary blast injury), and brain injuries are caused by thermal, chemical, and other factor (quaternary blast injury) (Jeff rey V Rosenfeld et al., 2013. Deborah Warden., 2006). The magnitude of blast wave is affected by several factors, include distance, blast energy and environment (Stephen J Wolf et al., 2009). After the high explosion, the gas quickly expand and compress the surrounding air. This process produce the positive phase of the blast (Figure 1.1). When the primary blast wave pass, the atmospheric pressure will drop and create a relative vacuum environment. The primary blast wave accelerate the different tissue with different speed rate, which is result in shearing forces, stretching, displacement. The air-fluid interfaces are the most vulnerable parts, such as middle ear, bowel, and lungs (Katherine H. Taber, et al., 2006). The blast-related TBI is resulted from subdural hemorrhage, contusion, and diffuse axonal injury. The Axon is injured by the shearing force produced by the primary blast wave. The white-gray matter connection at the frontal and temporal areas are the most common locations. The contusion is result from the brain

parenchyma impact on the skull (Figure 1.2). The frontal lobe, temporal lobe, and occipital lobe are the most common locations. The subdural hemorrhage is caused by tearing tributary surface veins when the brain relative move in the skull. The tributary surface veins connect dural venous sinus and the brain surface and commonly teared at the frontal and parietal lobe (Figure 1.3) (Katherine H. Taber, et al., 2006). The rabbit is exposure to a peak overpressue blast of 750 kPa, which is resulted in severe subdural hemorrhage (Figure 1.4) (Karin Rafaels, et al., 2011).

Over the years, different organizations have proposed a variety of diagnostic criteria for mTBI, including the American Congress of Rehabilitation Medicine (Kay et al., 1993), the CDC (CDC, 2003), and the World Health Organization (WHO) Task Force on Mild Traumatic Brain Injury (Holm L, et al., 2005). Currently, military medical providers use criteria for mild, moderate and severe TBI that include Glasgow Coma Scale (GCS)1 scores and the durations of LOC, altered consciousness, and PTA (The Management of Concussion/mTBI Working Group, 2009; Table 1.1).

TBI Severity	GCS	Alteration in Consciousness	LOC	PTA
Mild	13 to 15	≤24 h	0–30 min	≤24 h
Moderate	9 to 12	>24 h	>30 min to <24 h	>24 h to 7 d
Severe	3 to 8	>24 h	≥24 h	≥7 d

Table 1.1: mTBI Diagnostic Criteria

To identify devices for diagnosing mTBI early after injury, it is necessary first to consider various biologic and neurologic changes evoked by TBI more generally and the ways to potentially measure them. Brain injury is not a discrete entity — it is a continuum of cascading, often interrelated events. Waves of these events occurring over time are represented as “stages” of injury. Primary injury includes contusions,

lacerations, hemorrhage, and diffuse axonal injury. This is followed by secondary injuries comprising a wide range of cellular and physiologic changes that lead to additional injury and can exacerbate primary injury. A brief and simplified summary of injury events that may occur following TBI is provided in (Table 1.2). Ultimately, these changes can alter the functional integrity of brain cells. Cerebral blood flow (CBF) may become impaired (e.g., through decreased cerebral perfusion pressure [CPP]2) and deleterious sequelae, such as ischemia, may occur. In addition, homeostatic mechanisms designed to maintain cerebral integrity, such as cerebral autoregulation, may become compromised. These events may leave the brain unable to maintain adequate cerebral perfusion in the face of systemic blood pressure changes, and, in turn, vulnerable to insults caused by peripheral hypoxia and hypotension. Another pressing consequence of these injury cascades is edema and subsequent intracranial hypertension (elevated intracranial pressure [eICP]). Edema can result from multiple events, such as metabolic dysfunction and breakdown of the blood-brain barrier. As fluid in the cranium increases, ICP increases, and compensatory mechanisms for maintaining perfusion become exhausted. As a result, CBF is hindered, causing further injury.

Injury Associated with TBI
Primary Injury
✓ Contusion
✓ Laceration
✓ Hemorrhage
✓ Diffuse axonal injury
Secondary Injury
✓ Ischemia
✓ Oxidative stress
✓ Glutamate excitotoxicity
✓ Metabolic dysfunction
✓ Edema
✓ Neurochemical alterations
✓ Inflammation

Table 1.2: Examples of Primary and Secondary events associated with TBI

The EEG (electroencephalography) measures the summation of synaptic currents that arise on the dendrites and cell bodies of billions of cortical pyramidal cells, basically used in seizure monitoring based on EEG spike amplitude. QEEG (quantitative electroencephalography) is quantitative analysis measurement of the electrical activity of the brain through the use of high-speed computers by processing EEG band into sub-bands (delta, theta, alpha, beta bands) for amplitude, power (V^2/Hz), power spectrum density (PSD) and others. EEG is particularly attractive for field use because it is portable, relatively inexpensive and requires relatively short recording durations (Airoldi L, et al., 1999). Although routine EEG lacks sufficient sensitivity and specificity for diagnosing mTBI (Gaetz et al., 2001; Nuwer, et al., 2005), Quantitative EEG (QEEG), together with advanced analyses methods, shows promise for clinical applications.

Quantitative electroencephalography (QEEG) is used to diagnose mild traumatic brain injury (mTBI) and the postconcussion syndrome (PCS). 86% of mTBI patients have abnormal EEG (Zulfi Haneef et al., 2013). (Robert W. Thatcher, 2006) find that following traumatic injury, the high frequency bands (8-40 Hz) reduce power, which is related to injury the cortical gray matter. The delta band increase power in severe TBI patients, which is related to the injury the white matter. In another research, the mTBI athletes showed a significant decrease power in delta band in the standing posture as compared with the sitting posture (James Thompson, et al., 2004). In blast-related mTBI, a swine model shows that EEG wave appear arrhythmic and low-frequency spikes soon after blast (Figure 1.5) (Richard A. Bauman, et al., 2009). Compared to control group, blast related mTBI patients increase power in lower frequencies (delta, theta) at chronic phase (William C. Walker, 2014). After mild

traumatic brain injury, the frontal lobe most likely generate abnormal slow-waves, which suggest that front lobe is the most vulnerable lobe (Ming-Xiong Huang, et al., 2014). EEG has been proposed for TBI detection. At chronic phase, QEEG detection of mild TBI showed: Sensitivity=96.59%; Specificity=89.15%. (Thatcher 1989). But QEEG for acute TBI diagnosis has not been investigated.

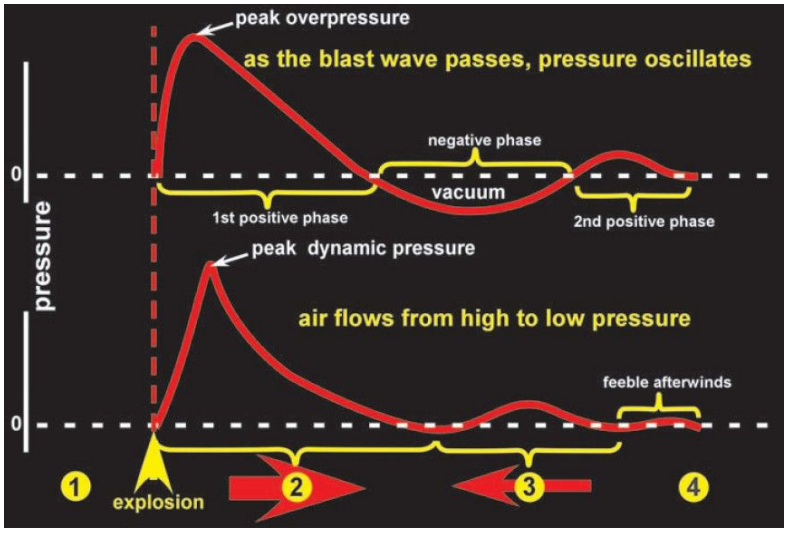

Figure 1.1: Atmospheric pressure changes after blast (adopted from Robin A. Hurley, et al., 2006).

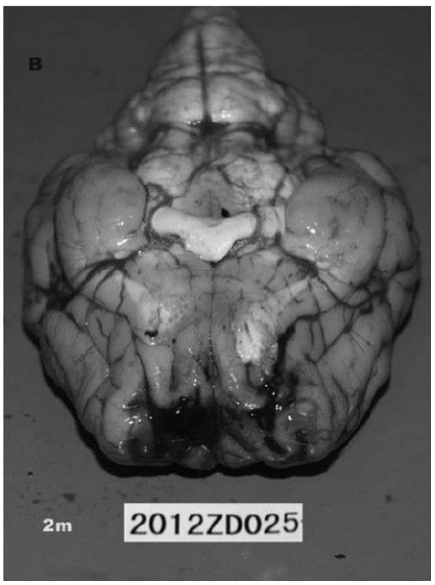

Figure 1.2: Goat prefrontal brain have severe subarachnoid hemorrhage after exposure to blast overpressue of 555 kPa (adopted from Bingcang Li, et al.,2014).

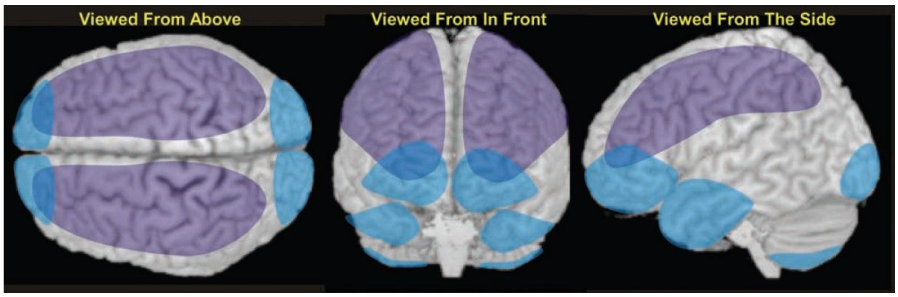

Figure 1.3: The most common locations for contusions (blue) and subdural hemorrhage (purple) (adopted from Robin A. Hurley, et al.,2006).

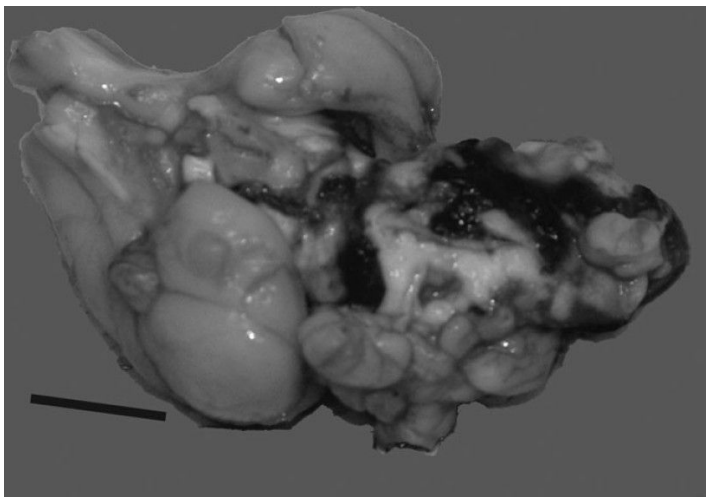

Figure 1.4: Rabbit brain have severe subdural hemorrhage after exposure to blast overpressue of 750 kPa (adopted from Karin Rafaels, et al.,2011).

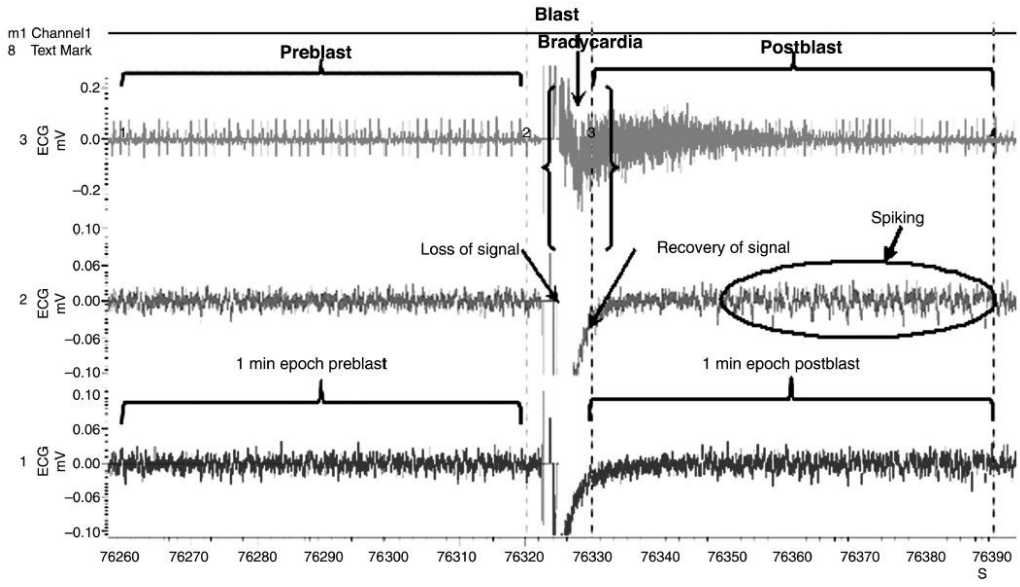

Figure 1.5: A sample recording of the EEG signals for channels 1 and 2 (bottom two records) and the ECG signal (top record) before, during, and after exposure to a moderately severe blast that was focused on the head. During the first minute after exposure the EEG signal appeared arrhythmic and although muted, low-frequency spiking appears in the EEG signals.

2.1. EEG Generation

When pyramidal neurons are activated in the cerebral cortex, the synaptic currents are produced within the pyramidal neuron dendrites. EEG system could measure electrical field over the scalp, which is generated by the synaptic currents.

Pyramidal neurons are the primary excitation cells, which are found in the hippocampus, the amygdala, and the cerebral cortex. The action potential is produced by summed post-synaptic graded potentials from electrical dipoles between the neuron soma and apical dendrites (Figure 1.6). The action potential in the brain is generated mostly by pumping in Na^+ and Cl^-, and pumping out K^+ (Gonzalo Alarcon et al., 2012).

The classic 3-layers concentric human head is consisted of inner brain, outer scalp, and intermediary skull (Figure 1.7) (Y. Lai et al., 2005). The EEG signals are attenuated by the skull, which are close to 80 times more than the other soft tissues (Stanley Rush et al., 1968). Thus, only a large amount of active neurons can produce enough action potential to be recorded by the scalp electrodes. The average numbers of neocortical neurons are 19 billion and 23 billion in female and male brains (range 20-90 years), respectively. In both sexes, the neocortical neurons approximately lose 10% over the life span (Bente Parkkenberg et al., 1997). Neurons interconnect with each other with synapses. Adults have total 1.6×10^{14} synapses in the neocortex (Yong Tang et al., 2001). The number of neurons lose 25 to 50% during aging, however the number of synapses increase during aging (John H. Morrison et al., 1997).

The human brain is mainly divided into three parts: cerebrum, cerebellum, and brain stem (Figure 1.8). The cerebrum is the most important part of the brain, includes

the regions for complex analysis, movement, sensation, and expression of emotions. The cerebellum control voluntary movements and posture balance. The brain stem regulate heart rate, respiration, and neurohormone balance (Teplan, M., 2002).

EEG is applied to diagnose brain death, sleep disorders, epilepsy seizure, coma, stroke, and tumor (Florian Mormann et al., 2000; Siddiqui et al., 2013; Brenner et al., 2003; Rositsa poryazova et al., 2015; Selvam, V.S et al., 2011). Compare to EEG (0.66) and MRI (0.66), PET have the most sensitivity (0.86) to diagnosis epilepsy, but MRI is three times and PET is six times the cost of EEG (John Dellabadia Jr, et al., 2002). Because swine brain have many convolutions in the cortex and a similar size of human brain. So swine brain can produce a similar EEG signal of human brain (Yoshio Okada, et al., 1999).

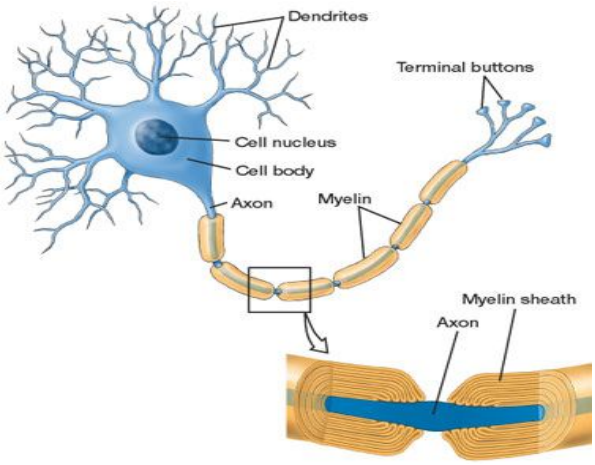

Figure 1.6: Structure of neuron (adopted from http://the-works.net/tag/ structure-of-neurons)

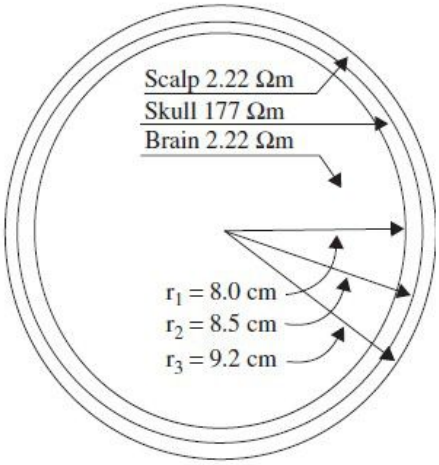

Figure 1.7: The three main layers of the brain including their approximate resistance and thickness (Ω=ohm)

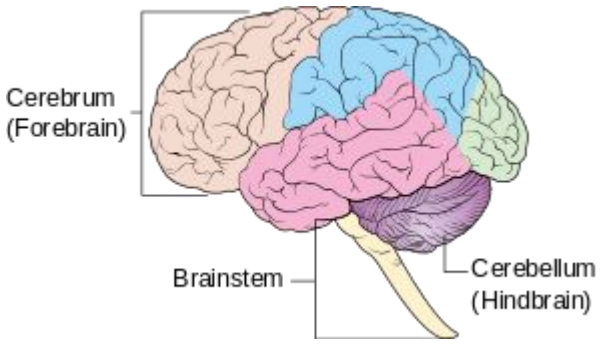

Figure 1.8: Structure of human brain (adopted from http://en.wikipedia.org/wiki/ Human _brain)

2.2. Brain Rhythms

Brain waves could be separated into delta band, theta band, alpha band, beta band from low to high frequencies (Figure 1.9).

Delta wave ranges from 0.5 Hz to 4 Hz. The delta wave generation depend on the activity of the brain reward system, which include the ventral tegmental area (VTA), the nucleus accumbens, the medial prefrontal cortex, and the nucleus

reticularis thalami (Figure 1.10). Delta oscillatory appear in the earlier developmental stage and deep sleep. During the motivation process, delta oscillations are related to reward mechanism and atavistic defensive mechanisms. During the cognitive process, delta waves are mostly associated with attention and detection of stimulus in the outside environment (Gennady G. Knyazev., 2012).

Theta wave ranges from 4 Hz to 8 Hz. Medial septum (MS) is considered to be the 'pace maker' of theta waves in most neurons of hippocampus (Figure 1.11) (Laura Lee Colgin., 2013). At the hippocampus, theta oscillations are centralized at CA1 pyramidal layer, and the amplitude of theta waves decrease from dorsal to ventral part of hippocampus (Figure 1.12) (Jagdish Patel et al., 2012). Hippocampal theta oscillation is associated with memory-guided behavior (Michael E. Hasselmo et al., 2005). Cortex theta oscillation is related to generate language (Dora Hermes et al., 2014).

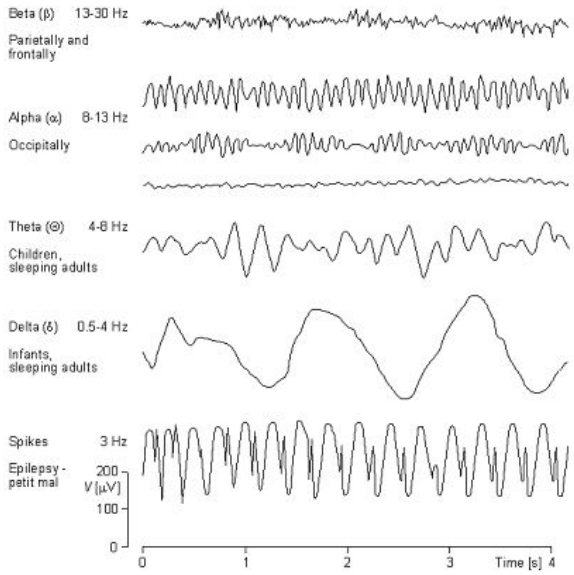

Figure 1.9: EEG waves (adopted from http://naozhendang.com).

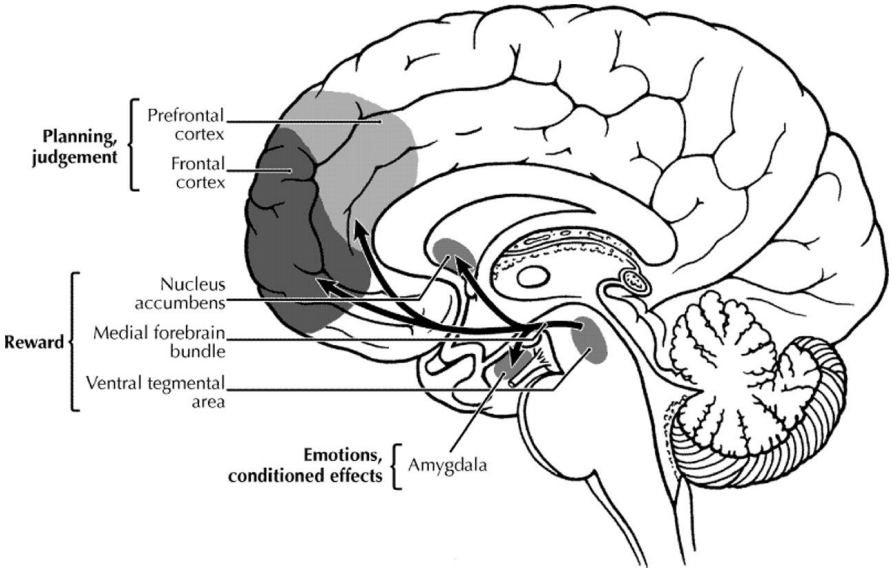

Figure 1.10: The pathway of reward system (adopted from https://philsphil. wordpress. com)

Alpha wave ranges from 8 Hz to 13 Hz. The alpha oscillation is mainly located at parietal, occipital, and inferior frontal regions of neocortex (Figure 1.13) (Kei Omata et al., 2013). During rapid eye movement (REM) sleep, alpha oscillations decrease after sleep deprivation (Cristina marzano et al., 2010). Upper Alpha component (10-13 Hz) was original from occipital areas, most likely reflects primary visual processing and feature extraction (W Klimesch, et al., 1997). Lower Alpha component (8-10 Hz) was prominent over parietal areas and more related to cognitive processing, attention and pulsatile communicate between brain and muscle (G. Pfurtscheller, 2003).

Beta wave ranges from 13 Hz to 30 Hz. The beta oscillation is generated by pyramidal tract neurons (Figure 1.14) (Preeya Khanna et al., 2015). The sensorimotor cortex beta wave is associated with voluntary movement in healthy subjects

(Gilbertson T et al., 2005). The cortex beta oscillation connect with muscle by the corticospinal tract. (Figure 1.15) (Karen M. Fisher et al., 2012).

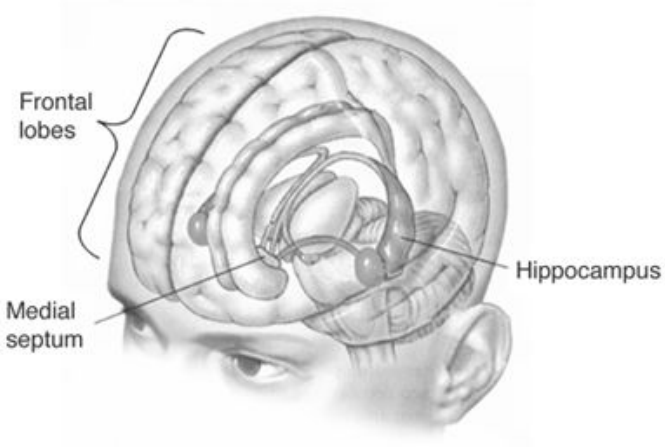

Figure 1.11: The position of Medial Septum (adopted from http://pubs.niaaa.nih.gov)

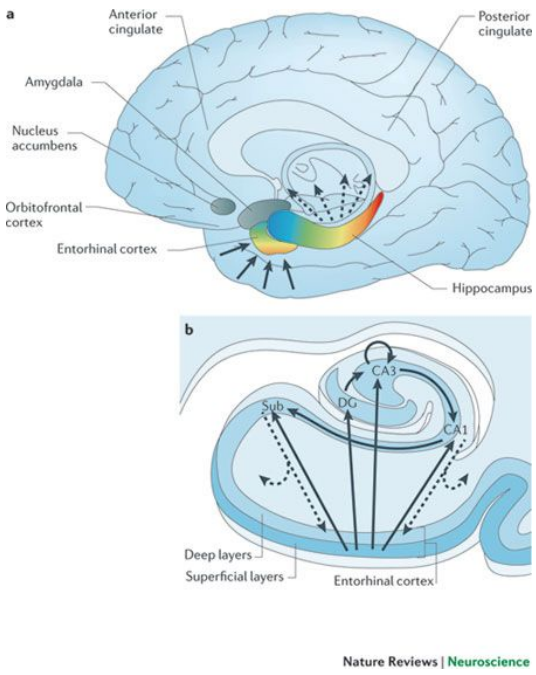

Figure 1.12: a. The hippocampal formation. b. hippocampal transverse axis (adopted from http://www.nature.com).

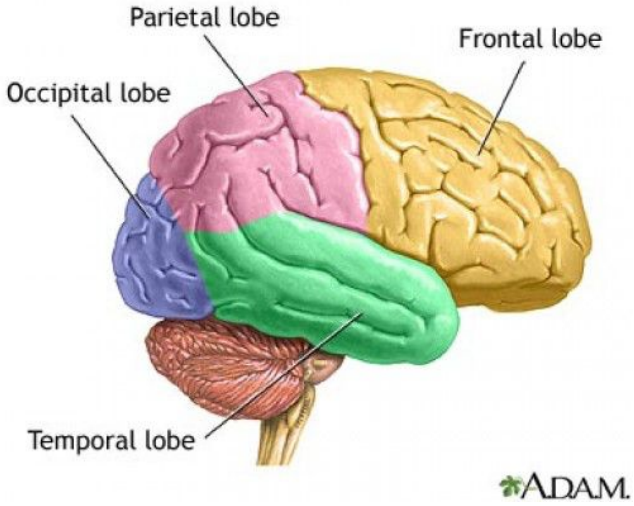

Figure 1.13: Cerebral Neocortex (adopted from http://www.md-health.com)

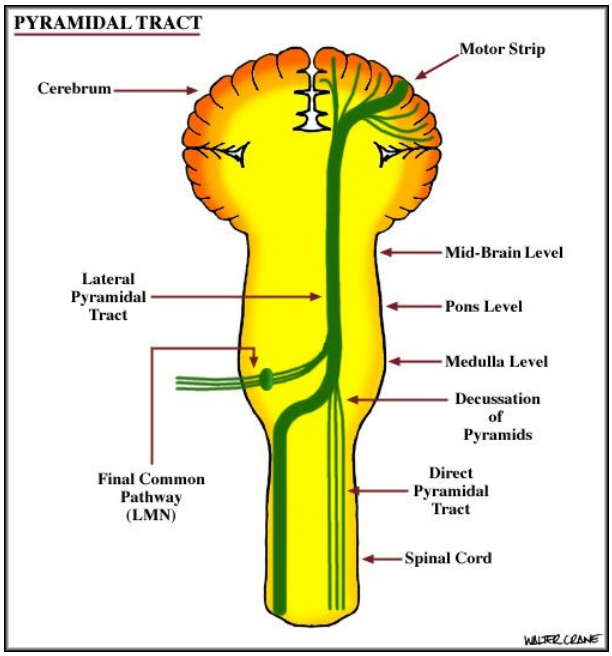

Figure 1.14: Pyramidal Tract (adopted from http://www.csuchico.edu)

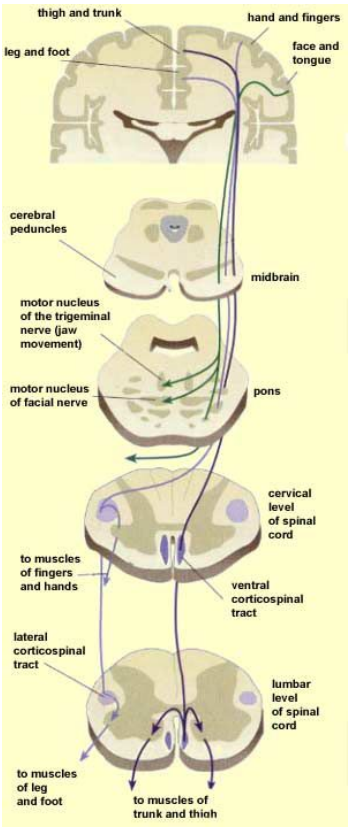

Figure 1.15: Corticospinal tract (adopted from http://thebrain.mcgill.ca)

2.3. EEG Recording and Measurement

In clinical practice, EEG recording is from 24 channels to 32 channels. The minimum digital sampling rate for each channel is 200 samples/s. The digitization resolution should be down to 0.5 μV and 12 bits. Input impedance must be higher than 100 MΩ and electrode impedance should be lower than 5 kΩ. The rejection ratio of each channel should be more than 110 dB. At 0.5–100 Hz, peak-to-peak noise should be less than 1.5 μV (Marc R. Nuwera et al., 1998).

2.3.1. Conventional Electrode Positioning

The conventional 21 electrodes position is recommended by the international federation of societies for electroencephalography and clinical neurophysiology (Figure 1.16) (Jasper, H., 1985).

The anatomy landmarks of the skull are used in this technique, such as inion, nasion, and the left and right preauricular points. At the anteroposterior axis, the skull could be divided into 5 separate points from the nasion point to the inion point (Figure 1.17). The 5 points are marked as Fp, F, C, P, and O point. The Fp and O points were 10% of total measurement away from nasion and inion, respectively. The F, C, and P points are 20% of total measurement between each other. At the central coronal plane, the skull also can be divide into 5 points from the left preauricular point to the right preauricular point through the C points (Figure 1.18). The 5 points are marked as T3, T4, C3, C4, and C. The T3 and T4 points are 10% of total measurement away from left and right preauricular points, respectively. The C3, C4, and C points are 20% of total measurement between each other. At the transverse plane, the lefte side of skull can be divided into 5 separate points from the point Fp to the point O through point T3 (Figure 1.19). The 5 points are marked as Fp1, O1, F1, T5, and T3. The Fp1 and O1 points are 10% of total measurement away from point Fp and point O, respectively. The F1, T5, and T3 points are 20% of total measurement between each other (George H. Klem et al., 1999).

The F7 and F8 points are projected on the frontal lobe (Figure 1.20A). The F3 and F4 points are located on the middle frontal or superior gyri. The C3 and C4 points

are projected on the postcentral gyrus or the precentral gyrus (Figure 1.20B, C). The O1, O2, T3 and T4 points are located on the middle occipital gyrus and the middle temporal gyrus, respectively (Figure 1.20D). The P3 and P4 points are projected on the angular gyrus (Figure 1.20E). The T5 and T6 points are located on the temporal lobe (Figure 1.20F) (Masako Okamoto et al., 2004).

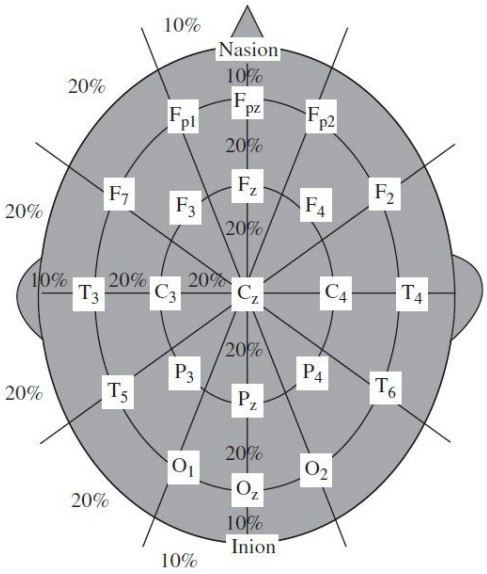

Figure 1.16: The conventional position of 21 electrodes (adopted from Saeid Sanei, et al., 2007).

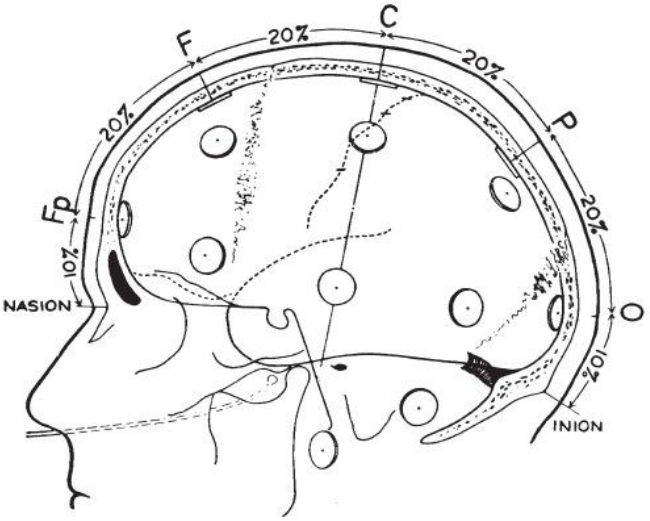

Figure 1.17: Lateral view of skull (adopted from George H. Klem, et al., 1999).

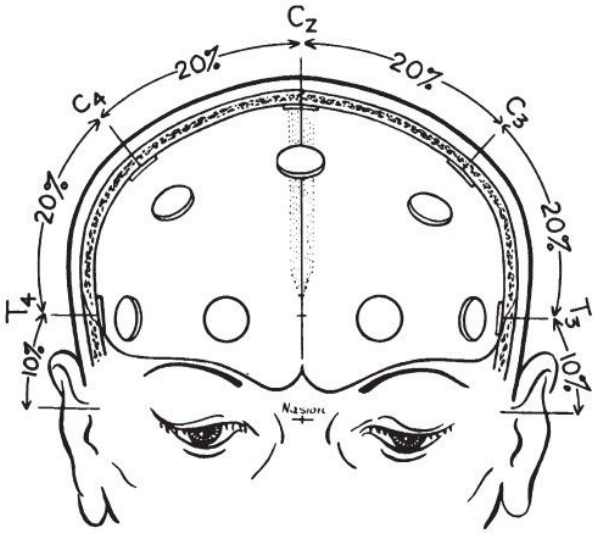

Figure 1.18: Frontal view of the skull (adopted from George H. Klem, et al., 1999).

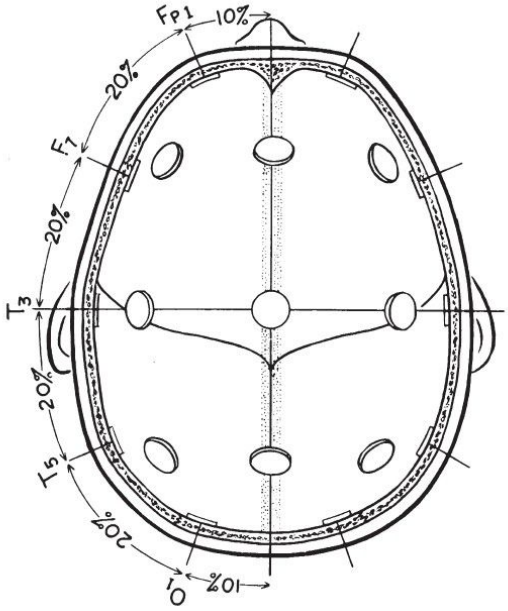

Figure 1.19: Superior view of skull (adopted from George H. Klem, et al., 1999).

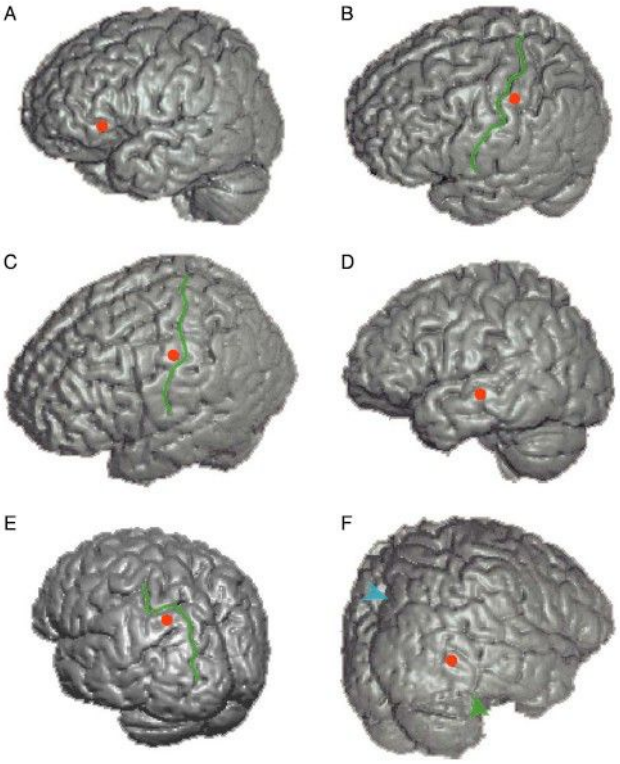

Figure 1.20: Cortical projection points from scalp.

2.3.2. Conditioning the Signals

The original EEG signals comprise frequency up to 300 Hz. Before signal processing, we should use highpass filter and lowpass filter to cut off frequence lower than 0.5 Hz and higher than 30 Hz respectively. The artifacts include system and patient-related artifacts. The patient-related artifacts contain electromyography (EMG) (Figure 1.21), electrocardiography (ECG) (Figure 1.22), electrooculography (EOG) (Figure 1.23), sweating and ballistocardiogram. The system artifacts include cable defects, electrical noise, power supply interference, electrodes impedance fluctuation (Figure 1.24) (Saeid Sanei et al., 2007).

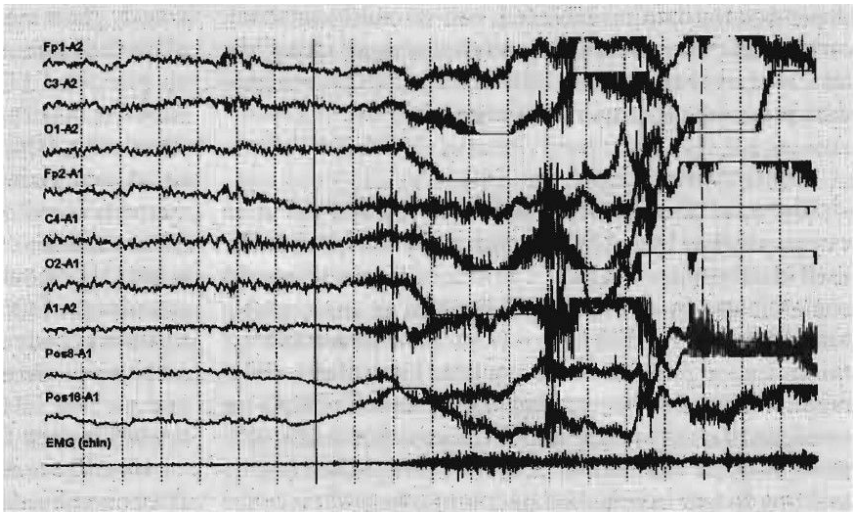

Figure 1.21: Muscle movement artifacts distort raw EEG signal (adopted from Peter Anderer, et al., 1999).

Figure 1.22: ECG artifacts distort the raw EEG signal (adopted from Joe-Air Jiang, et al., 2007).

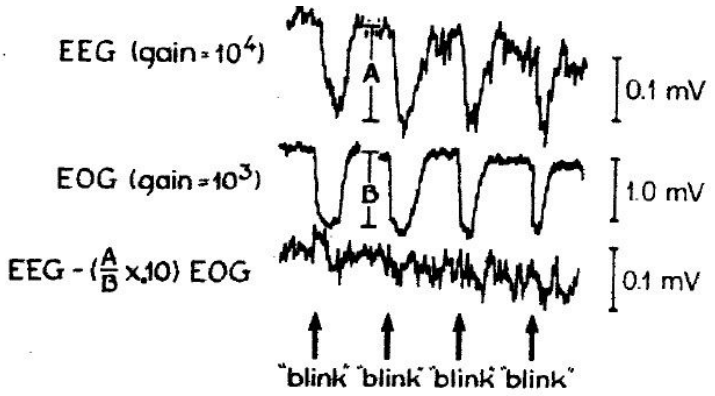

Figure 1.23: EOG artifacts distort the raw EEG signal (adopted from James C. Corby, et al., 1972).

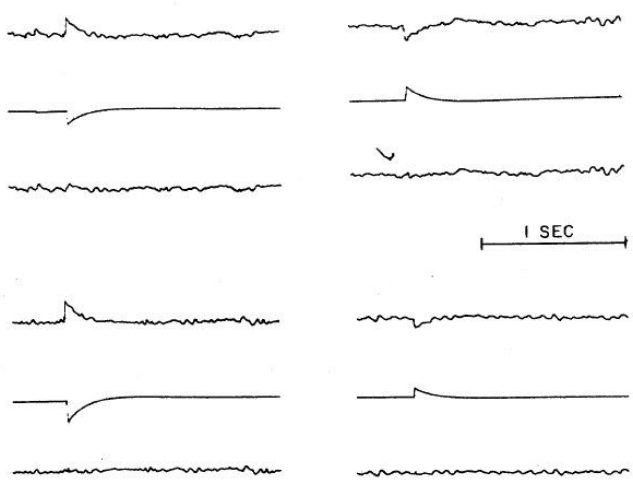

Figure 1.24: Electrode-pop artifacts (adopted from John S. Barlow., 1986).

2.4. Aging

Aging is characterized by dysfunction in executive system and memory system. In elder people, the cognition alterations is result from early neurodegeneration (Jaqust W., 2013). The cerebral blood flow (CBF) and cerebral metabolic rate of oxygen consumption (CMRO2) decrease with aging at the sensory-motor cortex and occipital cortex (Joel Aanerud et al., 2012).

Alpha oscillation reduce in elder participants, who suffer high work stress (Amanda C. Marshall et al., 2015). In healthy aging people, gamma oscillation increase is coordination with increasing the working memory activity (Mera S. Barra et al., 2014). In elderly subjects, the reduction of beta-band activity is related to deficit in sustaining attention (Mateusz Gola et al., 2013; Mateusz Gola et al., 2012).

2.5. Mental Disorders

2.5.1. Dementia

Dementia is resulted from the lose of cognitive level and death of brain cells (D. Pond., 2012). When the people have dementia, the delta band and theta band power will increase, and alpha band power will decrease (B. Jelles et al., 2008).

In elderly people, alzheimer's disease (AD) is the common reason of dementia. This disease mainly damage the memory and learning ability of the patients. Compared with the health people, AD patients increase delta band and theta band power, and decrease alpha band and beta band power (Lei Wu et al., 2014).

2.5.2. Epileptic Seizure and Nonepileptic Attacks

All over the world, epilepsy affect people from different age groups (World Health Organization, 2013, Fact sheet 999: epilepsy). A group of brain cells suddenly electric shock is the character of this disease. During the seizure attack, delta band power increase and alpha band, beta band, theta band power decrease (M. Valderramaa et al., 2012).

Psychogenic non-epileptic seizures (PNES) only change behavior, and don't change EEG signal (Ce´cile Hubsch et al., 2011). The diagnosis for non-epileptic siezures is based on EEG record, disease history and physical examination (Katherine H. Noe et al., 2012).

2.5.3. Psychiatric Disorders

Attention deficit hyperactivity disorder (ADHD) is prevalent in 3%–5% of children before 7 years old. Its character symptoms are inattention and/or hyperactivity (Monastra VJ et al., 2001). The theta band activity is the preliminary symptom of ADHD (sensitivity: 86%, specificity: 98%) (Monastra VJ et al., 1999; Nash Boutros et al., 2005). The reduction of beta band activity in ADHD patients are result in poor attention level (Geir Ogrim et al., 2012).

Bipolar disorder (BD) is characterized by alternating manic and depression (Anderson et al., 2012; Diagnostic and Statistical Manual of Mental Disorders (5^{th} ed), 2013). At the resting state, BD patients show beta band significantly increase power and theta band decrease power at frontal cortex and cingulate gyrus. But, the beta band power decrease after the mindfulness based cognitive therapy (MBCT) (Fleur M Howells et al., 2012).

The prevalence of schizophrenia is less than 1% all over the world. This disease affects all ethnicities and slightly more common in men. The symptoms of the schizophrenia patients include: delusions, hallucinations, and emotional expression decrease (Sarah D. Holder et al., 2014). When schizophrenia patients experience delusions and/or hallucinations, the gamma-band increase activity. However, after transcranial magnetic stimulation (TMS), the theta band and delta band increase activity with the loss of the symptoms (Marina Frantseva et al., 2014).

Autism is a developmental disease. It affect several behavioral domains, including language, cognitive, and social abilities (William Bosl et al., 2011). The

austism spectrum disorder (ASD) is result from reduction of connectivity in cortical auditory processing circuit. It is characterized by EEG change range from 12 Hz to 30 Hz (Frank H Duffy et al., 2012).

3.1. What is unknown for blast induced brain injury?

(Scott R. Sponheim et al., 2010) find the diminish of EEG phase was related to injury white matter tracts caused by blast-related mTBI. (Ming-Xiong Huang, et al., 2009) exam blast-related mild traumatic brain injury patients. The result show a large number of delta waves are visible during 15 minute EEG recording. The results above only show the EEG change at chronic phase after blast. We still don't know the EEG change at acute and subacute phase after blast.

3.2. What is the hypothesis for the study?

Recent, scientists find QEEG can monitor the cerebral ischemia and delayed cerebral infarction in the traumatic brain injury patients and animals (S. Gollwitzer, 2015; Shao-jie Zhang, et al., 2013). QEEG is sensitive to detect brain function change following mTBI (Michael Gaetz, 2001).

We suppose that the QEEG can detect brain activity abnormalities early after blast exposure.

3.3. What is purpose of this study?

In this study, we examine the relation between the blast-related mild TBI and the unique features of acute and subacute QEEG change of swine under anesthesia. And, we want to find the power threshold to detect the blast-related mTBI at the acute and subacute phase.

CHAPTER 2 MATERIALS AND METHODS

2.1. Subjects

Six swines (Yucatan minipigs, 50Kg weight) were sedated with ketamine and midazolam, and then propofol (0.83-1.66 mg/kg, iv) was given for further anesthesia and maintained with propofol (12-20 mg/kg/hr iv) for 3 hours after blast. The use of these swines were approved by the Ethics Committee of Wayne State University, Detroit, MI.

We were scheduled to perform open field blast testing of 6 anesthetized swine to obtain EEG data of brain response due to blast overpressure. The animal was moved onto a sling for the blast experiment, and the swine head was front to the blast wave (Figure 2.1). The level of anesthesia was maintained and monitored by a veterinarian to ensure the animal felt no pain. The target incident overpressures (IOP) were range from 410 kPa to 460 kPa (Table 2.1). The entire procedure took about 2 to 3 hours.

	The target incident overpressures (IOP)
Swine 1	413.7 kPa
Swine 2	441.3 kPa
Swine 3	432.3 kPa
Swine 4	421.3 kPa
Swine 5	460.6 kPa
Swine 6	468.2 kPa

Table 2.1: The target incident overpressures (IOP) of six swine

2.2. EEG data acquisition

Subjects were lied prostrate on the ambulance stretchers. The continuous EEG was recorded using Ag/AgCl electrodes (Biopac electrode EL503) mounted in a 4-channel Biopac data acquisition system (MP-36, Biopac, Goleta, CA) at 15 minutes before blast, and 15 minutes, 30 minutes, 2 hours, 24 hours, 48 hours, 72 hours post-blast. The MP36 connected with the computer via a USB Port (Figure 2.2). Conducting gel (Biopac GEL100) was injected onto each electrode recording surface to connect with the scalp and electrode impedance was below 5 kΩ. The electrical activity from the scalp was recorded at 4-sites: left parietal lobe, right parietal lobe, left front lobe and right front lobe. 8 electrodes were 2 cm away from the middle line suture. The frontal and parietal recording electrodes were 3.5 cm away from each other (Figure 2.3). The ground electrode was located anterior of the front lobe, served as reference. High-pass filter and Low-pass filter were incorporated into each MP unit channel, and set at 0.5 and 30 Hz, respectively. The Channel sampling rate was set at 10 K samples/second. EEG raw data was saved as Windows AcqKnowledge 3 Graph (*.acq) format for later analyses.

2.3. EEG data processing and analyses

The raw EEG data were processed offline using Acknowledge software (Version 4.2, Biopac, Goleta, CA). The typical electrode pop artifact (Figure 2.4) was abrupt vertical transient waveform, and showed in single electrode (Selim R et al., 2006). We manually removed the electrode pop artifact before the QEEG analyses.

Figure 2.1: Instrumented swine test: the pig head was front to the blast wave

Figure 2.2: 4-channels Biopac data acquisition system (MP-36) connects to the computer via a USB port.

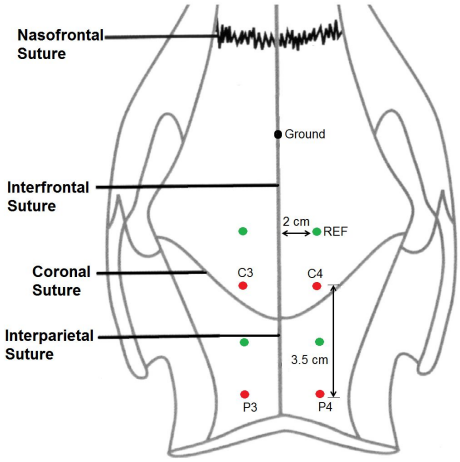

Figure 2.3: Recording electrodes were placed on the swine scalp over both frontal and parietal areas of the skull. 8 electrodes were 2 cm away from the middle line suture. Frontal and parietal recording electrodes were 3.5 cm away from each other. The ground electrode was located anterior of the front lobe, served as reference.

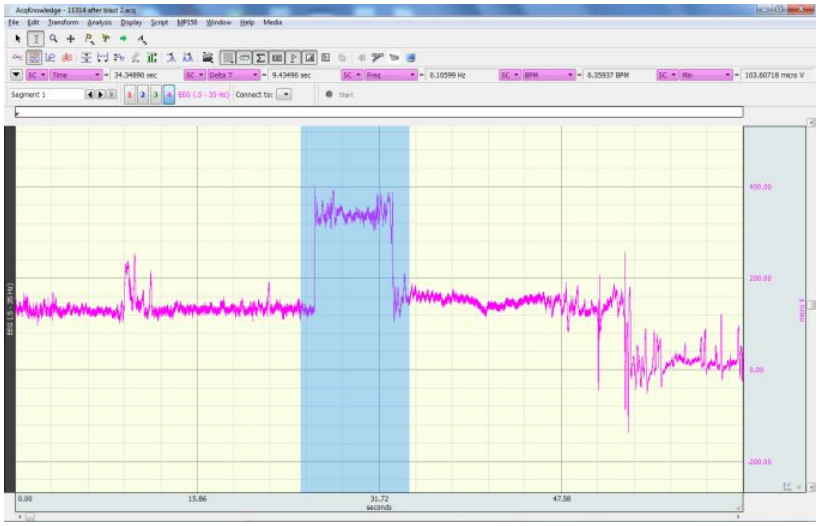

Figure 2.4: Electrode Pop Artifact (Blue highlight)

2.3.1. EEG Frequency Analysis

The EEG Frequency Analysis extracted frequency feature from EEG signals using fast fourier transform (FFT) ($F(S) = \int_{-\infty}^{\infty} f(x) e^{-2\pi i s x} dx$, f(x) is time-domain data, F(S) is frequency-domain data) (Figure 2.5). The EEG signals were divided into fixed-width time epochs. For each epoch, frequency data was extracted : 1. Mean Frequency (Hz), frequency at which the average power is reached. 2. Spectral Edge (Hz), frequency at which 90% of the total power is reached (AcqKnowledge® 4 Software Guide, 2001).

In this study, we set width of each epoch to be 2 seconds (Figure 2.6), and calculate 150 epochs. We could read overall mean frequency, spectral edge frequency 90 (SEF-90) from data sheet created by software (Figure 2.7).

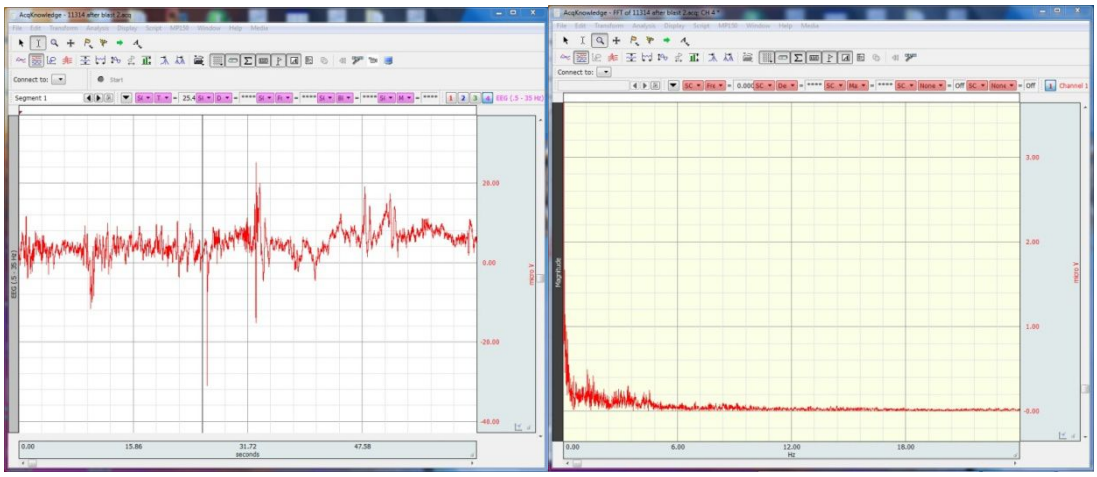

Figure 2.5: Acknowledge software convert time-domain data to frequency-domain data by fast fourier transform

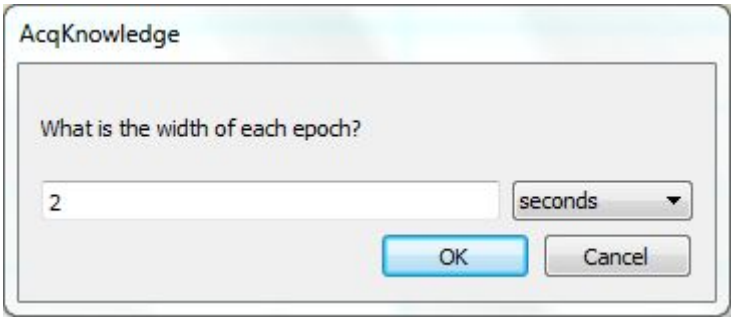

Figure 2.6: EEG Frequency Analysis epoch setting

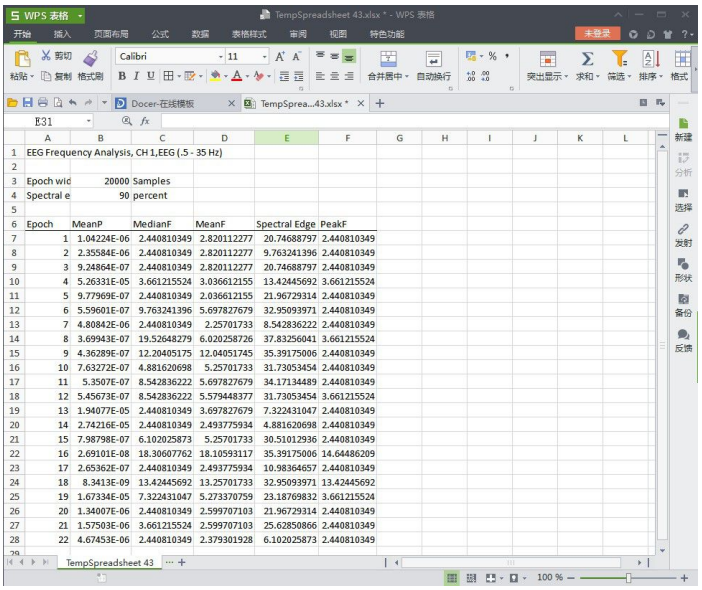

EEG Frequency Analysis, CH 1,EEG (.5 - 35 Hz)

Epoch wid 20000 Samples
Spectral e 90 percent

Epoch	MeanP	MedianF	MeanF	Spectral Edge	PeakF
1	1.04224E-06	2.440810349	2.820112277	20.74688797	2.440810349
2	2.35584E-06	2.440810349	2.820112277	9.763241396	2.440810349
3	9.24864E-07	2.440810349	2.820112277	20.74688797	2.440810349
4	5.26331E-05	3.661215524	3.036612155	13.42445692	3.661215524
5	9.77969E-07	2.440810349	2.036612155	21.96729314	2.440810349
6	5.59601E-07	9.763241396	5.697827679	32.95093971	2.440810349
7	4.80842E-06	2.440810349	2.25701733	8.542836222	2.440810349
8	3.69943E-07	19.52648279	6.020258726	37.83256041	3.661215524
9	4.36289E-07	12.20405175	12.04051745	35.39175006	2.440810349
10	7.63272E-07	4.881620698	5.25701733	31.73053454	2.440810349
11	5.3507E-07	8.542836222	5.697827679	34.17134489	2.440810349
12	5.45673E-07	8.542836222	5.579448377	31.73053454	3.661215524
13	1.94077E-05	2.440810349	3.697827679	7.322431047	2.440810349
14	2.74216E-05	2.440810349	2.493775934	4.881620698	2.440810349
15	7.98798E-07	6.102025873	5.25701733	30.51012936	2.440810349
16	2.69101E-08	18.30607762	18.10593117	35.39175006	14.64486209
17	2.65362E-07	2.440810349	2.493775934	10.98364657	2.440810349
18	8.3413E-09	13.42445692	13.25701733	32.95093971	13.42445692
19	1.67334E-05	7.322431047	5.273370759	23.18769832	3.661215524
20	1.34007E-06	2.440810349	2.599707103	21.96729314	2.440810349
21	1.57503E-06	3.661215524	2.599707103	25.62850866	2.440810349
22	4.67453E-06	2.440810349	2.379301928	6.102025873	2.440810349

Figure 2.7: Data sheet created by Acknowledge software

2.3.2. Power spectral density analysis

The power spectral density (PSD) analysis also divided the EEG signals into fixed-width time epochs (2 second). Raw data was divided into 300 epochs. For each epoch, AcqKnowledge's Welch periodogram method to estimate the power spectrum of that epoch (Figure 2.8) (AcqKnowledge® 4 Software Guide, 2001).

In our study, window option set Hamming ($w(n) = 0.54 - 0.46\cos(\frac{2\pi n}{N-1})$, n is overlapping segments, N is non-overlapping segments); window size, overlap length and FFT width set Automatic, respectively (Figure 2.9, 2.10). We manually extracted the delta band (0.5-4 Hz), theta band (4-8 Hz), lower alpha band (8-10 Hz), beta band (13-30 Hz) by frequency and read the mean power density value ((micro V)^2/Hz).

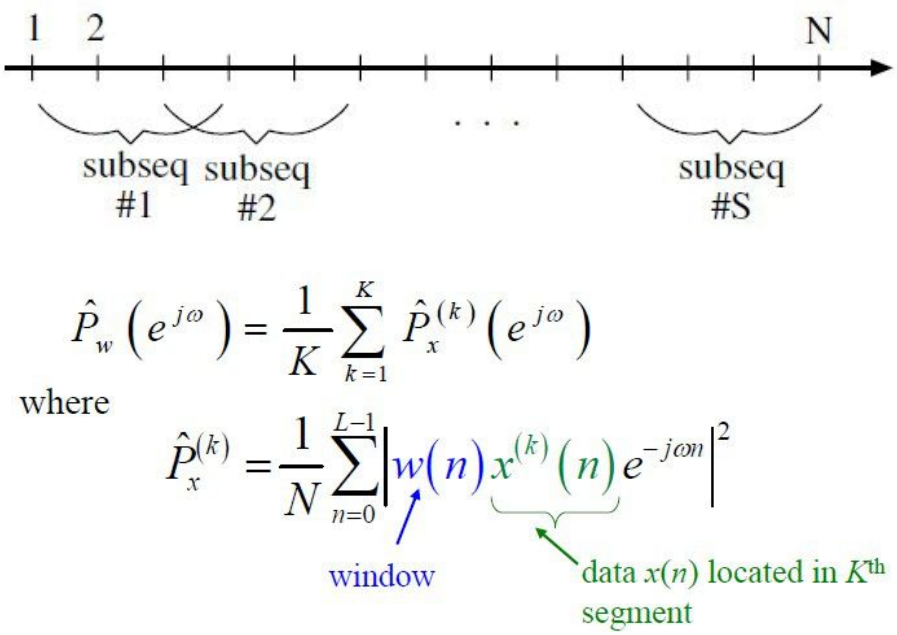

Figure 2.8: The signal is split up into 300 segments, each segment overlap 50% of other segment, which will give more epoch and better average value. Each segment multiply window function to decrease wave leakage.

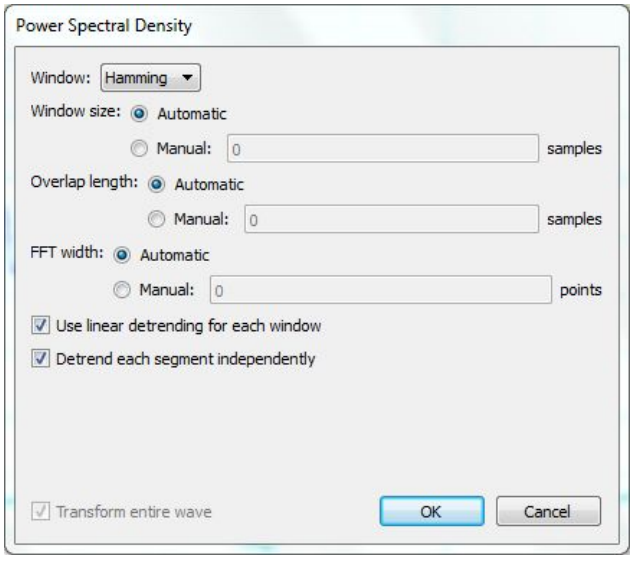

Figure 2.9: Power spectral density setting

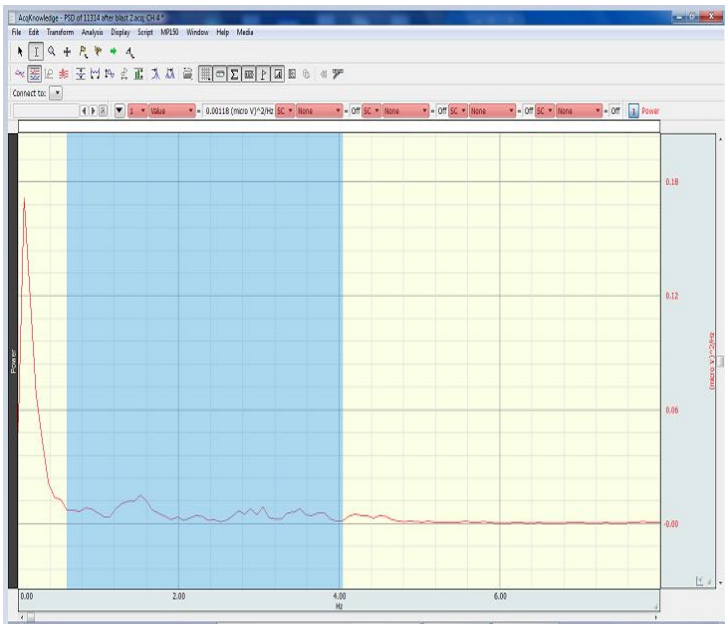

Figure 2.10: We manually choose frequency from 0.5 Hz-4 Hz (delta band), and read power value from above square frame.

2.4. Statistic Analysis

SPSS 17.0 (SPSS Inc., Chicago, IL) software was used for data analysis. Significance of differences between groups and time points was calculated using One Way ANOVA (PostHoc, LSD) and Repeated Measures of ANOVA (RMANOVA) tests (PostHoc, LSD). $P<0.05$ was considered as a significant difference.

CHAPTER 3 RESULTS

3.1. EEG Frequency data

The EEG mean frequency have no statistic significant before and after blast at left parietal, left front and right front recording site. At the right parietal recording site, EEG mean frequency decreased from 6.78 ± 2.01 Hz before blast to 3.36 ± 0.28 Hz, 3.10 ± 0.19, 3.47 ± 0.21, 3.43 ± 0.11 at 15 min, 2h, 1d, 2d after blast ($P<0.05$), returned to 5.25 ± 1.96 Hz, 4.52 ± 1.26 Hz at 30 min, 3d after blast ($P>0.05$) (Figure 3.1; Table 3.1).

The SEF-90 have no statistic significant before and after blast at left front recording site. At the left parietal recording site, SEF-90 decreased from 18.22 ± 3.51 Hz before blast to 10.27 ± 1.24 Hz, 10.84 ± 1.22 Hz at 15 min, 2d after blast ($P<0.05$), respectively, and returned to 14.25 ± 3.01 Hz, 17.27 ± 3.15, 14.94 ± 0.86 Hz, 11.03 ± 2.03 Hz at 30 min, 2h, 1d, 3d after blast ($P>0.05$), respectively. At the right parietal recording site, SEF-90 decreased from 20.46 ± 3.63 Hz before blast to 10.43 ± 1.26, 10.74 ± 1.18, 11.98 ± 1.15, 11.44 ± 0.72 at 15 min, 2h, 1d, 2d after blast ($P<0.05$), respectively, and returned to 13.84 ± 3.97, 13.21 ± 4.49 at 30 min, 3d after blast ($P>0.05$), respectively. At the right front recording site, SEF-90 decreased from 16.55 ± 4.14 Hz before blast to 9.31 ± 1.01 after blast ($P<0.05$), and returned to 16.10 ± 3.37, 15.09 ± 2.07, 12.52 ± 1.68, 10.10 ± 0.64, 13.29 ± 1.76 at 30 min, 2h, 1d, 2d, 3d after blast ($P>0.05$), respectively (Figure 3.2; Table 3.2).

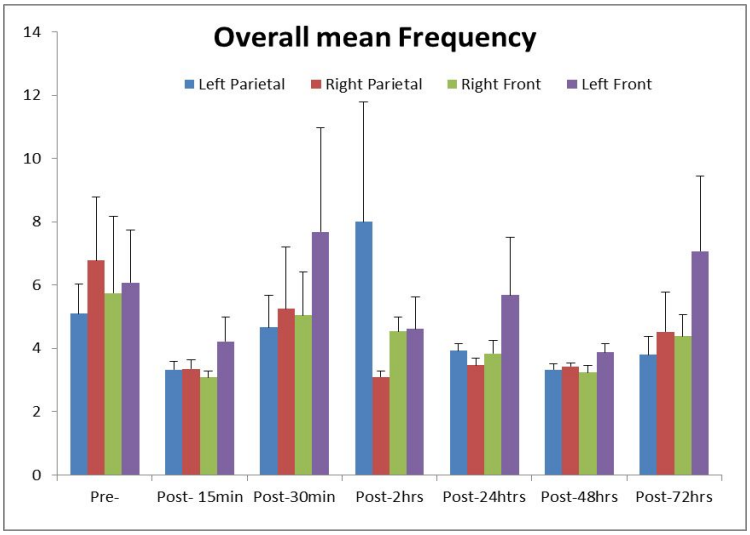

Figure 3.1: EEG mean frequency (Hz) change before and after blast at both front and parietal recording sites.

Overall mean frequency (Hz)

	Before blast	15 min	30 min	2h	1d	2d	3d
Left Parietal	5.09±0.94	3.32±0.26	4.66±1.02	8.00±3.78	3.93±0.23	3.33±0.18	3.79±0.57
Right Parietal	6.78±2.01	3.36±0.28	5.25±1.96	3.10±0.19	3.47±0.21	3.43±0.11	4.52±1.26
Left Front	6.08±1.67	4.21±0.78	7.68±3.30	4.62±1.02	5.68±1.82	3.88±0.27	7.06±2.39
Right Front	5.75±2.43	3.09±0.49	5.04±1.37	4.53±0.47	3.83±0.42	3.24±0.21	4.39±0.69

Table 3.1: The EEG mean frequency value before and after blast at both front and parietal recording sites. At right parietal recording site have statistic significant, other recording sites have no significant.

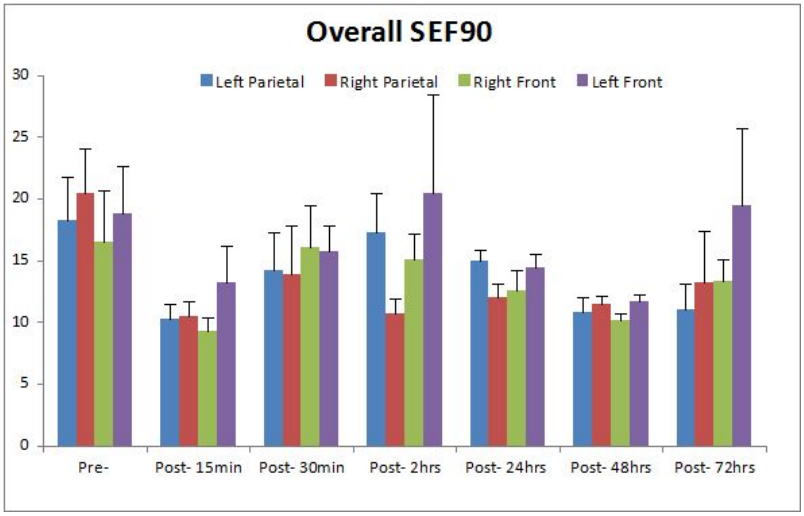

Figure 3.2: Spectral Edge Frequency 90 (SEF-90, Hz) change at both front and parietal recording sites.

Overall Spectral Edge Frequency (Hz)

	Before blast	15 min	30 min	2h	1d	2d	3d
Left Parietal	18.22±3.51	10.27±1.24	14.25±3.01	17.27±3.15	14.94±0.86	10.84±1.22	11.03±2.03
Right Parietal	20.46±3.63	10.43±1.26	13.84±3.97	10.74±1.18	11.98±1.15	11.44±0.72	13.21±4.49
Left Front	18.77±3.83	13.20±2.96	15.77±2.09	20.47±7.96	14.38±1.10	11.67±0.6	19.43±6.28
Right Front	16.55±4.14	9.31±1.01	16.10±3.37	15.09±2.07	12.52±1.68	10.10±0.64	13.29±1.76

Table 3.2: Spectral Edge Frequency 90 (SEF-90) value at both front and parietal recording sites. At left front recording site have no statistical significant, other sites have significant.

3.2. Different band of EEG data

EEG power change at both parietal and front regions after blast (Figure 3.3, 3.4, 3.5, 3.6).

The Lower Alpha band power (8-10 Hz) have no statistic significant before and after blast at right parietal, left front, right front recording site. At the left parietal recording site, Alpha power decreased from $5\times10^{-3}\pm4\times10^{-3}$ V^2/Hz before blast to $4.9\times10^{-4}\pm4\times10^{-4}$ V^2/Hz, $8.8\times10^{-4}\pm4\times10^{-4}$ V^2/Hz, $1.7\times10^{-4}\pm3\times10^{-5}$ V^2/Hz, $2.5\times10^{-4}\pm8\times10^{-5}$ V^2/Hz at 15 min, 2h, 1d, 2d after blast ($P<0.05$), respectively, and returned to $1.2\times10^{-3}\pm5\times10^{-4}$ V^2/Hz , $7.6\times10^{-4}\pm2\times10^{-4}$ V^2/Hz at 30 min, 3d after blast ($P>0.05$), respectively (Figure 3.7; Table 3.3).

The Beta band power and theta band power, Delta band power, and Alpha-Delta power ratio (ADR) have no statistic significant before and after blast at all recording sites (Figure 3.8, 3.9, 3.10, 3.11; Table 3.4, 3.5, 3.6, 3.7).

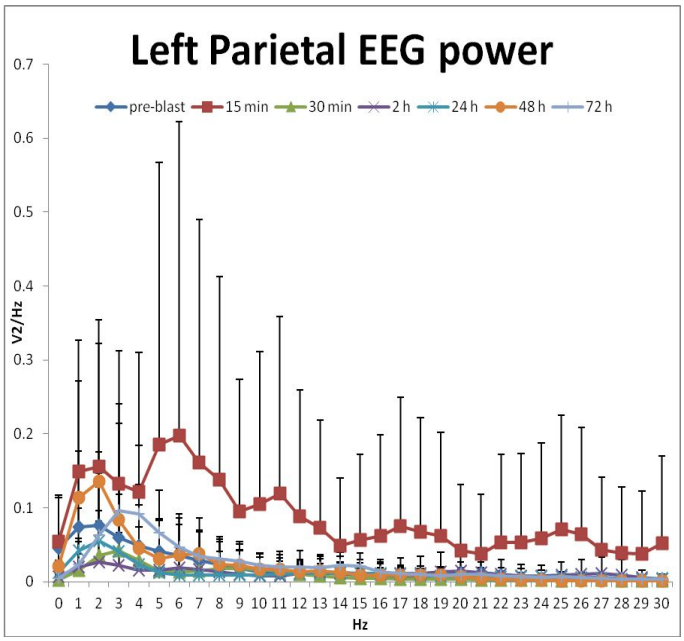

Figure 3.3: EEG power data was recorded at the left parietal region.

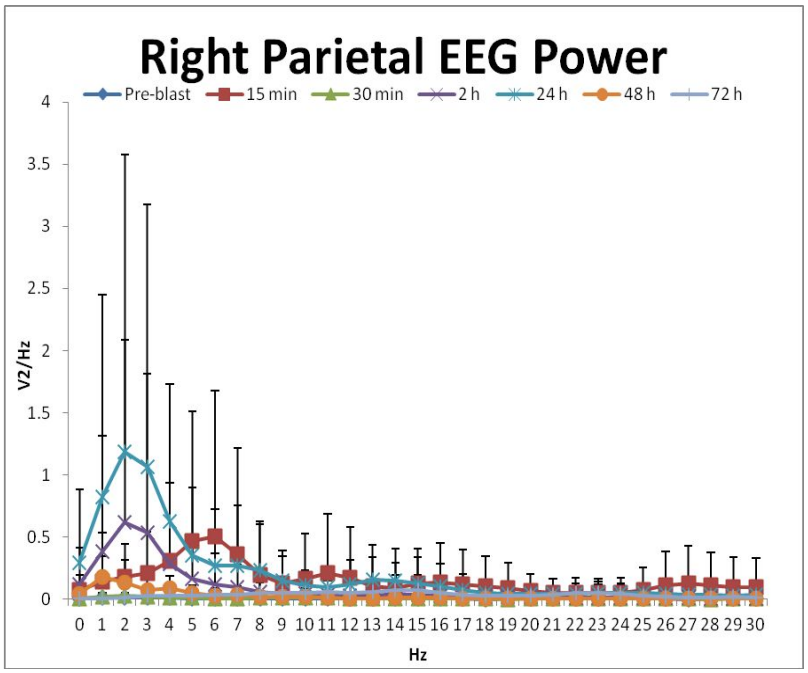

Figure 3.4: EEG power recorded at the right parietal region.

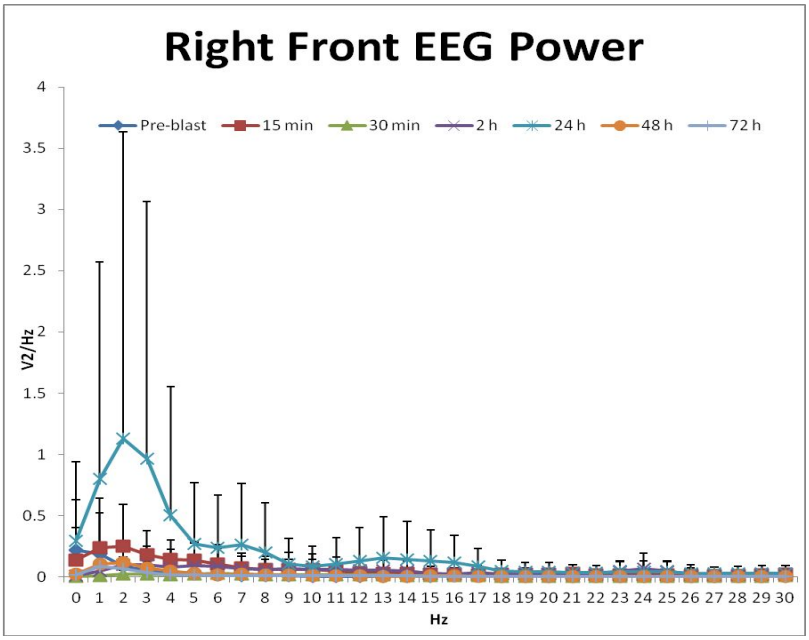

Figure 3.5: EEG power recorded at the right front region.

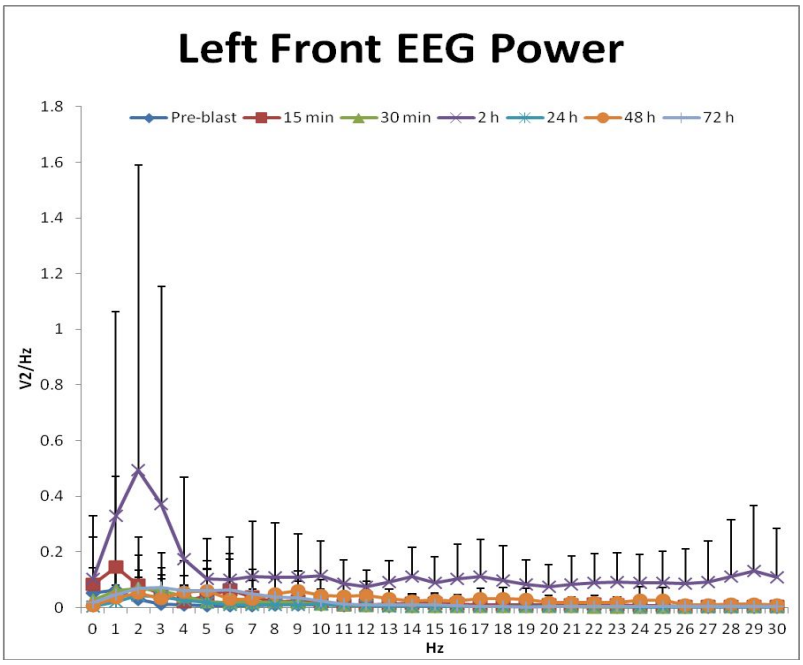

Figure 3.6: EEG power recorded at the left front region.

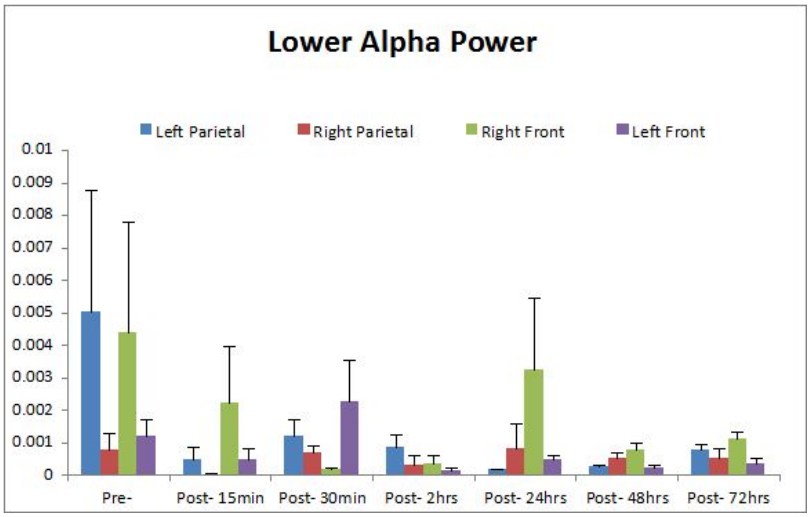

Figure 3.7: Lower Alpha power (V^2/Hz) change before and after blast at both front and parietal recording sites.

Lower Alpha power (V^2/Hz)							
	Before blast	15 min	30 min	2h	1d	2d	3d
Left Parietal	$5\times10^{-3}\pm4\times10^{-3}$	$4.9\times10^{-4}\pm4\times10^{-4}$	$1.2\times10^{-3}\pm5\times10^{-4}$	$8.8\times10^{-4}\pm4\times10^{-4}$	$1.7\times10^{-4}\pm3\times10^{-5}$	$2.5\times10^{-4}\pm8\times10^{-5}$	$7.6\times10^{-4}\pm2\times10^{-4}$
Right Parietal	$7.8\times10^{-4}\pm5\times10^{-4}$	$2.9\times10^{-5}\pm3\times10^{-5}$	$6.9\times10^{-4}\pm2\times10^{-4}$	$3.3\times10^{-4}\pm3\times10^{-4}$	$8.0\times10^{-4}\pm8\times10^{-4}$	$5.0\times10^{-4}\pm2\times10^{-4}$	$5.3\times10^{-4}\pm3\times10^{-4}$
Left Front	$1.2\times10^{-3}\pm5\times10^{-4}$	$4.9\times10^{-4}\pm3\times10^{-4}$	$2.2\times10^{-3}\pm1\times10^{-3}$	$1.3\times10^{-4}\pm1\times10^{-4}$	$4.8\times10^{-4}\pm1\times10^{-4}$	$2.3\times10^{-4}\pm1\times10^{-4}$	$3.6\times10^{-4}\pm2\times10^{-4}$
Right Front	$4.4\times10^{-3}\pm3\times10^{-3}$	$2.2\times10^{-3}\pm2\times10^{-3}$	$1.7\times10^{-4}\pm7\times10^{-5}$	$3.4\times10^{-4}\pm3\times10^{-4}$	$3.2\times10^{-3}\pm2\times10^{-3}$	$7.8\times10^{-4}\pm2\times10^{-4}$	$1.1\times10^{-3}\pm2\times10^{-4}$

Table 3.3: The Lower Alpha power (8-10 Hz) value before and after blast at both front and parietal recording sites. At left parietal recording site have statistical significant, other sites have no significant.

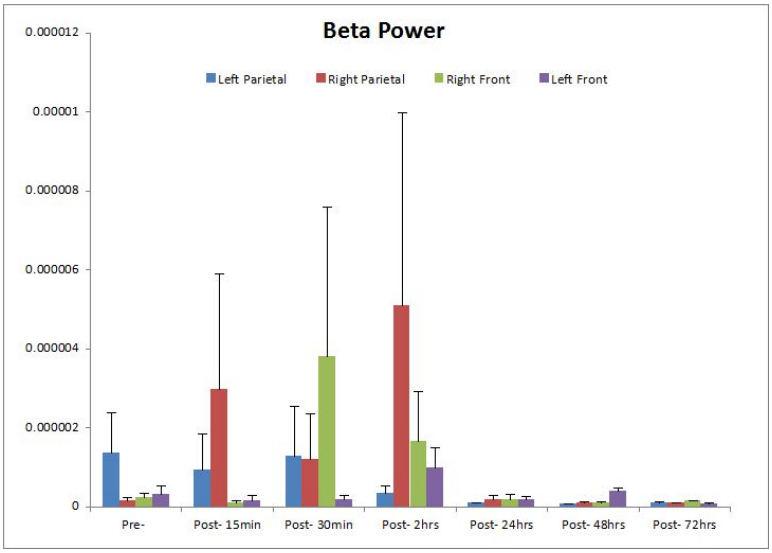

Figure 3.8: Beta band power (V^2/Hz) have no statistical significance before and after blast ($P>0.05$) .

	Beta power (V^2/Hz)						
	Before blast	15 min	30 min	2h	1d	2d	3d
Left Parietal	$1.4\times10^{-6}\pm1\times10^{-6}$	$9.4\times10^{-7}\pm9\times10^{-7}$	$1.3\times10^{-6}\pm1\times10^{-6}$	$3.5\times10^{-7}\pm2\times10^{-7}$	$1.0\times10^{-7}\pm2\times10^{-8}$	$7.0\times10^{-8}\pm2\times10^{-8}$	$1.2\times10^{-7}\pm2\times10^{-8}$
Right Parietal	$1.7\times10^{-7}\pm7\times10^{-8}$	$3.0\times10^{-6}\pm3\times10^{-6}$	$1.2\times10^{-6}\pm1\times10^{-6}$	$5.1\times10^{-6}\pm5\times10^{-6}$	$1.9\times10^{-7}\pm1\times10^{-7}$	$1.1\times10^{-7}\pm2\times10^{-8}$	$1.0\times10^{-7}\pm2\times10^{-8}$
Left Front	$3.3\times10^{-7}\pm2\times10^{-7}$	$1.6\times10^{-7}\pm1\times10^{-7}$	$1.9\times10^{-7}\pm1\times10^{-7}$	$9.8\times10^{-7}\pm5\times10^{-7}$	$1.9\times10^{-7}\pm9\times10^{-8}$	$3.9\times10^{-7}\pm8\times10^{-8}$	$7.0\times10^{-8}\pm3\times10^{-8}$
Right Front	$2.5\times10^{-7}\pm1\times10^{-7}$	$1.0\times10^{-7}\pm7\times10^{-8}$	$3.8\times10^{-6}\pm4\times10^{-6}$	$1.7\times10^{-6}\pm1\times10^{-6}$	$2.0\times10^{-7}\pm1\times10^{-7}$	$1.0\times10^{-7}\pm2\times10^{-8}$	$1.6\times10^{-7}\pm1\times10^{-8}$

Table 3.4: Beta band power (V^2/Hz) have no statistical significance before and after blast (P>0.05) .

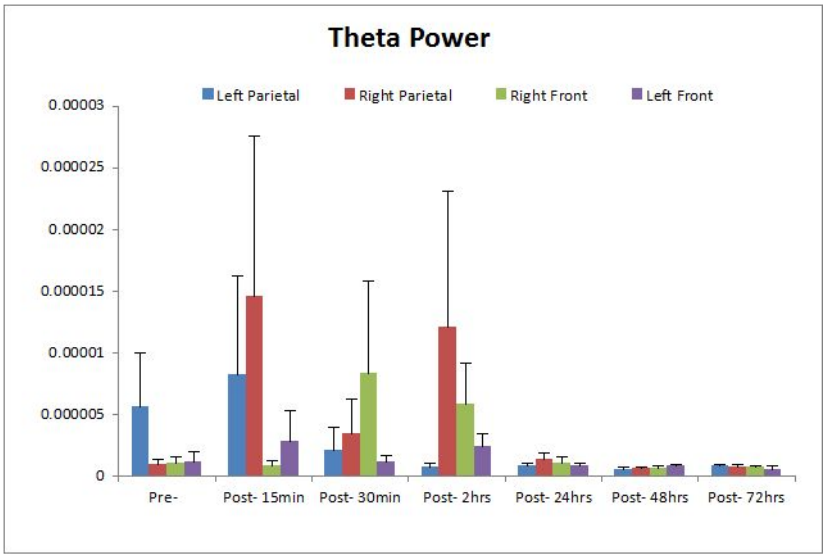

Figure 3.9: Theta band power (V^2/Hz) have no statistical significance before and after blast (P>0.05) .

Theta power (V^2/Hz)							
	Before blast	15 min	30 min	2h	1d	2d	3d
Left Parietal	$5.7\times10^{-6}\pm4\times10^{-6}$	$8.3\times10^{-6}\pm8\times10^{-6}$	$2.1\times10^{-6}\pm2\times10^{-6}$	$7.3\times10^{-7}\pm3\times10^{-7}$	$8.5\times10^{-7}\pm3\times10^{-7}$	$6.0\times10^{-7}\pm1\times10^{-7}$	$8.5\times10^{-7}\pm8\times10^{-8}$
Right Parietal	$9.9\times10^{-7}\pm4\times10^{-7}$	$1.5\times10^{-5}\pm1\times10^{-5}$	$3.5\times10^{-6}\pm3\times10^{-6}$	$1.2\times10^{-5}\pm1\times10^{-5}$	$1.4\times10^{-6}\pm5\times10^{-7}$	$6.8\times10^{-7}\pm7\times10^{-8}$	$8.1\times10^{-7}\pm2\times10^{-7}$
Left Front	$1.2\times10^{-6}\pm8\times10^{-7}$	$2.8\times10^{-6}\pm3\times10^{-6}$	$1.2\times10^{-6}\pm5\times10^{-7}$	$2.5\times10^{-6}\pm1\times10^{-6}$	$8.9\times10^{-7}\pm2\times10^{-7}$	$8.3\times10^{-7}\pm1\times10^{-7}$	$5.6\times10^{-7}\pm3\times10^{-7}$
Right Front	$1.1\times10^{-6}\pm5\times10^{-7}$	$8.8\times10^{-7}\pm4\times10^{-7}$	$8.4\times10^{-6}\pm7\times10^{-6}$	$5.9\times10^{-6}\pm3\times10^{-6}$	$1.1\times10^{-6}\pm5\times10^{-7}$	$6.8\times10^{-7}\pm1\times10^{-7}$	$8.1\times10^{-7}\pm5\times10^{-8}$

Table 3.5: Theta band power (V^2/Hz) have no statistical significance before and after blast (P>0.05) .

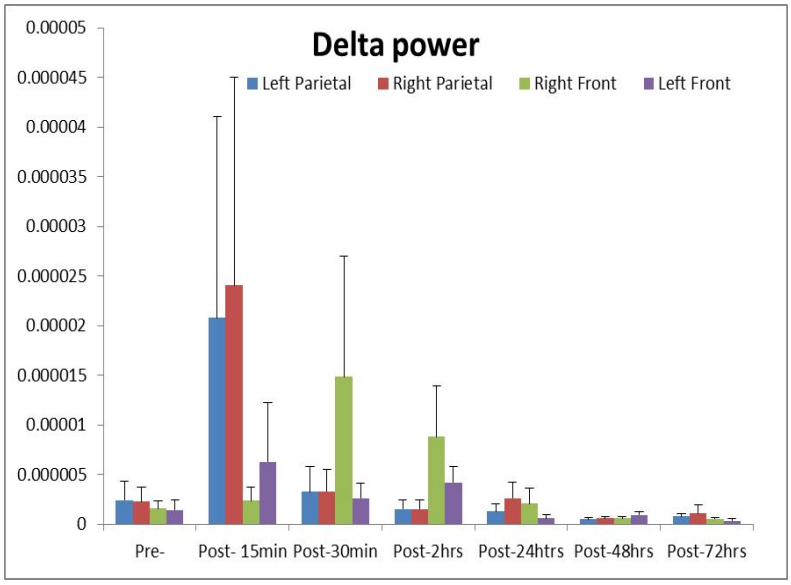

Figure 3.10: Delta band power (V^2/Hz) have no statistical significance before and after blast (P>0.05).

	Delta power (V^2/Hz)						
	Before blast	15 min	30 min	2h	1d	2d	3d
Left Parietal	$2.4\times10^{-6}\pm2\times10^{-6}$	$2.1\times10^{-5}\pm2\times10^{-5}$	$3.3\times10^{-6}\pm3\times10^{-6}$	$1.5\times10^{-6}\pm9\times10^{-7}$	$1.3\times10^{-6}\pm8\times10^{-7}$	$5.1\times10^{-7}\pm2\times10^{-7}$	$7.8\times10^{-7}\pm3\times10^{-7}$
Right Parietal	$2.3\times10^{-6}\pm2\times10^{-6}$	$2.4\times10^{-5}\pm2\times10^{-5}$	$3.3\times10^{-6}\pm2\times10^{-6}$	$1.6\times10^{-6}\pm9\times10^{-7}$	$2.6\times10^{-6}\pm2\times10^{-6}$	$5.8\times10^{-7}\pm1\times10^{-7}$	$1.1\times10^{-6}\pm9\times10^{-7}$
Left Front	$1.5\times10^{-6}\pm1\times10^{-6}$	$6.3\times10^{-6}\pm6\times10^{-6}$	$2.6\times10^{-6}\pm2\times10^{-6}$	$4.2\times10^{-6}\pm2\times10^{-6}$	$6.1\times10^{-7}\pm3\times10^{-7}$	$9.4\times10^{-7}\pm4\times10^{-7}$	$3.7\times10^{-7}\pm2\times10^{-7}$
Right Front	$1.6\times10^{-6}\pm8\times10^{-7}$	$2.4\times10^{-6}\pm1\times10^{-6}$	$1.5\times10^{-5}\pm1\times10^{-5}$	$8.8\times10^{-6}\pm5\times10^{-6}$	$2.1\times10^{-6}\pm2\times10^{-6}$	$6.1\times10^{-7}\pm2\times10^{-7}$	$5.3\times10^{-7}\pm2\times10^{-7}$

Table 3.6: Delta band power have no statistical significance before and after blast (P>0.05).

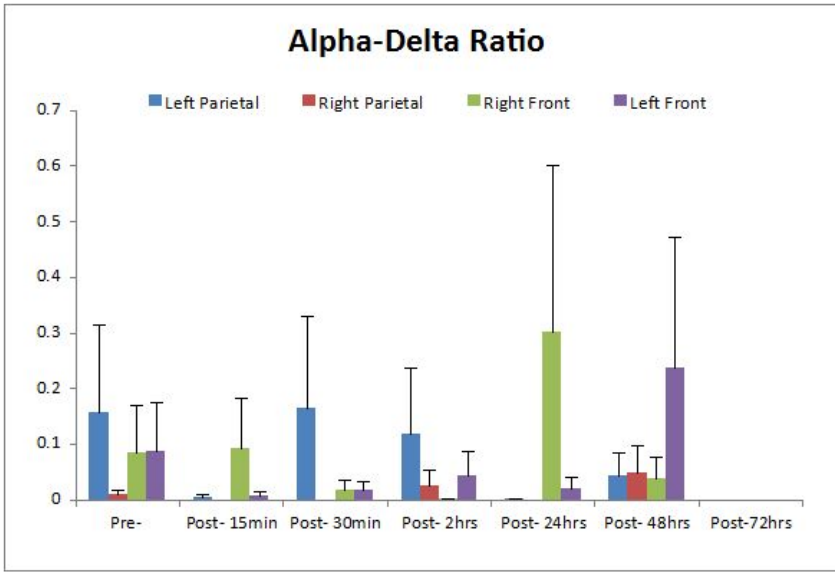

Figure 3.11: Alpha-Delta power ratio (ADR) have no statistical significance before and after blast (P>0.05).

Alpha-Delta power ratio (ADR)

	Before blast	15 min	30 min	2h	1d	2d	3d
Left parietal	$2\times10^{-1}\pm1.6\times10^{-1}$	$5\times10^{-3}\pm4.6\times10^{-3}$	$2\times10^{-1}\pm1.7\times10^{-1}$	$1.2\times10^{-1}\pm1.2\times10^{-1}$	$1.3\times10^{-3}\pm1.3\times10^{-3}$	$4.2\times10^{-2}\pm4.2\times10^{-2}$	$3\times10^{-7}\pm3.6\times10^{-8}$
Right parietal	$9\times10^{-3}\pm8.5\times10^{-3}$	$5\times10^{-6}\pm4.6\times10^{-6}$	$2\times10^{-6}\pm1.7\times10^{-6}$	$3\times10^{-2}\pm2.6\times10^{-2}$	$5\times10^{-7}\pm1.8\times10^{-7}$	$5\times10^{-2}\pm4.9\times10^{-2}$	$2\times10^{-7}\pm6.8\times10^{-8}$
Left front	$9\times10^{-2}\pm8.8\times10^{-2}$	$8\times10^{-3}\pm7.6\times10^{-3}$	$2\times10^{-2}\pm1.7\times10^{-2}$	$4.4\times10^{-2}\pm14.4\times10^{-2}$	$2\times10^{-2}\pm2\times10^{-2}$	$2.4\times10^{-1}\pm2.4\times10^{-1}$	$2.2\times10^{-7}\pm1.5\times10^{-9}$
Right front	$9\times10^{-2}\pm8.5\times10^{-2}$	$9.2\times10^{-2}\pm9.2\times10^{-2}$	$1.7\times10^{-2}\pm1.7\times10^{-2}$	$1.3\times10^{-3}\pm1.3\times10^{-3}$	$3\times10^{-1}\pm3\times10^{-1}$	$4\times10^{-2}\pm3.8\times10^{-2}$	$3\times10^{-7}\pm2.1\times10^{-8}$

Table 3.7: Alpha-Delta power ratio (ADR) have no statistical significance before and after blast ($P>0.05$).

CHAPTER 4 DISCUSSION

4.1. Summary of the work

In this research, we recorded and analyzed EEG data from swine brains before and after blasts by QEEG technology. The following conclusions are made from the project findings:

The EEG activity decreased fast frequency, and increased slower frequency after the blast. The EEG mean frequency have no statistic significant before and after blast at left parietal, left front and right front recording site. At the right parietal recording site, EEG mean frequency decreased from 6.78 ± 2.01 Hz before blast to 3.36 ± 0.28 Hz, 3.10 ± 0.19, 3.47 ± 0.21, 3.43 ± 0.11 at 15 min, 2h, 1d, 2d after blast ($P<0.05$), returned to 5.25 ± 1.96 Hz, 4.52 ± 1.26 Hz at 30 min, 3d after blast ($P>0.05$). The SEF-90 have no statistic significant before and after blast at left front recording site. At the left parietal recording site, SEF-90 decreased from 18.22 ± 3.51 Hz before blast to 10.27 ± 1.24 Hz, 10.84 ± 1.22 Hz at 15 min, 2d after blast ($P<0.05$), respectively, and returned to 14.25 ± 3.01 Hz, 17.27 ± 3.15, 14.94 ± 0.86 Hz, 11.03 ± 2.03 Hz at 30 min, 2h, 1d, 3d after blast ($P>0.05$), respectively. At the right parietal recording site, SEF-90 decreased from 20.46 ± 3.63 Hz before blast to 10.43 ± 1.26, 10.74 ± 1.18, 11.98 ± 1.15, 11.44 ± 0.72 at 15 min, 2h, 1d, 2d after blast ($P<0.05$), respectively, and returned to 13.84 ± 3.97, 13.21 ± 4.49 at 30 min, 3d after blast ($P>0.05$), respectively. At the right front recording site, SEF-90 decreased from 16.55 ± 4.14 Hz before blast to 9.31 ± 1.01 after blast ($P<0.05$), and returned to 16.10 ± 3.37, 15.09 ± 2.07, 12.52 ±

1.68, 10.10 ± 0.64, 13.29 ± 1.76 at 30 min, 2h, 1d, 2d, 3d after blast (P>0.05), respectively.

The Lower Alpha band power (8-10 Hz) have no statistic significant before and after blast at right parietal, left front, right front recording site. At the left parietal recording site, Alpha power decreased from $5\times10^{-3}\pm4\times10^{-3}$ V^2/Hz before blast to $4.9\times10^{-4}\pm4\times10^{-4}$ V^2/Hz, $8.8\times10^{-4}\pm4\times10^{-4}$ V^2/Hz, $1.7\times10^{-4}\pm3\times10^{-5}$ V^2/Hz, $2.5\times10^{-4}\pm8\times10^{-5}$ V^2/Hz at 15 min, 2h, 1d, 2d after blast (P<0.05), respectively, and returned to $1.2\times10^{-3}\pm5\times10^{-4}$ V^2/Hz , $7.6\times10^{-4}\pm2\times10^{-4}$ V^2/Hz at 30 min, 3d after blast (P>0.05), respectively. The Beta band power and theta band power, Delta band power, and Alpha-Delta power ratio (ADR) have no statistic significant before and after blast at all recording sites

4.2. EEG clinical significance

4.2.1. Overall mean frequency

Immediately after a mTBI, EEG wave showed from epileptiform, to suppressed and recovered to normal(Marc R. Nuwer, et al., 2005). In rat TBI model, the mean frequency decreased from 2.59 ± 0.18 Hz to 1.05 ± 0.20 Hz within 1-4 hours after controlled cortical impact (Xingjie Ping, et al., 2015). Cerebrolysin accelerated the recovery of QEEG slowing in mTBI patients, which was correlated with the improvement of attention and working memory (X. Anton Alvarez, et al., 2008). The slower frequencies were derived from cells in layers II-VI of cortex and thalamus.

The faster frequencies were generated by cells in layers IV and V of cortex (Amzica F et al., 2010). The reticular activating system was the control center to modulate all the EEG frequencies (Evans BM., 1976). The neurons in layers III, V, and VI of cortex are sensitive to cerebral ischemia, and cause the abnormal EEG changes (Jordan KG., 2004).

EEG frequency changes were related to cerebral blood flow (CBF) (Figure 4.1). During general anesthesia, EEG is an accurate monitor to show the cerebral blood flow change in cortex. The EEG frequency started to lose faster frequency, when the CBF declines to 25–35 ml/100 g/min. When the CBF decreased to 17–18 ml/100 g/min, the EEG frequency progressively increased slower frequency. The neurons start to lose transmembrane gradients when the EEG frequency declined to ischemic threshold (4 Hz) (Brandon Foreman, et al., 2012). EEG frequency declined to ischemic threshold within 20 seconds after clamping at carotid (Sharbrough FW et al., 1973).

This study showed mean frequency decreased from 6.78 ± 2.01 Hz pre-blast to 3.10 ± 0.19 Hz after blast ($P<0.05$) at the right parietal recording site. Our data suggest that blast exposure at 410-460KPa may cause transient brain dysfunction.

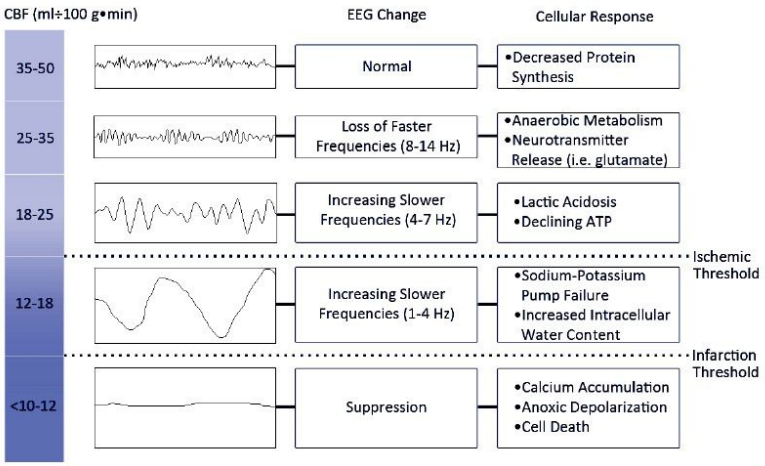

Figure 4.1: The relationship between cerebral blood flow (CBF) and electroencephalogram (EEG) (adopted from Brandon Foreman, et al., 2012.).

4.2.2. Overall Spectral Edge Frequency (SEF)

The SEF 90 means the EEG frequency is below 90 percent of the total power (Figure 4.2). In clinical applications, SEF 90 was used to monitor the depth of anesthesia. During adequate general anaesthesia, in both patients SEF 90 decreased from the awake baseline value of 18-20 Hz to 12-14 Hz. When a movement occurred during anaesthesia, SEF 90 increased to the awake baseline value of 18-20 Hz. During emergence from general anaesthesia, SEF returned to the awake baseline value of 18-20 Hz (Drummond JC et al., 1991) (Figure 4.3). To maintain general anaesthesia (no movement), patients received propofol 3-5 mg kg-1 h-1 i.v.. During general anaesthesia, the SEF 90 decreased from the baseline value of 14.04±3.21 Hz to 11.89 ±1.28 Hz. From 8 min to 2 min before movement, the SEF90 increased from 12.91 ± 2.22 Hz to 15.04 ± 3.05 Hz. When the patients started to move, the SEF 90 increased to the baseline value of 18.08 ± 3.72 Hz (D. Schwender et al., 1996). In

another study, patients maintained spinal anesthesia by propofol (4.2 (0.5) mg. kg^{-1}. h^{-1}). The SEF 90 was 12.2 ± 1.5 Hz during the general anesthesia. 1 min before the patients opened their eyes, the SEF 90 increased to 16.2 ± 1.9 Hz (Shuya Kiyama et al., 1997). (Robert P. Weenink, et al., 2011) used 16 pigs injected 0.05 ml/kg of air into the ascending pharyngeal artery to simulates swine model of cerebral arterial gas embolism. SEF 90 had no significant difference between high-ICP (intracranial pressure) group (n = 5) or low-ICP group (n = 8) at 240 minutes after injection (Figure 4.4). This result indicated the gas embolism had no effect on the SEF 90 value.

In our study, SEF 90 dropped from 16-20 Hz pre-blast to 9-10 Hz post-blast ($P<0.05$) at left parietal, right parietal, right front recording sites, which was lower SEF 90 under anesthesia, indicative of neuron functional inhibition.

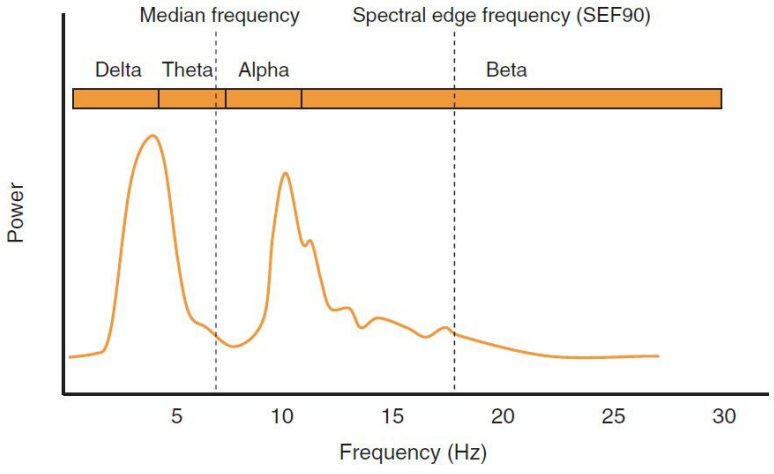

Figure 4.2: Schematic of power spectrum (adopted from P.H. Tonner, et al., 2006).

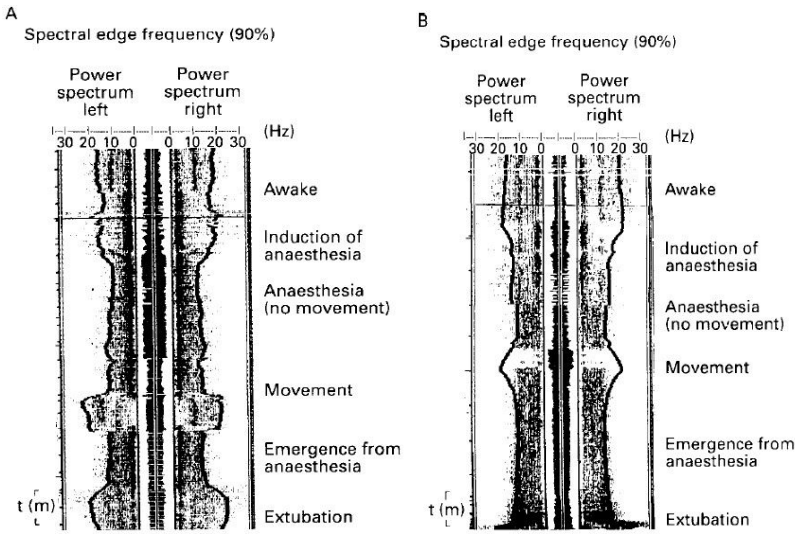

Figure 4.3: Induction and maintenance of general anaesthesia with isoflurane (A) and propofol (B). During adequate general anaesthesia, in both patients SEF 90 decreased from the baseline value of 18-20 Hz to 12-14 Hz. When a movement occurred during anaesthesia, SEF 90 increased to the baseline value of 18-20 Hz. During emergence from general anaesthesia, SEF 90 returned to the awake baseline value of 18-20 Hz (adopted from Drummond JC, et al., 1991.).

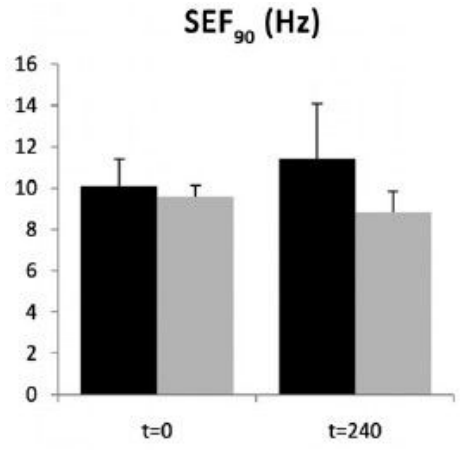

Figure 4.4: SEF-90 value of high-ICP group (black bar) versus low-ICP group (gray bars) at t=0 and t=240 min (P>0.05).

4.2.3. EEG power

mTBI injuries were related to increases in Delta, Theta, and Beta bands power and decreases in Alpha band power (Sladjana et al. 2008, Paul et al. 2015). Cortical arousal was associated with Alpha power changes and cortical activation was related to Delta, Theta, and Beta power changes (Barry et al. 2007). (Napoli et al., 2012) found rat mTBI group increased low-frequency band (4-10 Hz) power at the temporal and subcortical recording location, and Alpha band power decreased at the parietal recording location (Dunkley et al. 2015). In one swine blast-mTBI model, the EEG power shifted from the high frequencies (alpha, beta band) to the low frequencies (delta, theta band) soon after the blast, which was associated with severity of brain injury resulting from the seizures (Richard A. Bauman, et al., 2009).

Alpha activity reflected the severity of disturbed consciousness in the acute stage after TBI (Yuko Urakami, 2013). The Alpha band activities were modified by the interaction between cortico-cortical and thalamo-cortical neuron network (Lopes et al. 1980). When the alpha band activity desynchronized, sensomotor cortex prepare to and process sensory information and motor activity. However, when the Alpha band activity synchronized, the information process was reduced and motor behavior slowed down (G. Pfurtscheller, 1992). Alpha event related desynchroized (ERD) can be divided into upper components (10-13 Hz) and lower components (8-10 Hz). Upper Alpha band was dominated at the occipital areas and associated with the cognitive tasks, such as long-term memory and semantic function. Lower Alpha band was dominated at the parietal areas and related to the attention processes, such as

alertness and expectancy (Figure 4.5) (G. Pfurtscheller et al., 1994, C. Neuper, et al., 2001, W. Klimesch, et al., 1998). Moreover, lower Alpha band activity was the pulsatile signal connection between brain and muscle (Vallbo and Wessberg, 1993).

The reduction of Alpha power can enhance cognitive performance by increasing thalamus metabolic activity (Lindgren et al. 1999). In TBI patients, the reduction of Alpha band power was correlated with deficits in control of behaviour and increase lapses of attention (Richard A.P. Roche, et al., 2004, Paul M. Dockree, et al., 2004). In our study, lower Alpha band (8-10 Hz) power decreased from $5\times10^{-3}\pm4\times10^{-3}$ V^2/Hz before blast to $4.9\times10^{-4}\pm4\times10^{-4}$ V^2/Hz, $8.8\times10^{-4}\pm4\times10^{-4}$ V^2/Hz, $1.7\times10^{-4}\pm3\times10^{-5}$ V^2/Hz, $2.5\times10^{-4}\pm8\times10^{-5}$ V^2/Hz at 15 min, 2h, 1d, 2d after blast ($P<0.05$), respectively. The mTBI swine model have acute transient cortical dysfunction soon after blast. The mTBI swine model had acute transient cortical dysfunction after blast, which was result from disruption of cortical-cortical and cortical-thalamus network.

After voluntary movement and somatosensory stimulation, Beta band oscillations were induced in sensorimotor areas (Figure 4.6) (C. Neuper, et al., 2001). The Beta band oscillation was related to control submaximal muscle force (Halliday, et al., 1998; Kilner, et al., 2000). The decrease of Beta power was associated with movement preparation, execution and imagery (Kuhn et al. 2004). The Beta band power increased after execution of movement (Pfurtscheller and Lopes da Silva, 1999). Raised levels of Beta oscillations in basal ganglia thalamocortical networks are ‘anti-kinetic’ (Jenkinson and Brown, 2011). The Beta band activity of parkinson’s patients or dystonia increased in the basal ganglia thalamocortical circuits (Brown,

2007; Crowell et al., 2012). Beta band activity was associated with motor function. No significant changes of Beta band power was found in this study.

The Theta activity was generated in the deep structures of the brain with weak signal power (Blessing. 1997). The increase of hippocampal Theta band power has been associated with working memory, episodic memory, and encoding new information, especially spatial information (Figure 4.7) (Karrasch et al. 2004; Brian, et al., 2008). Compared with control animals, lateral fluid percussion TBI rats significantly decreased Theta band power in the ipsilateral hippocampus during the first 6 days after TBI (Figure 4.8). Theta band power increased above baseline levels during MSN (medial septal nucleus) stimulation in both TBI and sham animals (197.4 ±24.4% [n = 5] and 218.3±18.4% of baseline [n = 5]), respectively (Darrin J. Lee, et al., 2013). Moreover, Theta band activity at the frontal midline (fmθ) has been associated with focused attention, concentration, and creativity, and it may reflect the outcome of meditation (Missonnier et al., 2006). In the fronto-central midline region, older adults (68.4 year, range 60-80 years) had lower Theta activity than young people (21.9 years, range 18-27 years) in the resting state (Cummins et al. 2007). Theta band activity is associated with spatial navigation and memory functions. No significant changes of Theta band power was found in this study.

17% of TBI patients could develop paroxysmal Delta activity, and lasted for at least 1 day (Ronne-Engstrom E, et al., 2006). The blast related mTBI patients showed poor coordination of frontal neural function, which was resulted from damaged anterior white matter tracts (Scott R. Sponheim, et al., 2010). TBI patients generate

abnormal Delta waves originate from gray matter neurons that connect to white matter fiber with axonal injury. The axonal injury was result from tissue shearing and stretching (Ming-Xiong Huang et al., 2009). Despite the high correlations of the slow-wave generation characteristics in mild blast-induced and mild non-blast TBI (Figure 4.9). The percent-likelihood values in the mild non-blast TBI curve are significantly higher than the ones in the mild blast-induced TBI curve (Figure 4.10). The helmet and armor used by soldiers provides some protection against the over-pressure of blast (Ming-Xiong Huang, et al., 2014). (Evan Calabrese, 2014) quantified white matter injury of rat suffered repetitive blast exposure. Their results showed the microstructural significantly damaged after a second blast exposure (Figure 4.11). The diffuse axonal injury is most common at the frontotemporal corticomedullary junction, deep gray matter, corpus callosum, upper brainstem, and internal capsule (Figure 4.12) (Katherine H. Taber, 2006). Christine (2011) found traumatic axonal injury in soliders with blast-related mTBI were most common at the anterior limb of the internal capsule, uncinate fasciculus, and cingulum bundle. (Robert, et al., 2011) reported that blast exposure of rats cause acute and enduring axonal injury, especially at the brainstem and cerebellum. In our study, Delta band power have no statistical significance before and after blast ($P>0.05$). These results indicated that blast have restricted effect on the cortical-thalamic circuits.

Alpha to Delta ratio (ADR) was the ratio between Alpha band power and Delta band power. An increase in ADR was associated with brain activity switched from slow frequency to faster frequency. In the patient with mTBI, the Alpha-Delta ratio

immediately decreased after injury at the left and right hemisphere (Figure 4.13) (Jeremy J. Moeller, et al., 2011). In this study, Alpha-Delta power ratio (ADR) decreased 67% compared with pre-blast level at 15 minutes after blast, but not significant.

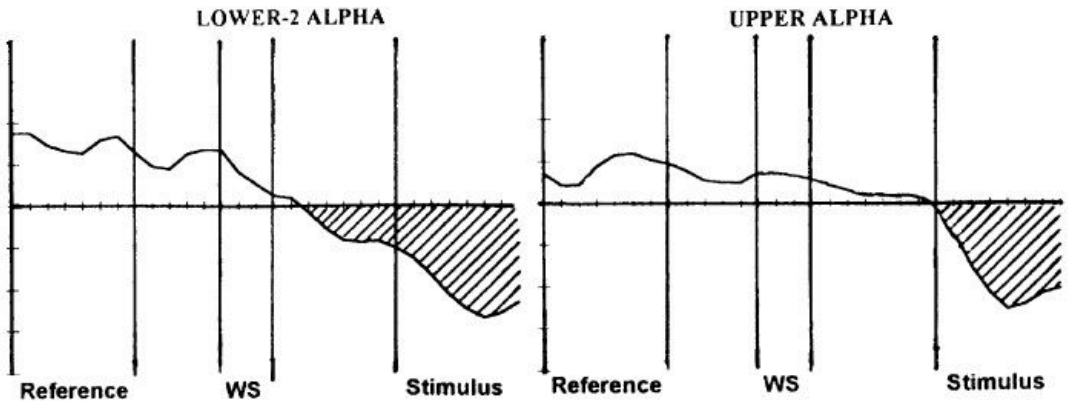

Figure 4.5: Lower-2 alpha band (8-10 Hz) reflects expectancy before the stimulus appear. The upper alpha band (10-13 Hz) reflects task performance (adopted from W. Klimesch, et al., 1998).

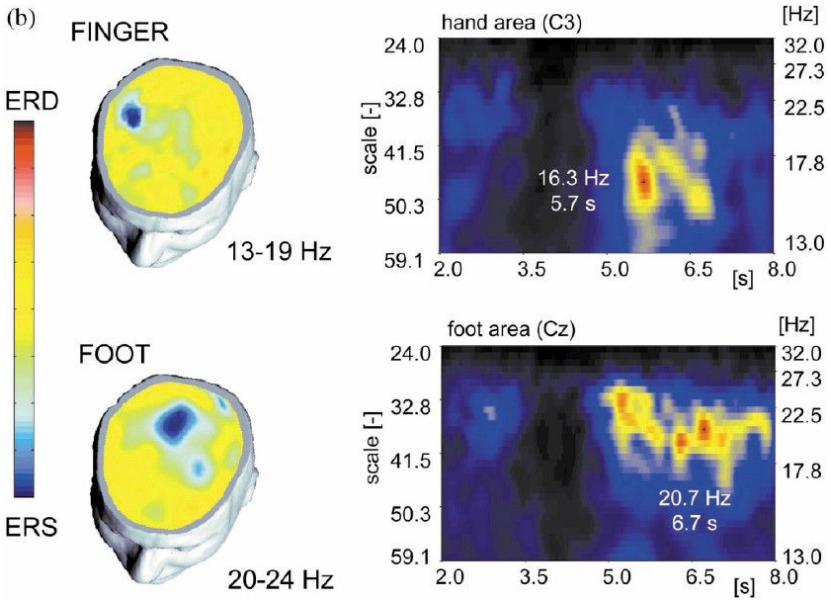

Figure 4.6: After onset of movement, Beta power decreased at the contralateral motorcortex and increased at the ispilateral motorcortex (adopted from C. Neuper, et al., 2001).

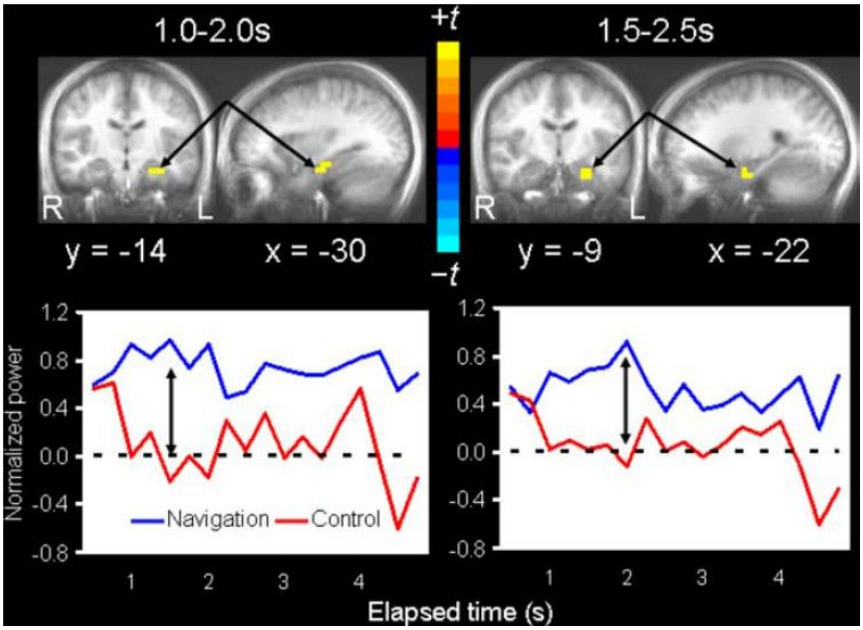

Figure 4.7: Theta peaked in the anterior portion of the left hippocampus 1-2 s after trial onset. Second, theta peaked slightly anterior and inferior to the left hippocampus,

in parahippocampal cortex, 1.5-2.5 s after trial onset. Theta power during goal-directed navigation were higher than theta power during aimless movements (adopted from Brian R. Cornwell, et al., 2008).

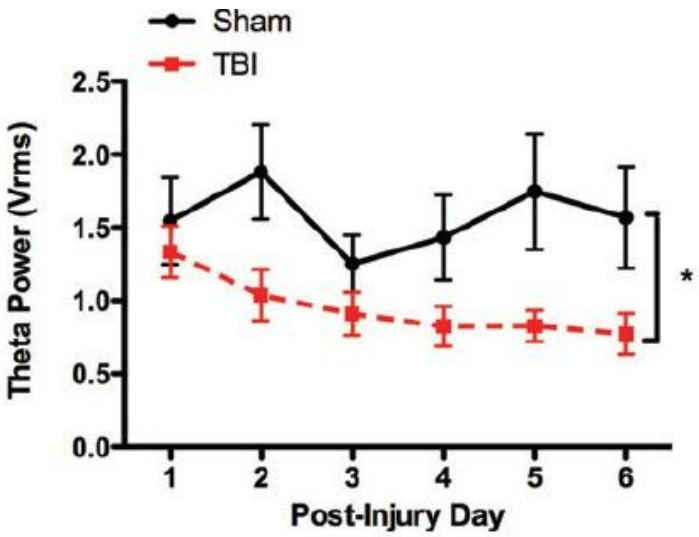

Figure 4.8: In the lateral fluid percussion of rats TBI model, hippocampal theta band power decreased during the first 6 days after injury (adopted from Darrin J Lee, et al., 2013).

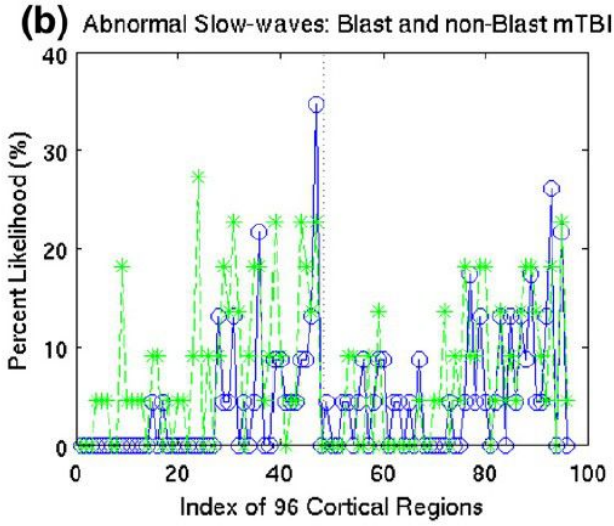

Figure 4.9: The percent of slow-wave generation for mild blast-induced (blue color) and non-blast (green color) TBI (adopted from Ming-Xiong Huang, et al., 2014)

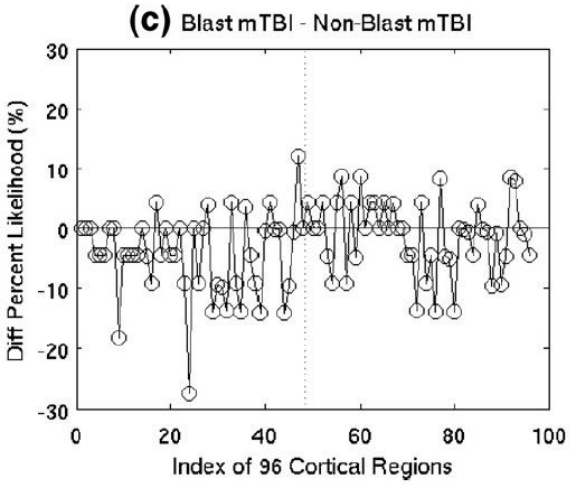

Figure 4.10: Blast-induced minus non-blast mTBI (adopted from Ming-Xiong Huang, et al., 2014)

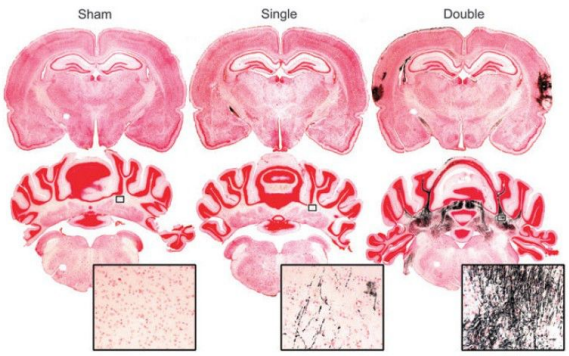

Figure 4.11: Silver degeneration-stained: sham control (left), single blast exposed (center) and double blast exposed (right) (adopted from Evan Calabrese, et al., 2014).

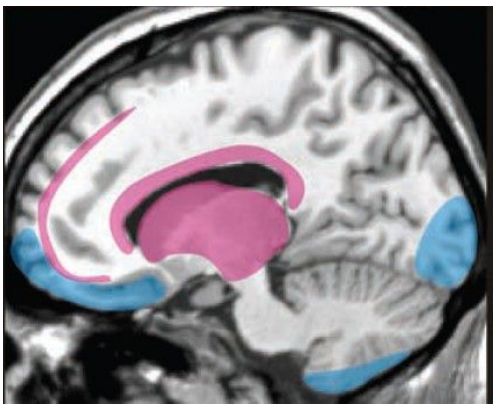

Figure 4.12: The most common locations for diffuse axonal injury (pink) (adopted from Katherine H. Taber, 2006).

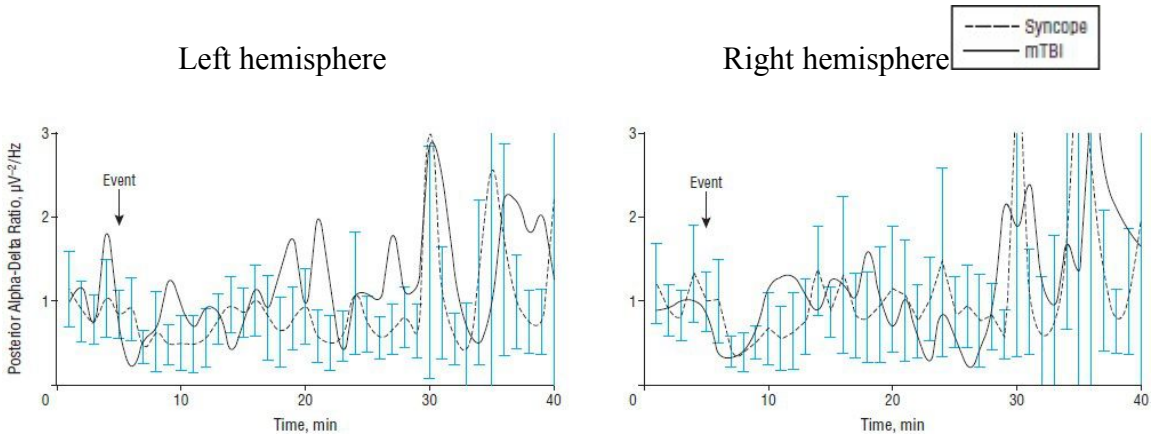

Figure 4.13: Alpha-Delta ratio decreased after injury at left and right hemisphere (Jeremy J. Moeller, et al., 2011).

4.3. Anesthesia effect

Propofol is an intravenous anesthetic medicine, which is used to induce a reversibly unconscious state. It is similar to Non-rapid eye movement (NREM) sleep (Shafer A., 1995). Compared to wakefulness subjects, scientists find the delta band and theta band increase power in the anterior regions and spread to posterior regions due to propofol-induced unconsciousness state (Michael Murphy et al., 2011; L. D. Gugino, et al., 2001). When increase the concentration of propofol during the infusion, the low frequency oscillation is progressively increase activity (Valerie Billard, et al., 1997). At cingulate gyrus and medial prefrontal cortex, the delta band, theta band and alpha band increase power after the subject lose conscious induced by propofol. The

loss of consciousness is resulted from suppression of corticocortical communication (Melanie Boly et al., 2012).

Ketamine is derived from phenylcyclohexylpiperidine (PCP), and mainly used as a sedative agent in animals (Sinner,B et al., 2008). Compared with placebo, ketamine significant decrease delta band oscillation (L Elliot Hong, et al., 2010). When the subjects are sedated by ketamine, the alpha band decrease power and the theta band increase power. When the ketamine and propofol are used together, the beta band significantly increase power (Ingo Bojak et al., 2013).

(Michael Murphy, 2011) studied EEG changes in humans during propofol anesthesia. The power of all frequency bands were increased after the loss of consciousness (Figure 4.14). (G. Plourde, et al., 1997) studied EEG changes in humans during ketamine anesthesia. The Theta band power was significantly increased, the Alpha band power was greatly decreased after loss consciousness (Figure 4.15). Mixure of porpofol and ketamine caused peak alpha wave shift to higher frequency. No significant change was found in delta band (Ingo Bojak, et al., 2013) (Figure 4.16). In our study, propofol was used for 3 hours of anesthesia in blast experiment, and ketamine was used for 24 hours, 48 hours, 72 hours anesthesia after blast. In our results, the Alpha band power was significantly decreased at acute and subacute phases after blast. The Beta band and Theta band power have no statistic significance after blast. Only Delta band power was greatly increased at acute phase after blast. These data suggest that changes of our QEEG reflect the further functional change caused by blast compared to anesthesia .

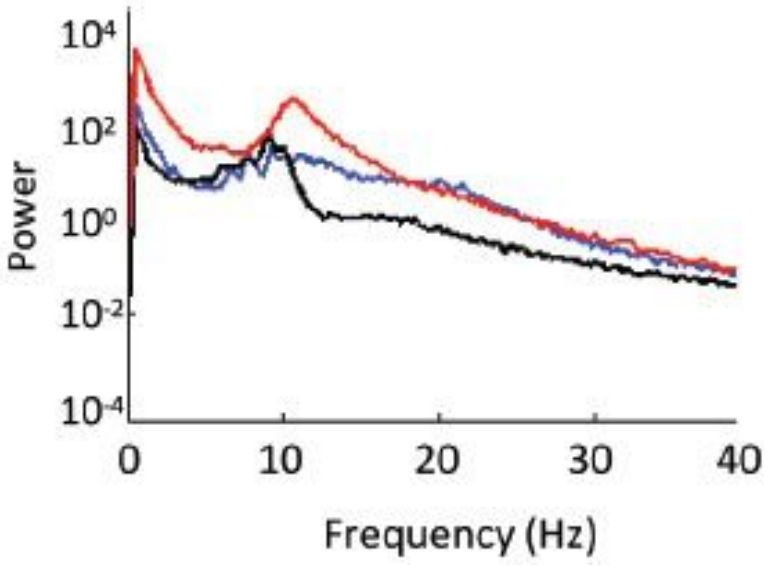

Figure 4.14: EEG recordings in humans during propofol anesthesia. A plot of power spectra from channel in waking (black), sedation (blue), and loss of consciousness (LOC) (adopted from Michael Murphy, et al., 2011)

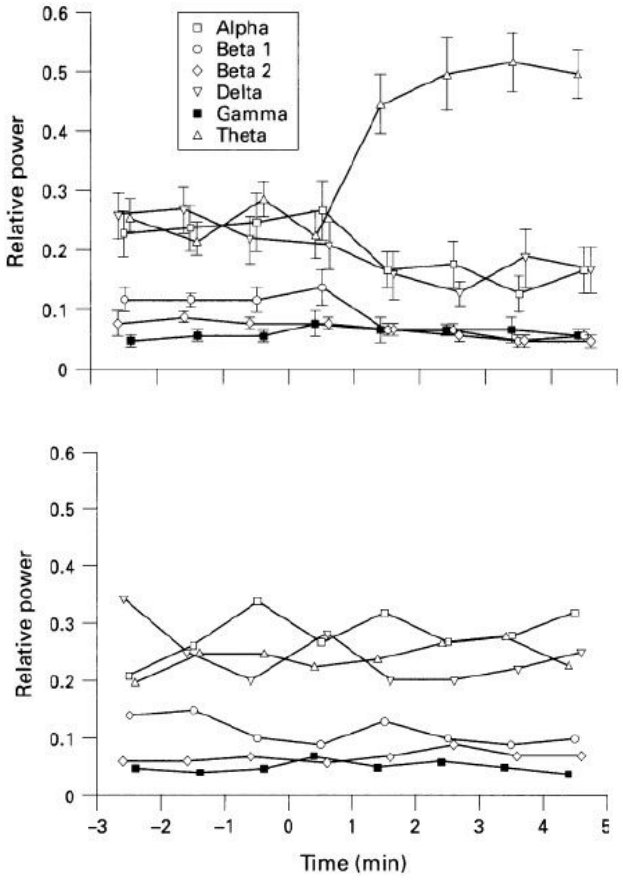

Figure 4.15: EEG recordings in humans during ketamine anesthesia. Ketamine was given at time 0. Top: result for patients. Bottom: result for controls (adopted from G. Plourde, et al., 1997)

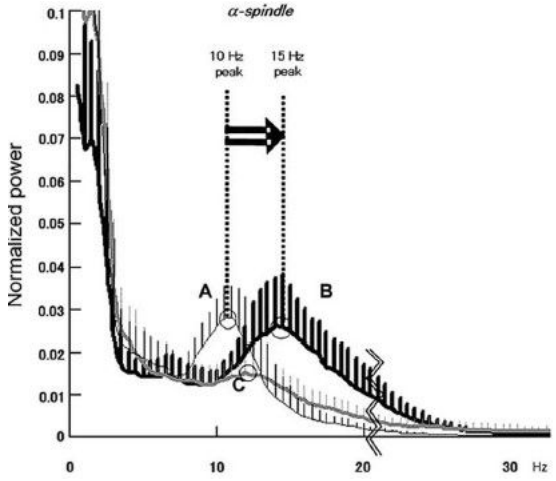

Figure 4.16: Compare to the control group, the peak alpha band activity is shifted to higher frequencies after ketamine combine propofol anesthesia (adopted from Ingo Bojak, et al., 2013)

4.4. Blast-related mTBI

4.4.1 Astrocyte proliferation

Astrocytes are characteristic star-shaped glial cells in the brain and spinal cord, and play a role in the repair and scarring process of the brain and spinal cord following traumatic injuries. Glial fibrillary acidic protein (GFAP) is the main intermediate filament protein in mature astrocytes, but also an important component of the cytoskeleton in astrocytes during development (J. Middeldorp E.M. Hol, 2011). Rats were subjected to head directed blast of 358 kPa for total 10 msec. CSF and

blood were collected at different times after blast. GFAP was significantly increased in the CSF and serum during 4-days and 24 hours after blast, respectively (Figure 4.17, 4.18) (Stanislav I. Svetlov, et al., 2010). (R. Hausmann et al., 2000) investigated astroglial GFAP expression following human brain injury. Compared to unaltered control tissue, GFAP immunoreactivity significantly increased numbers of GFAP positive astroglial cells adjacent to the cortical contusion from 1 day up to 4 weeks after brain injury (Figure 4.19).

In our GFAP study, swines were divided into sham group, medium blast group (300 kPa), high blast group (450 kPa). At 4 mm, 5mm, 6mm, front lobe of brain tissues were cut in to 40 μm thick frozen sections (Figure 4.20). The procedure for GFAP immunohistochemistry was adapted from previous reports (Alberto A,et al., 2002). The pictures were obtained from different regions of white matter under 10× digital microscope camera. Astrocyte cells were manually counted by a blinded observer using Image J software (Figure 4.21). At all blocks, the astrocytes proliferation of the medium and high blast group was much higher than the sham group ($P<0.01$), the high blast group was higher than the medium blast group ($P<0.05$) (Figure 4.22). These results may be result from CSF cavitation, because block 5 and block 6 were locate around the ventricular. Cavitation describes the process of vaporisation, bubble generation and bubble implosion. Cavitation will only occur if the local pressure declines to below the saturated vapor pressure of the liquid and subsequent recovery above the vapor pressure. The distribution of the relative increase in the peak brain strain due to cavitation for the 1000 kPa/4 ms blast

condition. The largest relative increases in brain tissue strain caused by CSF cavitation were in the periventricular tissues (Figure 4.23) (Matthew B. Panzer, et al., 2012). In this study, the EEG mean frequency, SEF 90 and Alpha band power significantly decreased ($P<0.05$) after blast at parietal recording site. These results indicated that the parietal regions have much seriously neuron injury than the front regions after blast.

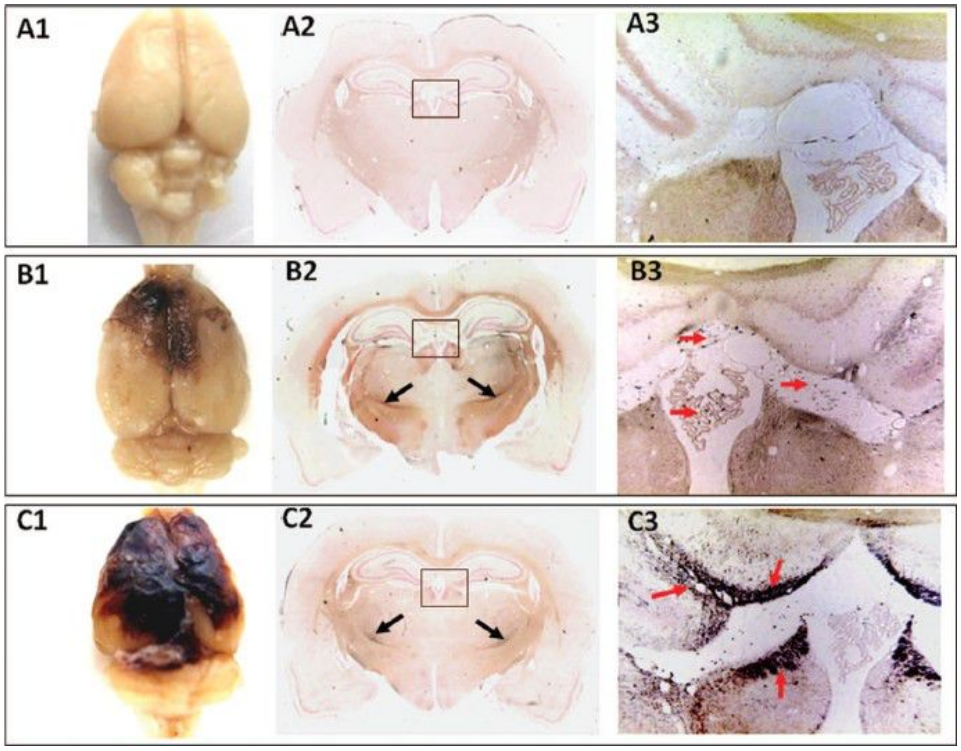

Figure 4.17: Rats brain anatomy at 48 hours and 5 days after blast (B and C), and sham (A). Gross pathology show: typical focal intracranial hematomas (B1, C1). Histopathology show: silver accumulation in nuclus subthalamicus (B2, C2). At higher magnification (10 ×) show: silver accumulation in perivascular and periventricular tissue zone (B3, C3) (adopted from Stanislav I. Svetlov, et al., 2010).

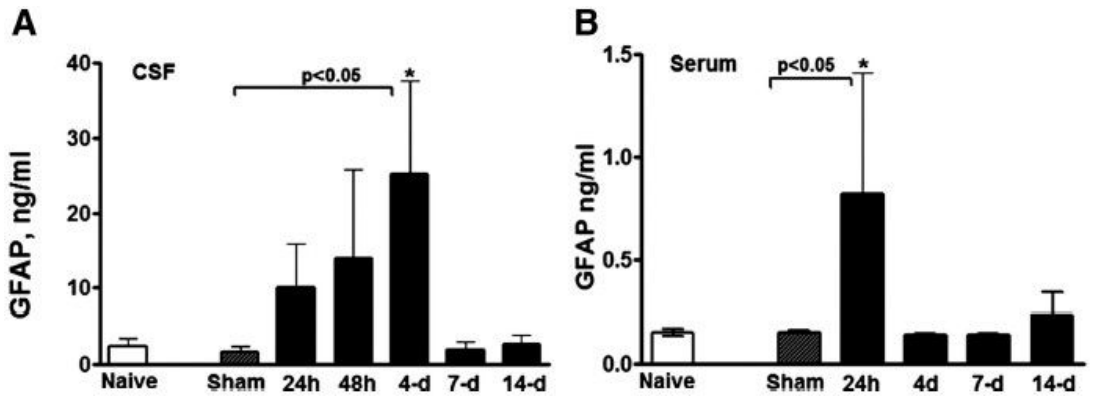

Figure 4.18: GFAP was significantly increased in the CSF and serum during 4-days and 24 hours after blast, respectively (adopted from Stanislav I. Svetlov, et al., 2010).

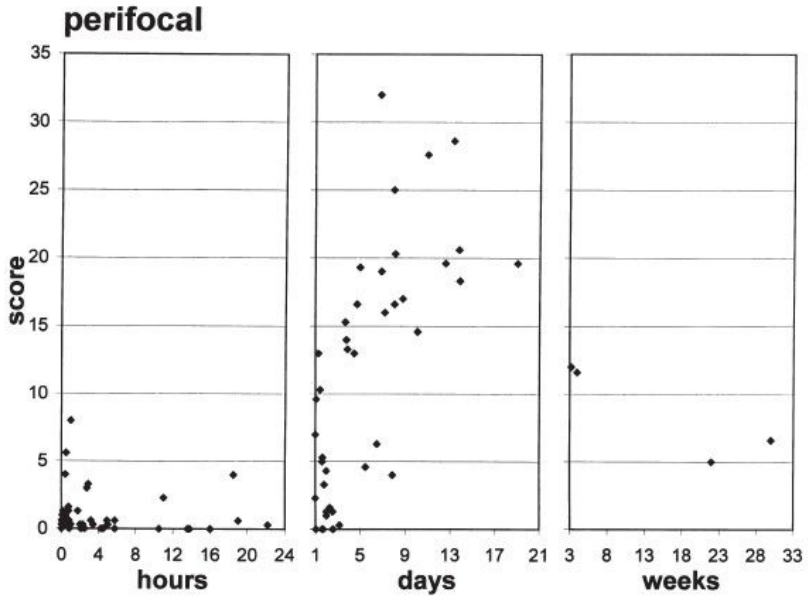

Figure 4.19: GFAP positive astroglial cells could be detected adjacent to the cortical contusion from 1 day up to 4 weeks after brain injury (adopted from R. Hausmann et al., 2000).

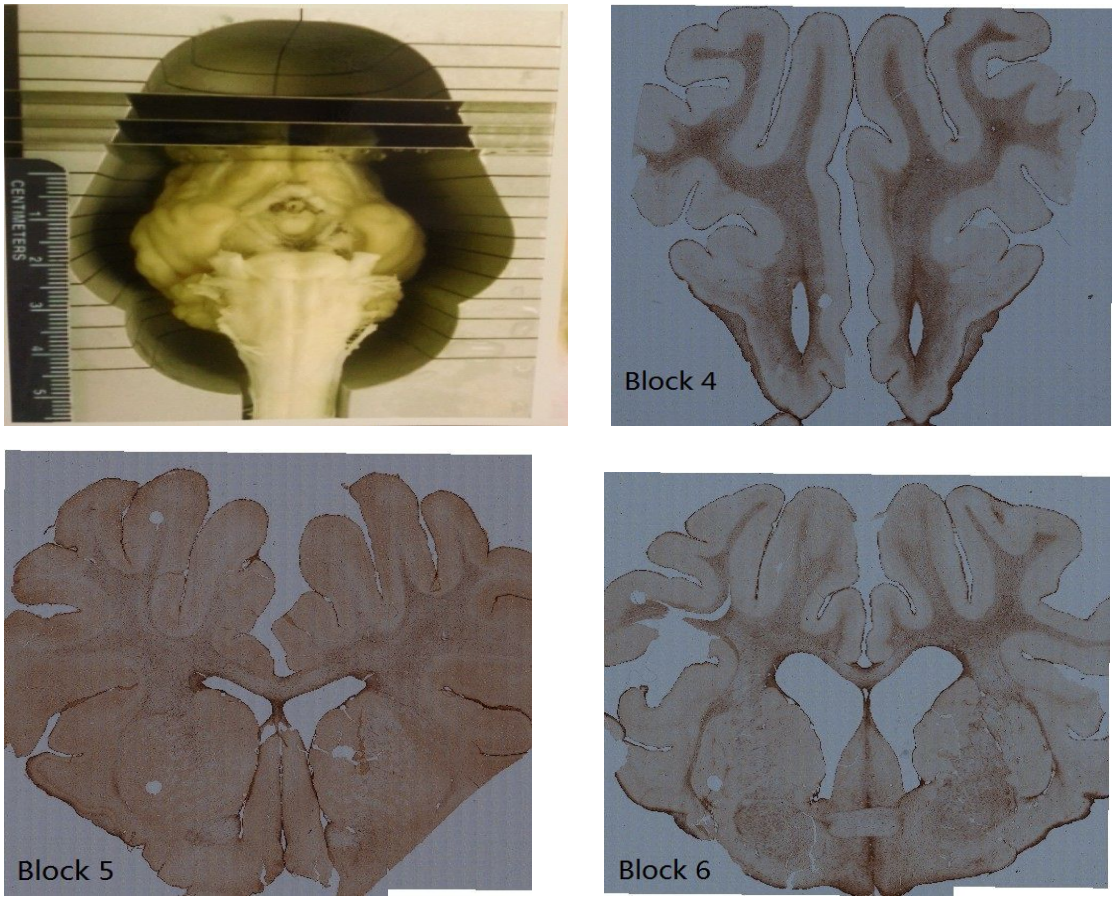

Figure 4.20: At 4 mm, 5mm, 6mm blocks of front lobe of brain tissues were cut in to 40 µm thick frozen sections.

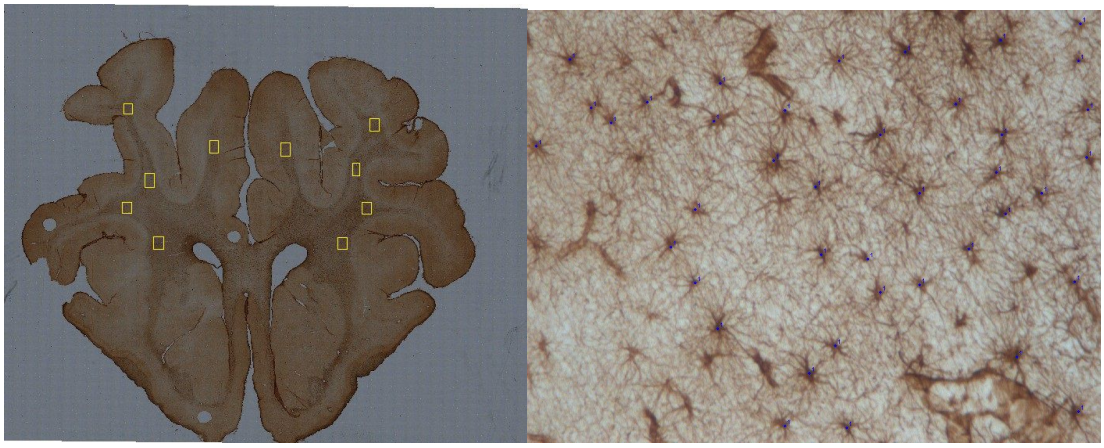

Figure 4.21: The pictures were obtained from different regions of white matter under 10×digital microscope camera. Astrocyte cells were manually counted by a blinded observer using Image J software.

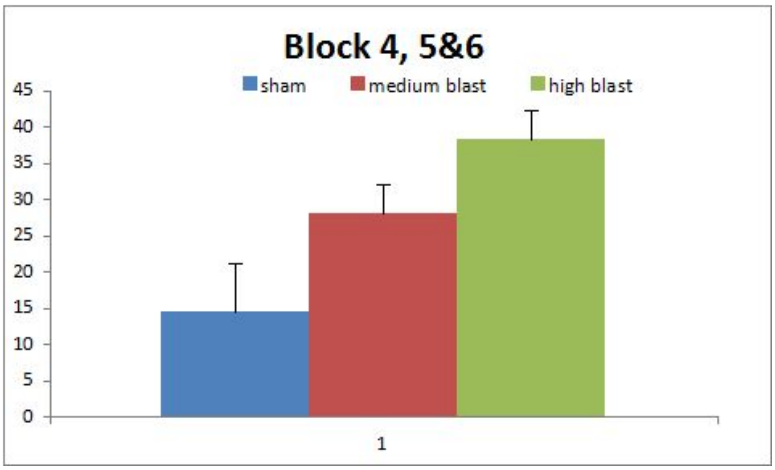

Figure 4.22: At all blocks, the astrocytes proliferation of the medium and high blast group was much higher than the sham group ($P<0.01$), the high blast group was higher than the medium blast group ($P<0.05$).

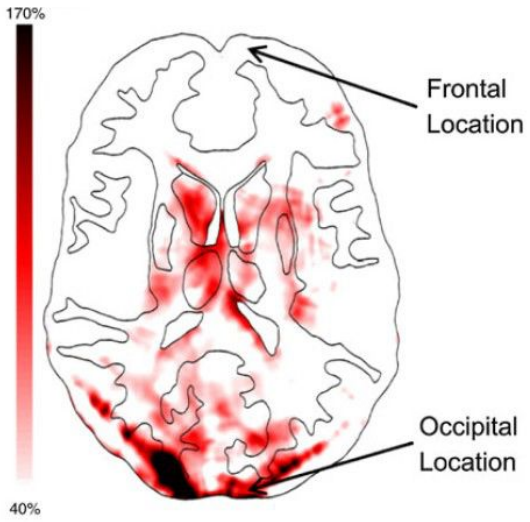

Figure 4.23: The largest relative increases in brain tissue strain caused by CSF cavitation were in the occipital region of the brain, and in the periventricular tissues (adopted from Matthew B. Panzer, et al., 2012).

4.4.2 Ripple effect

Recently, ripple mechanism had been proposed to explain the blast-induced vascular changes. When the blast wave strike the body, the kinetic energy would transfer to the brain through the main blood vessels (Figure 4.24). The energy could damage axonal fibers and neurons close to cerebral vessels (Ibolja cernak., 2008). The diameter of swine ascending pharyngeal (AP) artery was instantaneously reduced after blast. The diameter of the common carotid (CC) and the auricular artery also became narrowed (Figure 4.25) (Richard A. Bauman et al., 2009). Cynthia Bira et al. (2012) examined rats exposed with pressures from 90 to 193 kPa by function MRI (fMRI). The CBF of hippocampus, auditory cortex and thalamus were instantaneously decreased after blast (Figure 4.26). The hippocampus was the area of the brain involved in long-term memory and spatial navigation. (Patrick W et al., 2011) used high-velocity stretching of arterial lamellae to simulate blast wave impact on the vasculature. An hour after stretching, the injured tissues were hypersensitivity to contract by endothelin-1. One day after injury, the tissues showed prolonged hyper-contraction based on the blast force. In this study, the ripple effect may explain the change of the EEG frequency and power soon after blast.

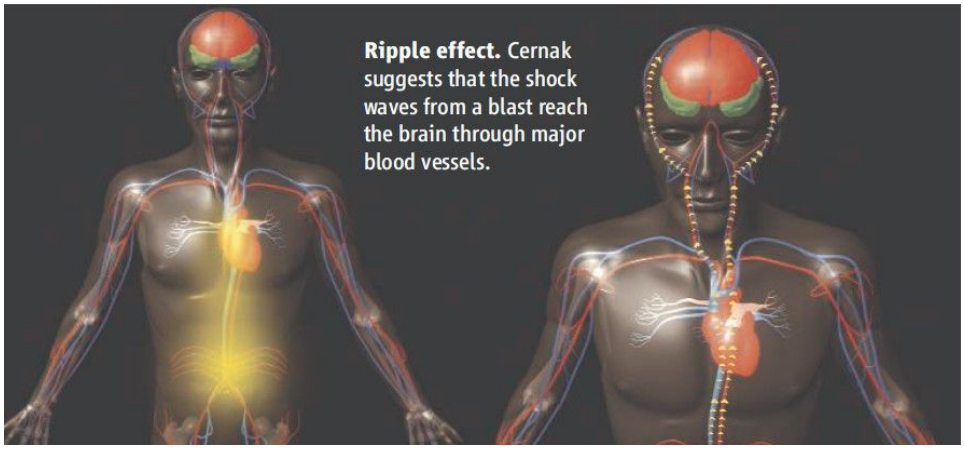

Figure 4.24: Ripple effect: blast wave reach the brain through major blood vessels (adopted from Ibolja cernak., 2008)

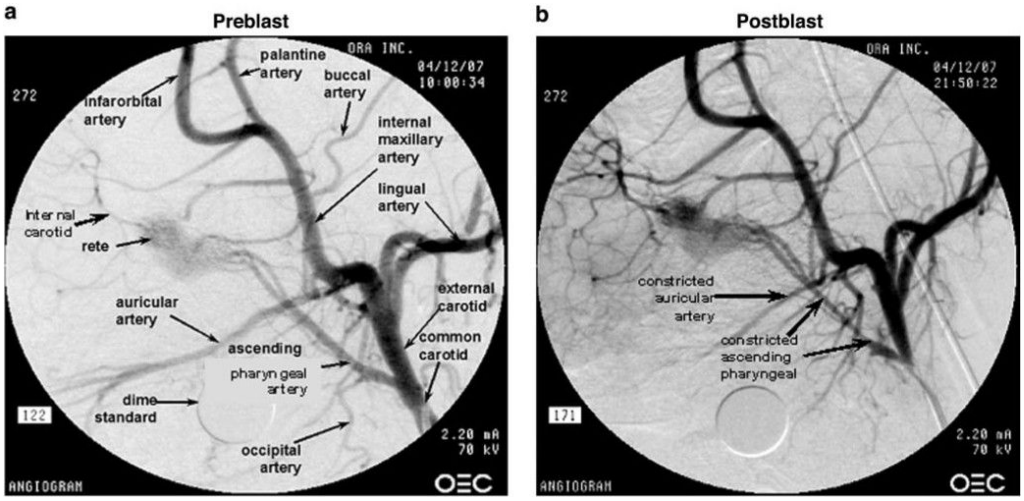

Figure 4.25: Blood vessel angiogram before and after blast. The diameter of swine ascending pharyngeal (AP) artery was instantaneously reduced after blast. The diameter of the common carotid (CC) and the auricular artery also became narrowed (adopted from Richard A. Bauman, et al., 2009).

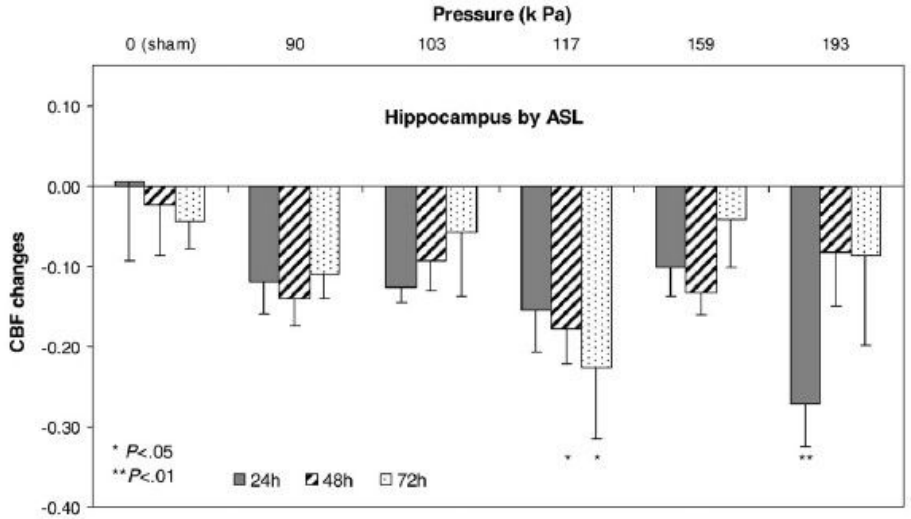
Pressure (k Pa)
0 (sham)
90
103
117
159
193
Hippocampus by ASL
CBF changes
0.10
0.00
-0.10
-0.20
-0.30
-0.40
* P<.05
**P<.01
24h
48h
72h

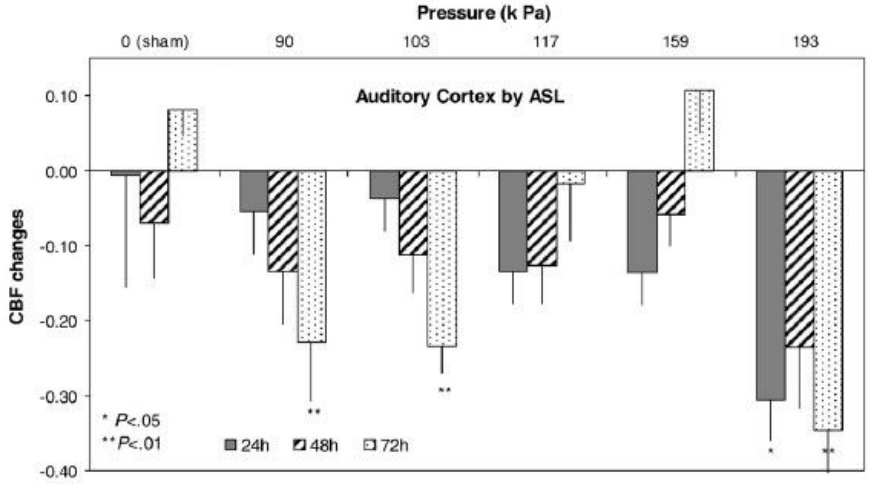
Pressure (k Pa)
0 (sham)
90
103
117
159
193
Auditory Cortex by ASL
CBF changes
0.10
0.00
-0.10
-0.20
-0.30
-0.40
* P<.05
**P<.01
24h
48h
72h

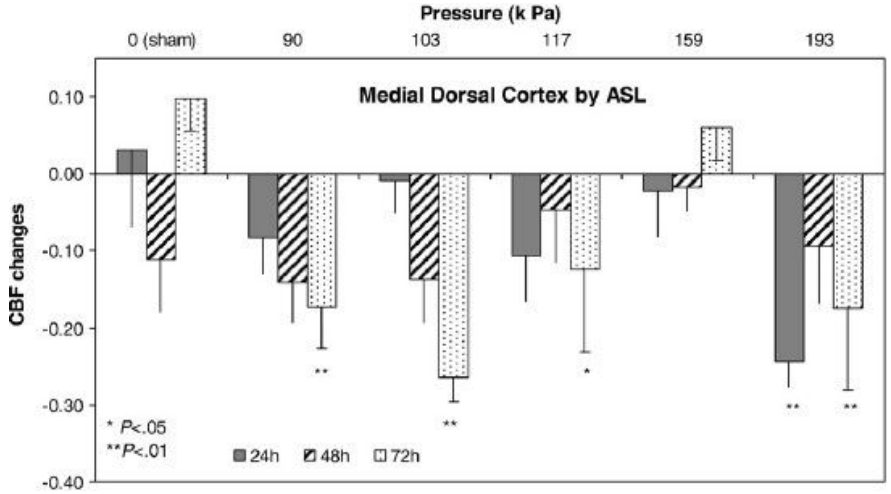
Pressure (k Pa)
0 (sham)
90
103
117
159
193
Medial Dorsal Cortex by ASL
CBF changes
0.10
0.00
-0.10
-0.20
-0.30
-0.40
* P<.05
**P<.01
24h
48h
72h

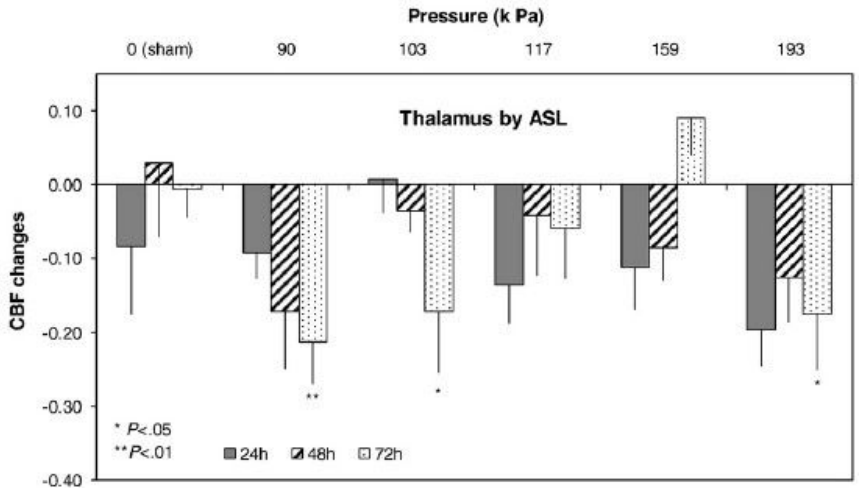

Figure 4.26: RCBF changes between pre- and post blast at the hippocampus, auditory cortex, medial dorsal cortex and thalamus vs. Various pressure (adopted from Cynthia Bir et al., 2012)

4.5. Limitation of experiment

In our experiment, we only have six swines in blast group and no sham group, because every swine should cost $10,000. We need more funds to support our future works.

4.6. Future work

In collaboration with ECE Department, we can consider using microelectrode EEG arrays in deep brain, which may directly record neuronal activity related to functional outcomes after blast.

APPENDIX：STATISTIC ANALYSIS RESULTS

Overall Mean Frequency

Multiple Comparisons

Overall Mean Frequency

LSD

(I) Time	(J) Time	Mean Difference (I-J)	Std. Error	Sig.	95% Confidence Interval	
					Lower Bound	Upper Bound
Pre-	Post- 15min	2.42918869*	.427213774	.000	1.59043929	3.26793809
	Post-30min	.26714961	.427213774	.532	-.57159979	1.10589901
	Post-2hrs	.86322694*	.427213774	.044	.02447754	1.70197634
	Post-24htrs	1.69709695*	.446210234	.000	.82105177	2.57314213
	Post-48hrs	2.45549877*	.427213774	.000	1.61674937	3.29424818
	Post-72hrs	.98367048	.515239198	.057	-.02789936	1.99524032
Post- 15min	Pre-	-2.42918869*	.427213774	.000	-3.26793809	-1.59043929
	Post-30min	-2.16203908*	.407332351	.000	-2.96175526	-1.36232291
	Post-2hrs	-1.56596175*	.407332351	.000	-2.36567793	-.76624557

	Post-24hrs	-.73209174	.427213774	.087	-1.57084114	.10665766
	Post-48hrs	.02631008	.407332351	.949	-.77340609	.82602626
	Post-72hrs	-1.44551821*	.498878208	.004	-2.42496649	-.46606992
Post-30min	Pre-	-.26714961	.427213774	.532	-1.10589901	.57159979
	Post-15min	2.16203908*	.407332351	.000	1.36232291	2.96175526
	Post-2hrs	.59607733	.407332351	.144	-.20363884	1.39579351
	Post-24hrs	1.42994734*	.427213774	.001	.59119794	2.26869674
	Post-48hrs	2.18834917*	.407332351	.000	1.38863299	2.98806534
	Post-72hrs	.71652087	.498878208	.151	-.26292741	1.69596916
Post-2hrs	Pre-	-.86322694*	.427213774	.044	-1.70197634	-.02447754
	Post-15min	1.56596175*	.407332351	.000	.76624557	2.36567793
	Post-30min	-.59607733	.407332351	.144	-1.39579351	.20363884
	Post-24hrs	.83387001	.427213774	.051	-.00487939	1.67261941
	Post-48hrs	1.59227183*	.407332351	.000	.79255566	2.39198801
	Post-72hrs	.12044354	.498878208	.809	-.85900474	1.09989183

Post-24htrs	Pre-	-1.69709695*	.446210234	.000	-2.57314213	-.82105177
	Post-15min	.73209174	.427213774	.087	-.10665766	1.57084114
	Post-30 min	-1.42994734*	.427213774	.001	-2.26869674	-.59119794
	Post-2hrs	-.83387001	.427213774	.051	-1.67261941	.00487939
	Post-48hrs	.75840183	.427213774	.076	-.08034758	1.59715123
	Post-72hrs	-.71342647	.515239198	.167	-1.72499631	.29814337
Post-48hrs	Pre-	-2.45549877*	.427213774	.000	-3.29424818	-1.61674937
	Post-15min	-.02631008	.407332351	.949	-.82602626	.77340609
	Post-30 min	-2.18834917*	.407332351	.000	-2.98806534	-1.38863299
	Post-2hrs	-1.59227183*	.407332351	.000	-2.39198801	-.79255566
	Post-24htrs	-.75840183	.427213774	.076	-1.59715123	.08034758
	Post-72hrs	-1.47182829*	.498878208	.003	-2.45127658	-.49238001
Post-72hrs	Pre-	-.98367048	.515239198	.057	-1.99524032	.02789936
	Post-15min	1.44551821*	.498878208	.004	.46606992	2.42496649
	Post-30 min	-.71652087	.498878208	.151	-1.69596916	.26292741

	Post-2hrs	-.12044354	.498878208	.809	-1.09989183	.85900474
	Post-24htrs	.71342647	.515239198	.167	-.29814337	1.72499631
	Post-48hrs	1.47182829*	.498878208	.003	.49238001	2.45127658

Based on observed means.

The error term is Mean Square(Error) = 9.955.

*. The mean difference is significant at the .05 level.

Overall Spectral Edge Frequency fc=90% (SEF-90)

Multiple Comparisons

SEF90

LSD

(I) Time	(J) Time				95% Confidence Interval	
		Mean Difference (I-J)	Std. Error	Sig.	Lower Bound	Upper Bound
Pre-	Post- 15min	7.800761754*	2.037640719	.000	3.77172754	11.82979597
	Post-30min	3.544507320	2.037640719	.084	-.48452689	7.57354153
	Post-3hrs	2.611052825	2.017799538	.198	-1.37874935	6.60085500
	Post-24htrs	5.093713924*	2.135073371	.018	.87202579	9.31540206

	Post-48hrs	7.487919867*	2.017799538	.000	3.49811769	11.47772204
	Post-72hrs	4.262978450	2.433557807	.082	-.54890402	9.07486092
Post- 15min	Pre-	-7.800761754E0	2.037640719	.000	-11.82979597	-3.77172754
	Post-30min	-4.256254435E0	1.965275222	.032	-8.14220009	-.37030878
	Post-3hrs	-5.189708929E0	1.944695856	.009	-9.03496293	-1.34445492
	Post-24htrs	-2.707047831	2.066123253	.192	-6.79240066	1.37830500
	Post-48hrs	-.312841888	1.944695856	.872	-4.15809589	3.53241212
	Post-72hrs	-3.537783304	2.373295304	.138	-8.23050851	1.15494191
Post-30min	Pre-	-3.544507320	2.037640719	.084	-7.57354153	.48452689
	Post- 15min	4.256254435*	1.965275222	.032	.37030878	8.14220009
	Post-3hrs	-.933454495	1.944695856	.632	-4.77870850	2.91179951
	Post-24htrs	1.549206604	2.066123253	.455	-2.53614622	5.63455943
	Post-48hrs	3.943412547*	1.944695856	.045	.09815854	7.78866655
	Post-72hrs	.718471130	2.373295304	.763	-3.97425408	5.41119634
Post-3hrs	Pre-	-2.611052825	2.017799538	.198	-6.60085500	1.37874935

	Post- 15min	5.189708929*	1.944695856	.009	1.34445492	9.03496293
	Post-30min	.933454495	1.944695856	.632	-2.91179951	4.77870850
	Post-24htrs	2.482661099	2.046558226	.227	-1.56400573	6.52932793
	Post-48hrs	4.876867042*	1.923896372	.012	1.07273993	8.68099415
	Post-72hrs	1.651925625	2.356282215	.484	-3.00715954	6.31101079
Post-24htrs	Pre-	-5.093713924E0	2.135073371	.018	-9.31540206	-.87202579
	Post- 15min	2.707047831	2.066123253	.192	-1.37830500	6.79240066
	Post-30min	-1.549206604	2.066123253	.455	-5.63455943	2.53614622
	Post-3hrs	-2.482661099	2.046558226	.227	-6.52932793	1.56400573
	Post-48hrs	2.394205943	2.046558226	.244	-1.65246089	6.44087277
	Post-72hrs	-.830735474	2.457455839	.736	-5.68987161	4.02840066
Post-48hrs	Pre-	-7.487919867E0	2.017799538	.000	-11.47772204	-3.49811769
	Post- 15min	.312841888	1.944695856	.872	-3.53241212	4.15809589
	Post-30min	-3.943412547E0	1.944695856	.045	-7.78866655	-.09815854
	Post-3hrs	-4.876867042E0	1.923896372	.012	-8.68099415	-1.07273993

	Post-24htrs	-2.394205943	2.046558226	.244	-6.440872 77	1.652460 89
	Post-72hrs	-3.224941417	2.356282215	.173	-7.884026 59	1.434143 75
Post-72hrs	Pre-	-4.262978450	2.433557807	.082	-9.074860 92	.5489040 2
	Post- 15min	3.537783304	2.373295304	.138	-1.154941 91	8.230508 51
	Post-30min	-.718471130	2.373295304	.763	-5.411196 34	3.974254 08
	Post-3hrs	-1.651925625	2.356282215	.484	-6.311010 79	3.007159 54
	Post-24htrs	.830735474	2.457455839	.736	-4.028400 66	5.689871 61
	Post-48hrs	3.224941417	2.356282215	.173	-1.434143 75	7.884026 59

*. The mean difference is significant at the 0.05 level.

Lower Alpha Band Power

Multiple Comparisons

A1Power

LSD

					95% Confidence Interval	
(I) Time	(J) Time	Mean Difference (I-J)	Std. Error	Sig.	Lower Bound	Upper Bound

Pre-	Post- 15min	.001836457*	.000917540	.048	.00001899	.00365393
	Post-30min	.001692235	.000872535	.055	-.00003609	.00342056
	Post-2hrs	.002313873*	.000984113	.020	.00036453	.00426321
	Post-24htrs	.001631837	.000917540	.078	-.00018563	.00344931
	Post-48hrs	.002339327*	.000917540	.012	.00052186	.00415680
	Post-72hrs	.002161372*	.001031226	.038	.00011871	.00420403
Post- 15min	Pre-	-.001836457*	.000917540	.048	-.00365393	-.00001899
	Post-30min	-.000144221	.000897567	.873	-.00192213	.00163369
	Post-2hrs	.000477416	.001006373	.636	-.00151602	.00247085
	Post-24htrs	-.000204619	.000941376	.828	-.00206930	.00166007
	Post-48hrs	.000502870	.000941376	.594	-.00136182	.00236755
	Post-72hrs	.000324915	.001052491	.758	-.00175987	.00240970
Post-30min	Pre-	-.001692235	.000872535	.055	-.00342056	.00003609
	Post- 15min	.000144221	.000897567	.873	-.00163369	.00192213
	Post-2hrs	.000621637	.000965518	.521	-.00129087	.00253414
	Post-24htrs	-.000060398	.000897567	.946	-.00183831	.00171751

	Post-48hrs	.000647091	.000897567	.472	-.0011308 2	.00242500
	Post-72hrs	.000469136	.001013496	.644	-.0015384 0	.00247668
Post-2hrs	Pre-	-.002313873*	.000984113	.020	-.0042632 1	-.0003645 3
	Post- 15min	-.000477416	.001006373	.636	-.0024708 5	.00151602
	Post-30min	-.000621637	.000965518	.521	-.0025341 4	.00129087
	Post-24htrs	-.000682036	.001006373	.499	-.0026754 7	.00131140
	Post-48hrs	.000025454	.001006373	.980	-.0019679 8	.00201889
	Post-72hrs	-.000152501	.001111006	.891	-.0023531 9	.00204819
Post-24htrs	Pre-	-.001631837	.000917540	.078	-.0034493 1	.00018563
	Post- 15min	.000204619	.000941376	.828	-.0016600 7	.00206930
	Post-30min	.000060398	.000897567	.946	-.0017175 1	.00183831
	Post-2hrs	.000682036	.001006373	.499	-.0013114 0	.00267547
	Post-48hrs	.000707489	.000941376	.454	-.0011572 0	.00257217
	Post-72hrs	.000529535	.001052491	.616	-.0015552 5	.00261432
Post-48hrs	Pre-	-.002339327*	.000917540	.012	-.0041568 0	-.0005218 6

	Post- 15min	-.000502870	.000941376	.594	-.0023675	.00136182
					5	
	Post-30min	-.000647091	.000897567	.472	-.0024250	.00113082
					0	
	Post-2hrs	-.000025454	.001006373	.980	-.0020188	.00196798
					9	
	Post-24htrs	-.000707489	.000941376	.454	-.0025721	.00115720
					7	
	Post-72hrs	-.000177955	.001052491	.866	-.0022627	.00190683
					4	
Post-72hrs	Pre-	-.002161372*	.001031226	.038	-.0042040	-.0001187
					3	1
	Post- 15min	-.000324915	.001052491	.758	-.0024097	.00175987
					0	
	Post-30min	-.000469136	.001013496	.644	-.0024766	.00153840
					8	
	Post-2hrs	.000152501	.001111006	.891	-.0020481	.00235319
					9	
	Post-24htrs	-.000529535	.001052491	.616	-.0026143	.00155525
					2	
	Post-48hrs	.000177955	.001052491	.866	-.0019068	.00226274
					3	

*. The mean difference is significant at the 0.05 level.

Beta Band Power

Multiple Comparisons

Beta Power

LSD

(I) Time	(J) Time				95% Confidence Interval	
		Mean Difference (I-J)	Std. Error	Sig.	Lower Bound	Upper Bound
Pre-	Post- 15min	-5.00763107894 74E-7	1.01453651 64838E-6	.622	-2.5094748 03947E-6	1.50794858 8157E-6
	Post-30min	-1.08444965789 47E-6	1.01453651 64838E-6	.287	-3.0931613 53947E-6	9.24262038 1574E-7
	Post-2hrs	-1.48548685789 47E-6	1.01453651 64838E-6	.146	-3.4941985 53947E-6	5.23224838 1574E-7
	Post-24htrs	3.729495479876 2E-7	1.05724871 83391E-6	.725	-1.7203293 35186E-6	2.46622843 1161E-6
	Post-48hrs	3.862480000000 0E-7	1.02746106 95870E-6	.708	-1.6480534 11713E-6	2.42054941 1713E-6
	Post-72hrs	4.296265087719 3E-7	1.16772506 28006E-6	.714	-1.8823878 47843E-6	2.74164086 5387E-6
Post- 15min	Pre-	5.007631078947 4E-7	1.01453651 64838E-6	.622	-1.5079485 88157E-6	2.50947480 3947E-6
	Post-30min	-5.83686550000 00E-7	1.00144517 42562E-6	.561	-2.5664782 99533E-6	1.39910519 9533E-6
	Post-2hrs	-9.84723750000 00E-7	1.00144517 42562E-6	.327	-2.9675154 99533E-6	9.98067999 5325E-7
	Post-24htrs	8.737126558823 5E-7	1.04469275 20529E-6	.405	-1.1947062 87876E-6	2.94213159 9641E-6
	Post-48hrs	8.870111078947 4E-7	1.01453651 64838E-6	.384	-1.1217005 88157E-6	2.89572280 3947E-6
	Post-72hrs	9.303896166666 7E-7	1.15636928 18710E-6	.423	-1.3591410 84012E-6	3.21992031 7346E-6
Post-30min	Pre-	1.084449657894 7E-6	1.01453651 64838E-6	.287	-9.2426203 81574E-7	3.09316135 3947E-6

	Post- 15min	5.836865500000 0E-7	1.00144517 42562E-6	.561	-1.3991051 99533E-6	2.56647829 9533E-6
	Post-2hrs	-4.01037200000 00E-7	1.00144517 42562E-6	.690	-2.3838289 49533E-6	1.58175454 9533E-6
	Post-24htrs	1.457399205882 4E-6	1.04469275 20529E-6	.166	-6.1101973 78759E-7	3.52581814 9641E-6
	Post-48hrs	1.470697657894 7E-6	1.01453651 64838E-6	.150	-5.3801403 81574E-7	3.47940935 3947E-6
	Post-72hrs	1.514076166666 7E-6	1.15636928 18710E-6	.193	-7.7545453 40125E-7	3.80360686 7346E-6
Post-2hrs	Pre-	1.485486857894 7E-6	1.01453651 64838E-6	.146	-5.2322483 81574E-7	3.49419855 3947E-6
	Post- 15min	9.847237500000 0E-7	1.00144517 42562E-6	.327	-9.9806799 95325E-7	2.96751549 9533E-6
	Post-30min	4.010372000000 0E-7	1.00144517 42562E-6	.690	-1.5817545 49533E-6	2.38382894 9533E-6
	Post-24htrs	1.858436405882 4E-6	1.04469275 20529E-6	.078	-2.0998253 78759E-7	3.92685534 9641E-6
	Post-48hrs	1.871734857894 7E-6	1.01453651 64838E-6	.068	-1.3697683 81574E-7	3.88044655 3947E-6
	Post-72hrs	1.915113366666 7E-6	1.15636928 18710E-6	.100	-3.7441733 40125E-7	4.20464406 7346E-6
Post-24htrs	Pre-	-3.72949547987 62E-7	1.05724871 83391E-6	.725	-2.4662284 31161E-6	1.72032933 5186E-6
	Post- 15min	-8.73712655882 35E-7	1.04469275 20529E-6	.405	-2.9421315 99641E-6	1.19470628 7876E-6
	Post-30min	-1.45739920588 24E-6	1.04469275 20529E-6	.166	-3.5258181 49641E-6	6.11019737 8759E-7
	Post-2hrs	-1.85843640588 24E-6	1.04469275 20529E-6	.078	-3.9268553 49641E-6	2.09982537 8759E-7

	Post-48hrs	1.329845201238 4E-8	1.05724871 83391E-6	.990	-2.0799804 31161E-6	2.10657733 5186E-6
	Post-72hrs	5.667696078431 4E-8	1.19401860 33749E-6	.962	-2.3073967 76271E-6	2.42075069 7840E-6
Post-48hrs	Pre-	-3.86248000000 00E-7	1.02746106 95870E-6	.708	-2.4205494 11713E-6	1.64805341 1713E-6
	Post- 15min	-8.87011107894 74E-7	1.01453651 64838E-6	.384	-2.8957228 03947E-6	1.12170058 8157E-6
	Post-30min	-1.47069765789 47E-6	1.01453651 64838E-6	.150	-3.4794093 53947E-6	5.38014038 1574E-7
	Post-2hrs	-1.87173485789 47E-6	1.01453651 64838E-6	.068	-3.8804465 53947E-6	1.36976838 1574E-7
	Post-24htrs	-1.32984520123 84E-8	1.05724871 83391E-6	.990	-2.1065773 35186E-6	2.07998043 1161E-6
	Post-72hrs	4.337850877193 0E-8	1.16772506 28006E-6	.970	-2.2686358 47843E-6	2.35539286 5387E-6
Post-72hrs	Pre-	-4.29626508771 93E-7	1.16772506 28006E-6	.714	-2.7416408 65387E-6	1.88238784 7843E-6
	Post- 15min	-9.30389616666 67E-7	1.15636928 18710E-6	.423	-3.2199203 17346E-6	1.35914108 4012E-6
	Post-30min	-1.51407616666 67E-6	1.15636928 18710E-6	.193	-3.8036068 67346E-6	7.75454534 0125E-7
	Post-2hrs	-1.91511336666 67E-6	1.15636928 18710E-6	.100	-4.2046440 67346E-6	3.74417334 0125E-7
	Post-24htrs	-5.66769607843 14E-8	1.19401860 33749E-6	.962	-2.4207506 97840E-6	2.30739677 6271E-6
	Post-48hrs	-4.33785087719 30E-8	1.16772506 28006E-6	.970	-2.3553928 65387E-6	2.26863584 7843E-6

Based on observed means.

The error term is Mean Square(Error) = 3.19E-011.

Theta Band Power

Multiple Comparisons

Theta Power

LSD

(I) Time	(J) Time				95% Confidence Interval	
		Mean Difference (I-J)	Std. Error	Sig.	Lower Bound	Upper Bound
Pre-	Post- 15min	-4.3579398007246E-6	3.0321131590069E-6	.153	-1.0352219781878187E-5	1.6363401804170417E-6
	Post-30min	-1.4847798007246E-6	3.0321131590069E-6	.625	-7.4790597818661866E-6	4.5095001804170417E-6
	Post-2hrs	-2.9985968423913E-6	3.0321131590069E-6	.324	-8.9928768235333533E-6	2.9956831387508750E-6
	Post-24htrs	1.2350547826087E-6	3.1770300823842E-6	.698	-5.0457160275937593E-6	7.5158255928112811E-6
	Post-48hrs	1.6068595445135E-6	3.1363085931420E-6	.609	-4.5934076713421342E-6	7.8071267603690369E-6
	Post-72hrs	1.5268881159420E-6	3.7003729387426E-6	.681	-5.7884956663476347E-6	8.8422718982318231E-6
Post- 15min	Pre-	4.3579398007246E-6	3.0321131590069E-6	.153	-1.6363401804177E-6	1.0352219781878187E-5

	Post-30min	2.873160000000 0E-6	2.99968320 88592E-6	.340	-3.0570081 91520E-6	8.80332819 1520E-6
	Post-2hrs	1.359342958333 3E-6	2.99968320 88592E-6	.651	-4.5708252 33187E-6	7.28951114 9853E-6
	Post-24htrs	5.592994583333 3E-6	3.14609429 11589E-6	.078	-6.2661828 70699E-7	1.18126074 5374E-5
	Post-48hrs	5.964799345238 1E-6	3.10496710 70569E-6	.057	-1.7350789 98750E-7	1.21031065 9035E-5
	Post-72hrs	5.884827916666 7E-6	3.67384662 58497E-6	.111	-1.3781151 62387E-6	1.31477709 9572E-5
Post-30min	Pre-	1.484779800724 6E-6	3.03211315 90069E-6	.625	-4.5095001 80417E-6	7.47905978 1866E-6
	Post- 15min	-2.87316000000 00E-6	2.99968320 88592E-6	.340	-8.8033281 91520E-6	3.05700819 1520E-6
	Post-2hrs	-1.51381704166 67E-6	2.99968320 88592E-6	.615	-7.4439852 33187E-6	4.41635114 9853E-6
	Post-24htrs	2.719834583333 3E-6	3.14609429 11589E-6	.389	-3.4997782 87070E-6	8.93944745 3737E-6
	Post-48hrs	3.091639345238 1E-6	3.10496710 70569E-6	.321	-3.0466678 99875E-6	9.22994659 0351E-6
	Post-72hrs	3.011667916666 7E-6	3.67384662 58497E-6	.414	-4.2512751 62387E-6	1.02746109 9572E-5
Post-2hrs	Pre-	2.998596842391 3E-6	3.03211315 90069E-6	.324	-2.9956831 38750E-6	8.99287682 3533E-6
	Post- 15min	-1.35934295833 33E-6	2.99968320 88592E-6	.651	-7.2895111 49853E-6	4.57082523 3187E-6
	Post-30min	1.513817041666 7E-6	2.99968320 88592E-6	.615	-4.4163511 49853E-6	7.44398523 3187E-6
	Post-24htrs	4.233651625000 0E-6	3.14609429 11589E-6	.181	-1.9859612 45403E-6	1.04532644 9540E-5

	Post-48hrs	4.605456386904 8E-6	3.10496710 70569E-6	.140	-1.5328508 58208E-6	1.07437636 3202E-5
	Post-72hrs	4.525484958333 3E-6	3.67384662 58497E-6	.220	-2.7374581 20720E-6	1.17884280 3739E-5
Post-24htrs	Pre-	-1.23505478260 87E-6	3.17703008 23842E-6	.698	-7.5158255 92811E-6	5.04571602 7593E-6
	Post- 15min	-5.59299458333 33E-6	3.14609429 11589E-6	.078	-1.1812607 45374E-5	6.26618287 0699E-7
	Post-30min	-2.71983458333 33E-6	3.14609429 11589E-6	.389	-8.9394474 53737E-6	3.49977828 7070E-6
	Post-2hrs	-4.23365162500 00E-6	3.14609429 11589E-6	.181	-1.0453264 49540E-5	1.98596124 5403E-6
	Post-48hrs	3.718047619047 6E-7	3.24663374 45509E-6	.909	-6.0465677 19759E-6	6.79017724 3569E-6
	Post-72hrs	2.918333333333 3E-7	3.79433247 95830E-6	.939	-7.2093020 23900E-6	7.79296869 0567E-6
Post-48hrs	Pre-	-1.60685954451 35E-6	3.13630859 31420E-6	.609	-7.8071267 60369E-6	4.59340767 1342E-6
	Post- 15min	-5.96479934523 81E-6	3.10496710 70569E-6	.057	-1.2103106 59035E-5	1.73507899 8750E-7
	Post-30min	-3.09163934523 81E-6	3.10496710 70569E-6	.321	-9.2299465 90351E-6	3.04666789 9875E-6
	Post-2hrs	-4.60545638690 48E-6	3.10496710 70569E-6	.140	-1.0743763 63202E-5	1.53285085 8208E-6
	Post-24htrs	-3.71804761904 76E-7	3.24663374 45509E-6	.909	-6.7901772 43569E-6	6.04656771 9759E-6
	Post-72hrs	-7.99714285714 29E-8	3.76030190 44568E-6	.983	-7.5138306 70262E-6	7.35388781 3119E-6
Post-72hrs	Pre-	-1.52688811594 20E-6	3.70037293 87426E-6	.681	-8.8422718 98231E-6	5.78849566 6347E-6

	Post- 15min	-5.88482791666 67E-6	3.67384662 58497E-6	.111	-1.3147770 99572E-5	1.37811516 2387E-6
	Post-30min	-3.01166791666 67E-6	3.67384662 58497E-6	.414	-1.0274610 99572E-5	4.25127516 2387E-6
	Post-2hrs	-4.52548495833 33E-6	3.67384662 58497E-6	.220	-1.1788428 03739E-5	2.73745812 0720E-6
	Post-24htrs	-2.91833333333 33E-7	3.79433247 95830E-6	.939	-7.7929686 90567E-6	7.20930202 3900E-6
	Post-48hrs	7.997142857142 9E-8	3.76030190 44568E-6	.983	-7.3538878 13119E-6	7.51383067 0262E-6

Based on observed means.

The error term is Mean Square(Error) = 2.01E-010.

Delta Band Power

Multiple Comparisons

Delta Power

LSD

(I) Time	(J) Time				95% Confidence Interval	
		Mean Difference (I-J)	Std. Error	Sig.	Lower Bound	Upper Bound
Pre-	Post- 15min	-1.1460391818E-5	.000004908 56	.021	-.000021180 7	-.0000017 401
	Post-30min	-.0000040860	.000004908 56	.407	-.000013806 3	.00000563 43

	Post-2hrs	-.0000022093	.000004959 33	.657	-.000012030 1	.00000761 16
	Post-24htrs	.0000002751	.000005137 96	.957	-.000009899 5	.00001044 96
	Post-48hrs	.0000013071	.000005073 47	.797	-.000008739 8	.00001135 39
	Post-72hrs	.0000012347	.000005968 01	.836	-.000010583 5	.00001305 30
Post- 15min	Pre-	.0000114604*	.000004908 56	.021	.0000017401	.00002118 07
	Post-30min	.0000073744	.000004800 67	.127	-.000002132 2	.00001688 10
	Post-2hrs	.0000092511	.000004852 57	.059	-.000000358 3	.00001886 05
	Post-24htrs	.0000117354*	.000005034 98	.021	.0000017648	.00002170 61
	Post-48hrs	.0000127675*	.000004969 16	.011	.0000029272	.00002260 78
	Post-72hrs	.0000126951*	.000005879 59	.033	.0000010519	.00002433 83
Post-30min	Pre-	.0000040860	.000004908 56	.407	-.000005634 3	.00001380 63
	Post- 15min	-.0000073744	.000004800 67	.127	-.000016881 0	.00000213 22
	Post-2hrs	.0000018767	.000004852 57	.700	-.000007732 7	.00001148 62
	Post-24htrs	.0000043611	.000005034 98	.388	-.000005609 6	.00001433 17
	Post-48hrs	.0000053931	.000004969 16	.280	-.000004447 2	.00001523 34

	Post-72hrs	.0000053207	.00000587959	.367	-.0000063224	.0000169639
Post-2hrs	Pre-	.0000022093	.00000495933	.657	-.0000076116	.0000120301
	Post- 15min	-.0000092511	.00000485257	.059	-.0000188605	.0000003583
	Post-30min	-.0000018767	.00000485257	.700	-.0000114862	.0000077327
	Post-24htrs	.0000024843	.00000508449	.626	-.0000075844	.0000125530
	Post-48hrs	.0000035163	.00000501932	.485	-.0000064233	.0000134560
	Post-72hrs	.0000034440	.00000592204	.562	-.0000082833	.0000151713
Post-24htrs	Pre-	-.0000002751	.00000513796	.957	-.0000104496	.0000098995
	Post- 15min	-1.1735445000E-5	.00000503498	.021	-.0000217061	-.0000017648
	Post-30min	-.0000043611	.00000503498	.388	-.0000143317	.0000056096
	Post-2hrs	-.0000024843	.00000508449	.626	-.0000125530	.0000075844
	Post-48hrs	.0000010320	.00000519588	.843	-.0000092572	.0000113213
	Post-72hrs	.0000009597	.00000607242	.875	-.0000110653	.0000129847
Post-48hrs	Pre-	-.0000013071	.00000507347	.797	-.0000113539	.0000087398
	Post- 15min	-1.2767481905E-5	.00000496916	.011	-.0000226078	-.0000029272

	Post-30min	-.0000053931	.00000496916	.280	-.0000152334	.0000044472
	Post-2hrs	-.0000035163	.00000501932	.485	-.0000134560	.0000064233
	Post-24htrs	-.0000010320	.00000519588	.843	-.0000113213	.0000092572
	Post-72hrs	-.0000000723	.00000601795	.990	-.0000119895	.0000118448
Post-72hrs	Pre-	-.0000012347	.00000596801	.836	-.0000130530	.0000105835
	Post- 15min	-1.2695135833E-5	.00000587959	.033	-.0000243383	-.0000010519
	Post-30min	-.0000053207	.00000587959	.367	-.0000169639	.0000063224
	Post-2hrs	-.0000034440	.00000592204	.562	-.0000151713	.0000082833
	Post-24htrs	-.0000009597	.00000607242	.875	-.0000129847	.0000110653
	Post-48hrs	.0000000723	.00000601795	.990	-.0000118448	.0000119895

Based on observed means.

The error term is Mean Square(Error) = 2.77E-010.

*. The mean difference is significant at the .05 level.

Alpha-Delta power ratio

Multiple Comparisons

ADR

LSD

(I) Time	(J) Time				95% Confidence Interval	
		Mean Difference (I-J)	Std. Error	Sig.	Lower Bound	Upper Bound
Pre-	Post- 15min	.05651412935	.07308492185	.441	-.0880756480	.2011039067
	Post-30min	.03082668635	.07308492185	.674	-.1137630910	.1754164637
	Post-3hrs	.04004970096	.07308492185	.585	-.1045400764	.1846394783
	Post-24htrs	-2.54802619687E-3	7.30849218530E-2	.972	-.1471378035	.1420417511
	Post-48hrs	-7.55762531256E-4	7.23664289333E-2	.992	-.1439240875	.1424125625
	Post-72hrs	8.45145964622E-2	9.77126546131E-2	.389	-.1087982048	.2778273977
Post- 15min	Pre-	-5.65141293507E-2	7.30849218530E-2	.441	-.2011039067	.0880756480
	Post-30min	-2.56874430048E-2	6.93344447013E-2	.712	-.1628573498	.1114824638
	Post-3hrs	-1.64644283892E-2	6.93344447013E-2	.813	-.1536343352	.1207054784
	Post-24htrs	-5.90621555475E-2	6.93344447013E-2	.396	-.1962320624	.0781077513
	Post-48hrs	-5.72698918819E-2	6.85766684546E-2	.405	-.1929406290	.0784008453
	Post-72hrs	2.80004671115E-2	9.49400984374E-2	.769	-.1598271633	.2158280976

Post-30min	Pre-	-3.08266863459E-2	7.30849218530E-2	.674	-.1754164637	.1137630910
	Post- 15min	2.56874430048E-2	6.93344447013E-2	.712	-.1114824638	.1628573498
	Post-3hrs	9.22301461564E-3	6.93344447013E-2	.894	-.1279468922	.1463929214
	Post-24htrs	-3.33747125427E-2	6.93344447013E-2	.631	-.1705446194	.1037951943
	Post-48hrs	-3.15824488771E-2	6.85766684546E-2	.646	-.1672531860	.1040882883
	Post-72hrs	5.36879101164E-2	9.49400984374E-2	.573	-.1341397203	.2415155406
Post-3hrs	Pre-	-4.00497009615E-2	7.30849218530E-2	.585	-.1846394783	.1045400764
	Post- 15min	1.64644283892E-2	6.93344447013E-2	.813	-.1207054784	.1536343352
	Post-30min	-9.22301461564E-3	6.93344447013E-2	.894	-.1463929214	.1279468922
	Post-24htrs	-4.25977271584E-2	6.93344447013E-2	.540	-.1797676340	.0945721797
	Post-48hrs	-4.08054634928E-2	6.85766684546E-2	.553	-.1764762006	.0948652736
	Post-72hrs	4.44648955007E-2	9.49400984374E-2	.640	-.1433627349	.2322925259
Post-24htrs	Pre-	2.54802619687E-3	7.30849218530E-2	.972	-.1420417511	.1471378035
	Post- 15min	5.90621555475E-2	6.93344447013E-2	.396	-.0781077513	.1962320624
	Post-30min	3.33747125427E-2	6.93344447013E-2	.631	-.1037951943	.1705446194

	Post-3hrs	4.25977271584E-2	6.93344447013E-2	.540	-.0945721797	.1797676340
	Post-48hrs	1.79226366561E-3	6.85766684546E-2	.979	-.1338784735	.1374630008
	Post-72hrs	8.70626226591E-2	9.49400984374E-2	.361	-.1007650078	.2748902531
Post-48hrs	Pre-	7.55762531256E-4	7.23664289333E-2	.992	-.1424125625	.1439240875
	Post- 15min	5.72698918819E-2	6.85766684546E-2	.405	-.0784008453	.1929406290
	Post-30min	3.15824488771E-2	6.85766684546E-2	.646	-.1040882883	.1672531860
	Post-3hrs	4.08054634928E-2	6.85766684546E-2	.553	-.0948652736	.1764762006
	Post-24htrs	-1.79226366561E-3	6.85766684546E-2	.979	-.1374630008	.1338784735
	Post-72hrs	8.52703589935E-2	9.43881164428E-2	.368	-.1014652411	.2720059591
Post-72hrs	Pre-	-8.45145964622E-2	9.77126546131E-2	.389	-.2778273977	.1087982048
	Post- 15min	-2.80004671115E-2	9.49400984374E-2	.769	-.2158280976	.1598271633
	Post-30min	-5.36879101164E-2	9.49400984374E-2	.573	-.2415155406	.1341397203
	Post-3hrs	-4.44648955007E-2	9.49400984374E-2	.640	-.2322925259	.1433627349
	Post-24htrs	-8.70626226591E-2	9.49400984374E-2	.361	-.2748902531	.1007650078
	Post-48hrs	-8.52703589935E-2	9.43881164428E-2	.368	-.2720059591	.1014652411

REFERENCES

Amanda C. Marshall, Nicholas R. Cooper, Rebecca Segrave, Nicolas Geeraert, (2015). The effect of long-term stress exposure on aging cognition: a behavioral & eeg investigation. J. Neurobiology of aging.

Anderson, IM, Haddad, PM, Scott, J. Bipolar disorder, J. Clinical research ed, 2012, 345: e8508.

American Psychiatry Association. Diagnostic and Statistical Manual of Mental Disorders (5th ed). Arlington: American Psychiatric Publishing. 2013, pp: 123–154.

Alberto A. Rasia-Filho, Léder L. Xavier, Paula dos Santos, et al. Glial fibrillary acidic protein immunodetection and immunoreactivity in the anterior and posterior medial amygdala of male and female rats. Brain Research Bulletin, 58(2002), No. 1, pp. 67–75.

Airoldi L, Beghi E, Boglium G, Crespi V, Frattola L, 1999. Rational use of EEG in adults in clinical practice. J Clin Neurophysiol, 16(5): 456-61.

Bente Parkkenberg, Hans Jorgen G. Gundersen., 1997. Neocortical Neuron Number in Humans: Effect of Sex and Age. J. Comparative Neurology, 384:312–320.

Brenner, Richard P., 2003. EEG in encephalopathy and coma.American journal of electroneurodiagnostic technology, Volume 43, Issue 3, 164.

Biopac systems, Inc. AcqKnowledge® 4 Software Guide, 2001.

Brown, P. (2007). Abnormal oscillatory synchronisation in the motor sys- tem leads to impaired movement. Curr.Opin.Neurobiol. 17, 656–664.

Barry RJ, Clarke AR, Johnstone SJ, Magee Ca, Rushby Ja (2007). EEG differences between eyes-closed and eyes-open resting conditions. Clinical neurophysiology: official journal of the International Federation of Clinical Neurophysiology, 118: 2765–2773.

Barry, R.J., Johnstone, S.J., Clarke, A.R., (2003). A review of electrophysiology in attention-deficit/hyperactivity disorder: II. Event-related potentials. Clinical Neurophysiology, 114, 184–198.

Bear, M.F., Huber, K.M., Warren, S.T., (2004). The mGluR theory of fragile X mental retardation. Trends Neuroscience 27, 370–377.

Brandon Foreman, Claassen J., 2012. Quantitative EEG for the detection of brain ischemia. Critical Care, 16: 216.

Brian R. Cornwell, Linda L. Johnson, Tom Holroyd, Frederick W. Carver, Christian Grillon (2008). Hippocampal and Parahippocampal Theta during Goal-Directed Spatial Navigation Predicts Performance on a Virtual Morris Water Maze. The journal of Neuroscience, 28(23): 5983-8990.

Blessing, W. W. The lower brainstem and bodily homeostasis. New York: Oxford University Press, 1997.

Belanger HG, Kretzmer T, Yoash-Gantz R, Pickett T, Tupler LA. Cognitive sequelae of blast-related versus other mechanisms of brain trauma. Journal of the International Neuropsychological Society : JINS. Jan 2009;15(1):1-8.

Cristina marzano, Michele ferrara, Giuseppe curcio, Luigi De Gennaro., 2010. The effects of sleep deprivation in humans: topographical electroencephalogram changes in non-rapid eye movement (NREM) sleep versus REM sleep.J. Sleep Res, 19, 260-268.

Ce´cile Hubsch, Cedric Baumann, Coraline Hingray, Nicolaie Gospodaru, Jean-Pierre Vignal, Herve Vespignani, Louis Maillard., 2011. Clinical classification of psychogenic non-epileptic seizures based on video-EEG analysis and automatic clustering. J. Neurol Neurosurg Psychiatry, 82:955-960.

Cynthia Bira, Pamela VandeVorda, Yimin Shen, Waqar Razac, E. Mark Haacke., 2012. Effects of variable blast pressures on blood flow and oxygen saturation in rat brain as evidenced using MRI. Magnetic Resonance Imaging, 30: 527–534.

Christine L. Mac Donald, Ann M. Johnson, Dana Cooper, Elliot C. Nelson, Nicole J. Werner, Joshua S. Shimony, Abraham Z. Snyder, Marcus E. Raichle, John R. Witherow, Raymond Fang, Stephen F. Flaherty, David L. Brody., 2011. Detection of Blast-Related Traumatic Brain Injury in U.S. Military Personnel. The new england journal of medicine, 364; 22: 2091-2100.

Crowell, A.L., Ryapolova-Webb, E.S., Ostrem, J.L., Galifianakis, N.B., Shimamoto, S.,Lim, D.A., Starr, P.A. (2012). Oscillationsin sensorimotorcortex inmovement disorders: an electrocorticography study. Brain 135, 615–630.

Cummins TD, Finnigan S (2007). Theta power is reduced in healthy cognitive aging. Int J Psychophysiol, 66: 10–7.

Ciraulo DL, Frykberg ER. The surgeon and acts of civilian terrorism: blast injuries. Journal of the American College of Surgeons. Dec 2006;203(6):942-950.

CDC report to congress on mild traumatic brain injury in the United States: Steps to prevent a serious public health problem, 2003.

Dora Hermes , Kai J.Miller, Mariska J. Vansteensel , Erik Edwards, Cyrille H. Ferrier, Martin G. Bleichner , Peter C. van Rijen , Erik J. Aarnoutse, Nick F. Ramsey., 2014. Cortical theta wanes for language. J. NeuroImage, 85: 738–748.

Duncan Wallace., 2009. Improvised explosive devices and traumatic brain injury: the military experience in Iraq and Afghanistan. J. Australasian Psychiatry, Vol 17, No 3, pp. 218-224.

Department of Defense worldwide numbers for traumatic brain injury. http://dvbic.dcoe.mil/dod-worldwide-numbers-tbi (accessed March 1, 2015).

Deborah Warden., 2006. Military TBI During the Iraq and Afghanistan Wars. J. Head Trauma Rehabil, Vol. 21, No. 5, pp. 398-402.

Drummond JC, Brann CA, Perkins DE, Wolfe DE., 1991. A comparison of median frequency, spectral edge frequency, a frequency band power ratio, total power, and dominance shift in the determination of depth of anesthesia. J. *Acta Anaesthesiol Scand,* 35 (8): 693-9.

Darrin J. Lee, Gene G. Gurkoff, Ali Lzadi, Robert F. Berman, Arne D. Ekstrom, J. Paul Muizelaar, Bruce G. Lyeth, Kiarash Shahlaie (2013). Medial septal nucleus theta frequency deep brain stimulation improves spatial working memory after traumatic brain injury. Journal of neurotrauma, 30: 131-139.

B.T. Dunkley, L. Da Costac, A. Bethunec, R. Jetlyd, E.W. Pangb, M.J. Taylora, S.M. Doesburga (2015). Low-frequency connectivity is associated with mild traumatic brain injury. NeuroImage: Clinical 7: 611–621.

Evans BM., 1976. Patterns of arousal in comatose patients. *J. Neurol Neurosurg Psychiatry,* 39: 392–402.

Evan Calabrese, Fu Du, Robert H. Garman, G. Allan Johnson, Cory Riccio, Lawrence C. Tong, Joseph B. Long., 2014. Diffusion Tensor Imaging Reveals White Matter Injury in a Rat Model of Repetitive Blast-Induced Traumatic Brain Injury. J. Neurotrauma, 31: 938–950.

Florian Mormann, Klaus Lehnertz, Peter David, Christian E. Elger., 2000. Mean phase coherence as a measure for phase synchronization and its application to the EEG of epilepsy patients. J. Physica, D 144: 358–369.

Francisco J. Urbano, Nebojsa Kezunovic, James Hyde, ChristenSimon, PaigeBeck, EdgarGarcia-Rill., 2012. Gamma band activity in the reticular activating system. J. Sleep and Chronobiology, Volume 3, Article 6, 1-16.

Fleur M Howells, Victoria L Ives-Deliperi, Neil R Horn, Dan J Stein., 2012. Mindfulness based cognitive therapy improves frontal control in bipolar disorder: a pilot EEG Study. J. BMC Psychiatry, 12: 15.

Frank H Duffy, Heidelise Als., 2012. A stable pattern of EEG spectral coherence distinguishes children with autism from neurotypical controls - a large case control study. J. BMC Medicine, 10:64.

Gonzalo Alarcon, Antonio Valentin., 2012. Introduction to Epilepsy. Cambridge University Press.

Rositsa poryazova, Reto huber, Ramin khatami, Esther werth, Peter brugger, Krizstina barath, Christian R. Baumann, Claudio L. Bassetti., 2015. Topographic sleep EEG changes in the acute and chronic stage of hemispheric stroke. J. Sleep Res, 24, 54-65.

Gennady G. Knyazev., 2012. EEG delta oscillations as a correlate of basic homeostatic and motivational processes. J. Neuroscience and Biobehavioral Reviews, 36, 677–695.

Gilbertson T, Lalo E, Doyle L, Di Lazzaro V, Cioni B, 2005. Existing motor state is favored at the expense of new movement during 13–35 Hz oscillatory synchrony in the human corticospinal system. J. Neurosci, 25: 7771–7779.

George H. Klem, Hans Otto LuÈders, H.H. Jasper, C. Elger., 1999. The ten-twenty electrode system of the International Federation. Guidelines of the International Federation of Clinical Physiology.

Geir Ogrim, Juri Kropotov, Knut Hestad., 2012. The quantitative EEG theta/beta ratio in attention deficit/hyperactivity disorder and normal controls: Sensitivity, specificity, and behavioral correlates. J. Psychiatry Research, 198: 482–488.

Gaetz, M., & Bernstein, D. M., 2001. The current status of electrophysiologic procedures for the assessment of mild traumatic brain injury. Journal of Head Trauma Rehabilitation, 16, 386−405.

G. Plourde, J. Baribeau, V. Bonhomme (1997). Ketamine increases the amplitude of the 40-Hz auditory steady-state response in humans. British journal of anaesthesia, 78: 524-529.

Halgren E, Boujon C, Clarke J, Wang C, Chauvel P., 2002. Rapid distributed fronto-parieto-occipital processing stages during working memory in humans. J. Cereb Cortex, 12: 710 –728.

Hagerman, R.J., Hagerman, P.J., (2002). Fragile X Syndrome: Diagnosis, Treatment, and Research, 3rd ed. Johns Hopkins University Press, Baltimore.

Halliday DM, Conway BA, Farmer SF, Rosenber JR, 1998. Using electroencephalography to study functional coupling between cortical activity and electromyograms during voluntary contractions in humans. Neurosci Lett, 241: 5-8.

Hoge CW, McGurk D, Thomas JL, Cox AL, Engel CC, Castro CA. Mild traumatic brain injury in U.S. Soldiers returning from Iraq. The New England journal of medicine. Jan 31 2008;358(5):453-463.

Holm L, Cassidy JD, Carroll LJ, Borg J, 2005. Summary of the WHO collaborating centre for neutrotrauma task force on mild traumatic brain injury. J Rehabil Med, 37(3): 137-41.

Igor Timofeev, Maxim Bazhenov, Josée Seigneur, Terrence Sejnowski. Neuronal Synchronization and Thalamocortical Rhythms in Sleep, Wake and Epilepsy. Jasper's Basic Mechanisms of the Epilepsies. 4th edition.

Ingo Bojak, Harry C. Day, DavidT. J. Liley., 2013. Ketamine, propofol, and the EEG: a neural field analysis of HCN1-mediated interactions. J. Frontiers in Computational Neuroscience, Volume7, Article 22.

Ibolja cernak., 2008. Shell shock revisited: solving the puzzle of blast trauma. Science, Volume 319, 406-408.

John H. Morrison, Patrick R. Hof., 1997. Life and Death of Neurons in the Aging Brain. J. Science, Vol 278, No. 5337, 412-419.

Jagdish Patel, Shigeyoshi Fujisawa, Antal Berenyi, Sebastien Royer, Gyorgy Buzsaki., 2012. Traveling Theta Waves along the Entire Septotemporal Axis of the Hippocampus. J. Neuron, 75, 410–417.

Jasper, H., 1958. Report of committee on methods of clinical exam in EEG, Electroencephalogr. Clin. Neurophysiol, 10: 370–375.

Jaqust W, 2013. Vulnerable neural systems and the borderland of brain aging and neurodegeneration. Neuron, 77(2): 219-34.

Joel Aanerud, Per Borghammer, M Mallar Chakravarty, Kim Vang, Anders B Rodell, Kristjana Y Jonsdottir, Arne Moller, Mahmoud Ashkanian, Manouchehr S Vafaee, Peter Iversen, Peter Johannsen, Albert Gjedde., 2012. Brain energy metabolism and blood flow differences in healthy aging. Journal of Cerebral Blood Flow & Metabolism, 32, 1177–1187.

B. Jelles, P. Scheltens, W. M. van der Flier, E. J. Jonkman, F. H. L. da Silva, C. J. Stam., 2008. Global dynamical analysis of the EEG in Alzheimer's disease:

Frequency-specific changes of functional interactions. J. *Clinical Neurophysiology*, vol. 119, no. 4: 837–841.

Jeff rey V Rosenfeld, Alexander C McFarlane, Peter Bragge, Rocco A Armonda, Jamie B Grimes, Geoff rey S Ling., 2013. Blast-related traumatic brain injury. J. Lancet Neurol, 12: 882-93.

Jenkinson,N.,and Brown, P. (2011). Newinsightsintotherelationship between dopamine, beta oscillations and motor function. Trends Neurosci, 34, 611–618.

J. Middeldorp E.M. Hol (2011). GFAP in health and disease. Progress in Neurobiology, 93: 421-443.

James Thompson, Wayne Sebastianelli, Semyon Slobounov, 2004. EEG and postural correlates of mild traumatic brain injury in athletes. Neuroscience Letters, 377: 158-163.

Jeremy J. Moeller, Bin Tu, Carl W. Bazil, 2011. Quantitative and Qualitative analysis of ambulatory electroencephalography during mild traumatic brain injury. Arch Neurol, 68 (12)：1595-1598.

John Dellabadia Jr, William L. Bell, John W. Keyes Jr, Vincent P. Mathews, Stephen S. Glazier, 2002. Assessment and cost comparison of sleep-deprived EEG, MRI and PET in the prediction of surgical treatment for epilepsy. Seizure, 11: 303-309.

Kei Omata, Takashi Hanakawa, Masako Morimoto, Manabu Honda., 2013. Spontaneous Slow Fluctuation of EEG Alpha Rhythm Reflects Activity in

Deep-Brain Structures: A Simultaneous EEG-fMRI Study. J. PLOS ONE, Volume 8, Issue 6, e66869.

Karen M. Fisher, Boubker Zaaimi, Timothy L. Williams, Stuart N. Baker, Mark R. Baker., 2012. Beta-band intermuscular coherence: a novel biomarker of upper motor neuron dysfunction in motor neuron disease. J. Brain, 135; 2849–2864.

Katherine H. Noe, Madeline Grade, Cynthia M. Stonnington, Erika Driver-Dunckley, Dona E.C. Locke., 2012. Confirming psychogenic nonepileptic seizures with video-EEG: Sex matters. J. Epilepsy & Behavior, 23: 220–223.

Klaus Linkenkaer-Hansen, Vadim V. Nikulin, Satu Palva, Risto J. Ilmoniemi, and J. Matias Palva., 2004. Prestimulus Oscillations Enhance Psychophysical Performance in Humans. J. Neuroscience, 24 (45): 10186 –10190.

Kuhn AA, Williams D, Kupsch A, Limousin P, Hariz M, Schneider GH, Yarrow K, Brown P (2004). Event-related beta desynchronization in human subthalamic nucleus correlates with motor performance. J Brain, 127: 735-746.

Karrasch M, Laine M, Rapinoja P, Krause CM (2004). Effects of normal aging on eventrelated desynchronization/synchronization during a memory task in humans. Neurosci Lett, 366: 18–23.

Katherine H. Taber, Deborah L. Warden, Robin A. Hurley (2006). Blast-Related Traumatic Brain Injury: What is known? J Neuropsychiatry Clin Neurosci, 18:2, 141-145.

Kilner JM, Baker SN, Salenius S, Hair R, Lemon RN, 2000. Human cortical muscle coherence is directly related to specific motor parameters. J Neurosci, 20: 8838-45.

Karin Rafaels, Cameron R. Rovert S. Salzar, Matthew B. Panzer, William Woods, Sanford Feldman, Thomas Cummings, Bruce Capehart, 2011. Survivial risk assessment for primary blast exposures to the head. Neurotrauma, 28: 2319-2328.

Kay, Thomas, 1993. Neuropsychological treatment of mild traumatic brain injury. The journal of Head Trauma Rehabilitation, 8(3): 74-85.

Y. Lai, W. van Drongelen, L. Ding, K.E. Hecox, V.L. Towle, D.M. Frim, B. He., 2005.Estimation of in vivo human brain-to-skull conductivity ratio from simultaneous extra- and intra-cranial electrical potential recordings. Clinical Neurophysiology, 116 , 456–465.

Laura Lee Colgin., 2013. Mechanisms and Functions of Theta Rhythms. J. Annu. Rev. Neurosci, 36:295–312.

Lei Wu, Ying Chen, Jiong Zhou., 2014. A Promising Method to Distinguish Vascular Dementia From Alzheimer's Disease With Standardized Low-Resolution Brain Electromagnetic Tomography and Quantitative EEG. J. Clinical EEG and Neuroscience, Vol. 45 (3): 152–157.

F.H. Lopes da Silva, J.E. Vos, H. Mooibroek, A. van Rotterdam,(1980). Relative contributions of intracortical and thalamo-cortical processes in the generation of

alpha rhythms, revealed by partial coherence analysis, Electroenceph. clin. Neurophysiol. 50, 449–456.

Lindgren KA, Larson CL, Schaefer SM, Abercrombie HC, Ward RT, Oakes TR, Holden JE, Perlman SB, Benca RM, Davidson RJ (1999) Thalamic metabolic rate predicts EEG alpha power in healthy control subjects but not in depressed patients. Biol Psychiatry 45(8):943–952.

L. D. Gugino, R. J. Chabot, L. S. Prichep, E. R. John, L. S. Aglio, 2001. Quantitative EEG changes associated with loss and return of consciousness in healthy adult volunteers anaesthetized with propofol or sevoflurane. British journal of anaesthesia, 87(3): 421-8.

L Elliot Hong, Ann Summerfelt, Robert W Buchanan, Patricio O'Donnell, Gunvant K Thaker, Martin A Weiler, Adrienne C Lahti, 2010. Gamma and delta neural oscillations and association with clinical symptoms under subanesthetic ketamine. Neuropsychopharmacology, 35: 632-640.

Michael E. Hasselmo, Howard B. Eichenbaum., 2005. Hippocampal mechanisms for the context-dependent retrieval of episodes. J . *Neural Netw,* 18 (9): 1172–1190.

Marc R. Nuwera, Giancarlo Comib, Ronald Emersonc, Anders Fuglsang-Frederiksend, Jean-Michel Guerite, Hermann Hinrichsf, Akio Ikedag, Fransisco Jose C. Luccash, Peter Rappelsburger., 1998. IFCN standards for digital recording of clinical EEG. Electroencephalography and clinical Neurophysiology, 106 :259–261.

Masako Okamoto, Haruka Dan, Kuniko Sakamoto, Kazuhiro Takeo, Koji Shimizu, Satoru Kohno, Ichiro Oda, Seiichiro Isobe, Tateo Suzuki, Kaoru Kohyama, Ippeita Dan., 2004. Three-dimensional probabilistic anatomical cranio-cerebral correlation via the international 10–20 system oriented for transcranial functional brain mapping. J. NeuroImage, 21: 99–111.

Mera S. Barra, Natasha Radhub, Crissa L. Gugliettid, Reza Zomorrodib, Tarek K. Rajjib, Paul Ritvod, Zafiris J. Daskalakisb., 2014. Age-related differences in working memory evoked gamma oscillations. J. Brain research, 1576: 43-51.

Mateusz Gola, Mikołaj Magnuski, Izabela Szumska, Andrzej Wróbel., 2013. EEG beta band activity is related to attention and attentional deficits in the visual performance of elderly subjects. International Journal of Psychophysiology, 89: 334–341.

Mateusz Gola, Jan Kamiński, Aneta Brzezicka, Andrzej Wróbel., 2012. Beta band oscillations as a correlate of alertness — Changes in aging. International Journal of Psychophysiology, 85: 62–67.

Monastra VJ, Lubar JF, Linden M., 2001. The development of a quantitative electroencephalographic scanning process for attention deficit-hyperactivity disorder: Reliability and validity studies. J. Neuropsychology, 15: 136–144.

Monastra VJ, Lubar JF, Linden M., 1999. Assessing attention deficit hyperactivity disorder via quantitative electroencephalography: an initial validation study. J. Neuropsychology, 13: 424–433.

Marina Frantseva, Jie Cui, Faranak Farzan, Lakshminarayan V. Chinta, Jose Luis Perez Velazquez, Zafiris Jeffrey Daskalakis., 2014. Disrupted Cortical Conductivity in Schizophrenia: TMS–EEG Study. J. Cerebral Cortex, 24: 211–221.

Michael Murphy, Marie-Aurélie Bruno, Brady A. Riedner, Pierre Boveroux, Quentin Noirhomme, P Eric C. Landsness, Jean-Francois Brichant, Christophe Phillips, Marcello Massimini, Steven Laureys, Giulio Tononi, Mélanie Boly., 2011. Propofol Anesthesia and Sleep: A High-Density EEG Study. J. SLEEP, Vol. 34, No. 3: 283-291.

Melanie Boly, Rosalyn Moran, Michael Murphy, Pierre Boveroux, Marie-Aurelie Bruno, Quentin Noirhomme, Didier Ledoux, Vincent Bonhomme, Jean-Francois Brichant, Giulio Tononi, Steven Laureys, Karl Friston., 2012. Connectivity Changes Underlying Spectral EEG Changes during Propofol-Induced Loss of Consciousness. The Journal of Neuroscience, 32 (20): 7082–7090.

Ming-Xiong Huang, Rebecca J. Theilmann, Ashley Robb, Annemarie Angeles, Sharon Nichols, Angela Drake, John D'Andrea, Michael Levy, Martin Holland, Tao Song, Sheng Ge, Eric Hwang, Kevin Yoo, Li Cui, Dewleen G. Baker, Doris Trauner, Raul Coimbra, Roland R. Lee., 2009. Integrated Imaging Approach with MEG and DTI to Detect Mild Traumatic Brain Injury in Military and Civilian Patients. J. Neurotrauma, 26: 1213–1226.

Ming-Xiong Huang, Sharon Nichols, Ashley Robb, Annemarie Angeles, Angela Drake, 2012. An automatic MEG low-frequency source imaging approach for

detecting injuries in mild and moderate TBI patients with blast and non-blast causes. Neuroimage, 61: 1067-1082.

Ming-Xiong Huang, Sharon Nichols, Dewleen G. Baker, Ashley Robb, Annemarie Angeles, Kate A. Yurgil, Angela Drake, Michael Levy, Tao Song, Robert McLay, Rebecca J. Theilmann, Mithun Diwakar, Victoria B. Risbrough, Zhengwei Ji, Charles W. Huang, Douglas G. Chang, Deborah L. Harrington, Laura Muzzatti, Jose M. Canive, J. Christopher Edgar, Yu-Han Chen, Roland R. Lee, 2014. Single-subject-based whole-brain MEG slow-wave imaging approach for detecting abnormality in patients with mild traumatic brain injury. NeuroImage: Clinical 5: 109-119.

Marie-Pierre Deiber, Etienne Sallard, Catherine Ludwig, Catherine Ghezzi, Jérôe Barral, VicenteIbañz., 2012. EEG alpha activity reflects motor preparation rather than the mode of action selection . J. Frontiers in Integrative Neuroscience , Volume 6, Article 59.

Missonnier P, Deiber MP, Gold G, Millet P, Gex-Fabry Pun M, Fazio-Costa L, (2006). Frontal theta event-related synchronization: comparison of directed attention and working memory load effects. J Neural Transm, 113: 1477–86.

Michael Gaetz, Daneil M. Bernstein, 2001. The current status of electrophysiologic procedures for the assessment of mild traumatic brain injury. J Head trauma rehabil, 16(4): 386-405.

Matthew B. Panzer, Barry S. Myers, Bruce P. Capehart, Cameron R. Bass, 2012. Annals of biomedical engineering, 40(7): 1530-1544.

Marc R. Nuwer, David A. Hovda, Lara M. Schrader, Paul M. Vespa, 2005. Routine and quantitative EEG in mild traumatic brain injury. Clinical Neurophysiology, 116: 2001-2025.

Management of concussion/mild traumatic brain injury, 2009. Clinical Practice Guideline.

Nash Boutros, Liana Fraenkel, Alan Feingold., 2005. A Four-Step Approach for Developing Diagnostic Tests in Psychiatry: EEG in ADHD as a Test Case. J. Neuropsychiatry Clin Neurosci, 17 (4): 455-464.

A. Napoli, M. Barbe, K. Darvish, I. Obeid. Assessing Traumatic Brain Injuries Using EEG Power Spectral Analysis and Instantaneous Phase (2012). 34th Annual International Conference of the IEEE EMBS San Diego, California USA, 28 August - 1 September.

C. Neuper, G. Pfurtscheller (2001). Event-related dynamics of cortical rhythms: frequency-specific features and functional correlates. International journal of Psychophysiology, 43: 41-58.

Nuwer MR, Hovda DA, Schrader LM, Vespa PM, 2005. Routine and quantitative EEG in mild traumatic brain injury. Clin Neurophysiol, 116(9): 2001-25.

Owens BD, Kragh JF, Jr., Wenke JC, Macaitis J, Wade CE, Holcomb JB. Combat wounds in operation Iraqi Freedom and operation Enduring Freedom. The Journal of trauma. Feb 2008;64(2):295-299.

Preeya Khanna, Jose M Carmena., 2015. Neural oscillations: beta band activity across motor networks. J. Current Opinion in Neurobiology, 32:60–67.

D. Pond., 2012. Dementia an update on management. J. Australian Family Physician, vol. 41, no. 12: 936–939.

Patrick W. Alford, Borna E. Dabiri, Josue A. Goss, Matthew A. Hemphill, Mark D. Brigham, and Kevin Kit Parker., 2011. Blast-induced phenotypic switching in cerebral vasospasm. J. PNAS, vol. 108 , no. 31: 12705–12710.

Paul E. Rapp, David O. Keyser, Alfonso Albano, Rene Hernandez, Douglas B. Gibson, Robert A. Zambon, W. David Hairston, John D. Hughes, Andrew Krystal, Andrew S. Nichols. Traumatic brain injury detection using electrophysiological methods (2015). Frontiers in Human Neuroscience,Volume 9, Article 11.

Palva S, Palva M (2011). Functional roles of alpha-band phase synchronization in local and large-scale cortical networks. Front Psychol, 2:204 – 8.

Pfurtscheller G., Lopes da Silva F (1999). Event-related EEG/MEG synchronization and desynchronization: basic principles. Clin. Neurophysiol., 110: 1842-1857.

G. Pfurtscheller (1994). Event-related desynchronization (ERD) during visual processing. International journal of psychophysiology, 16: 147-153.

Paul M. Dockree, Simon P. Kelly, Richard A.P. Roche, Michael J. Hogan, Richard B. Reilly, Ian H. Robertson, 2004. Behavioural and physiological impairments of sustained attention after traumatic brain injury. Cognitive Brain Research, 20: 403-414.

Richard A. Bauman, Geoffrey Ling, Lawrence Tong, Adolph Januszkiewicz, Denes Agoston, Nihal Delanerolle, Young Kim, Dave Ritzel, Randy Bell, James

Ecklund, Rocco Armonda, Faris Bandak, Steven Parks., 2009. An introductory characterization of a combat-casualty-care relevant swine model of closed head injury resulting from exposure to explosive blast. J. Neurotrauma, 26: 841-860.

Richard A.P. Roche, Paul M. Dockree, Hugh Garavan, John J. Foxe, Ian H. Robertson, Shane M. O'Mara, 2004. EEG alpha power changes reflect response inhibition deficits after traumatic brain injury (TBI) in humans. Neuroscience Letters, 362: 1-5.

Robert H. Garman, Larry W. Jenkins, Robert C. Switzer, Richard A. Bauman, Lawrence C. Tong, Peter V. Swauger, Steven A. Parks, David V. Ritzel, C. Edward Dixon, Robert S.B. Clark, Hu¨ lya Bayır, Valerian Kagan, Edwin K. Jackson, Patrick M. Kochanek (2011). Blast Exposure in Rats with Body Shielding Is Characterized Primarily by Diffuse Axonal Injury. JOURNAL OF NEUROTRAUMA 28:947–959.

Robert W. Thatcher, 2006. Electroencephalography and mild traumatic brain injury. Foundation of sport-related brain injuries, 241-265.

Robert P. Weenink, Xavier C.E. Vrijdag, Michel J. A.M. Van Putten, Markus W. Hollmann, Markus F. Stevens, Thomas M. Van Gulik, Robert A. Van Hulst, 2011. Quantitative electroencephalography in a swine model of cerebral arterial gas embolism. Clinical Neurophysiology, 123: 411-417.

Ronne-Engstrom E, Winkler T, 2006. Continuous EEG monitoring in patients with traumatic brain injury reveals a high incidence of epileptiform activity. Acta Neurol Scand, 114: 47-53.

Stanley Rush, Daniel A. Driscoll., 1968. Current Distribution in the Brain From Surface Electrodes. Anesthesia and analgesia, Vol 47, No. 6, 717-723.

Siddiqui, Mohd Maroof., 2013. EEG signals play major role to diagnose sleep disorder. International journal of electronics and computer science engineering, Volume 2, 503-505.

Selvam, V.S. , Sriram Eng. Coll, Chennai, India , Shenbagadevi, S., 2011. Brain tumor detection using scalp eeg with modified Wavelet-ICA and multi layer feed forward neural network.

Saeid Sanei, J. A. Chambers., 2007. EEG signal processing.

Sarah D. Holder, Amelia Wayhs., 2014. Schizophrenia. J. American Family Physician, Volume 90, Number 11: 776-782.

Shafer A., 1995. Metaphor and anesthesia. J. Anesthesiology, 83: 1331-42.

Sinner,B., Graf,B.M., 2008. Ketamine Handb Exp Pharmacol, 182: 313–333.

Stephen J Wolf, Vikhyat S Bebarta, Carl J Bonnett, Peter T Pons, Stephen V Cantrill., 2009. Blast injuries. J. Lancet, 374: 405–15.

Selim R. Benbadis., 2006. Introduction to sleep electroencephalography. Sleep: A Comprehensive Handbook.

Sharbrough FW, Messick JM Jr, Sundt TM Jr., 1973. Correlation of continuous electroencephalograms with cerebral blood flow measurements during carotid endarterectomy. J. Stroke, 4: 674–683.

D. Schwender, M. Daunderer, S. Mulzer, S. Klasing, U. Finsterer, K. Peter., 1996. Spectral edge frequency of the electroencephalogram to monitor ‘depth’ of

anaesthesia with isoflurane or propofol. British Journal of Anaesthesia, 77: 179-184.

Shuya Kiyama, Koichi Tsuzaki., 1997. Titration of propofol infusion using processed electroencephalogram during combined general and spinal anesthesia. Journal of Anesthesia, 11: 250-254.

P. Sauseng, W. Klimesch, C. Gerloff , F.C. Hummel., 2009. Spontaneous locally restricted EEG alpha activity determines cortical excitability in the motor cortex. J. Neuropsychologia, 47: 284–288.

Salmelin R, Hari R., 1994. Spatiotemporal characteristics of sensorimotor neuromagnetic rhythms related to thumb movement. J. Neuroscience, 60: 537–550.

Sladjana Spasic, Milka Culic, Gordana Grbic, Ljiljana Martac, Slobodan Sekulic, Dragosav Mutavdzic. Spectral and Fractal Analysis of Cerebellar Activity After Single and Repeated Brain Injury (2008). Bulletin of Mathematical Biology, 70: 1235–1249.

Scott R. Sponheim, Kathryn A. McGuire, Seung Suk Kang, Nicholas D. Davenport, Selin Aviyente, Edward M. Bernat, Kelvin O. Lim (2010). Evidence of disrupted functional connectivity in the brain after combat-related blast injury. Neuroimage 54: S21-S29.

Stanislav I. Svetlov, Victor Prima, Daniel R. Kirk, Hector Gutierrez, Kenneth C. Curley, Ronald L. Hayes, Kevin K. W. Wang, 2010. Morphologic and biochemical characterization of brain injury model of controlled blast

overpressure exposure. The journal of trauma Injury, Infection, and Critical Care, 69(4): 795-804.

Teplan, M., 2002, Fundamentals of EEG measurements, J. *Measmt Sci Rev*, 2(2).

Yuko Urakami, 2013. Electrophysiologic Evaluation of Diffuse Axonal Injury after Traumatic Brain Injury. J Neurol Neurophysiol, 4: 157.

M. Valderramaa, C. Alvaradoa, S. Nikolopoulosa, J. Martineriea, C. Adama, V. Navarroa, M. Le Van Quyena., 2012. Identifying an increased risk of epileptic seizures using a multi-feature EEG–ECG classification. J. Biomedical Signal Processing and Control, 7: 237– 244.

Von Stein A, Chiang C, Konig P., 2000. Top-down processing mediated by interareal synchronization. J. Proc Natl Acad Sci USA, 97: 14748 –14753.

Vallbo AB, Wessberg J, 1993. Organization of motor output in slow finger movements in man. J Physiol, 469:673-91. Clin Pharmacol Ther, 61: 45-88.

Valerie Billard, Pedro L. Gambus, Nassib Chamoun, Donald R. Stanski, Steven L. Shafer (1997). A comparison of spectral edge, delta power and bispectral index as EEG measures of alfentanil, propofol, and midazolam drug effect.

William Jagust., 2013. Vulnerable Neural Systems and the Borderland of Brain Aging and Neurodegeneration. J. Neuron, 77: 219-234.

World Health Organization, Factsheet 999: epilepsy. <http://www.who. int/mediacentre/factsheets/fs999/en/S>, 2013.

William Bosl, Adrienne Tierney, Helen Tager-Flusberg, Charles Nelson., 2011. EEG complexity as a biomarker for autism spectrum disorder risk. J. BMC Medicine, 9: 18.

W Klimesch, M Doppelmayr, Th Pachinger, B Ripper, 1997. Brain oscillatons and human memory: EEG correlates in the upper alpha and theta band. Neuroscience letters, 238(1-2): 9-12.

W. Kimesch, M. Doppelmayr, H. Russegger, T. Pachinger, J. Schwaiger, 1998. Induced alpha band power changes in the human EEG and attention. Neuroscience letters, 244: 73-76.

William C. Walker, 2014. Epidemiological study of mild traumatic brain injury sequelae caused by blast exposure during operations iraqi freedom and enduring freedom. Final report for U.S. Army medical research and materiel command, Fort Detrick, Maryland 21705-5012.

X. Anton Alvarez, Carolina Sampedro, Jesus Figueroa, Ivan Tellado, Andres Gonzalez, Manuel Garcia-Fantini, Ramon Cacabelos, Dafin Muresanu, Herbert Moessler, 2008. Reductions in qEEG slowing over 1 year and after treatment with cerebrolysin in patients with moderate-severe traumatic brain injury. J Neural Transm, 115: 683-692.

Xingjie Ping, Xiaoming Jin, 2015. Transition from initial hypoactivity to hyperactivity in cortical traumatic brain injury in vivo. Journal of Neurotrauma, 2015. 3913.

Yong Tang, Jens R. Nyengaard, Didima M.G. DE Groot, Hans Jorgen G. Gundersen., 2001. Total Regional and Global Number of Synapaes in the Human Brain Neocortex. J. Synapse, 41: 258-273.

Yoshio Okada, Airi Lahteenmaki, Chibing Xu, 1999. Comparison of MEG and EEG on the basis of somatic evoked responses elicited by stimulation of the snout in the juvenile swine. Clinical Neurophysiology, 110 (2): 214-229.

Zulfi Haneef, Harvey S. Levin, James D. Frost, Jr, and Eli M. Mizrahi., 2013. Electroencephalography and Quantitative Electroencephalography in Mild Traumatic Brain Injury. J. Neurotrauma, 30: 653–656.

ABSTRACT

QUANTITATIVE BRAIN ELECTRICAL ACTIVITY IN THE INITIAL SCREENING OF MILD TRAUMATIC BRAIN INJURIES AFTER BLAST

by

CHENGPENG ZHOU

August 2015

Advisor: Dr. John Michael Cavanaugh, Dr. Chaoyang Chen

Major: Biomedical Engineering

Degree: Master of Science

Objective: Quantitative electroencephalography (QEEG) has been reported to be sensitive in the diagnosis and measurement of mild traumatic brain injury (mTBI) in civilian setting and thus may be a promising tool in individuals who have been exposed to blast forces. Using a swine model, this study investigated EEG changes early after blast exposure. The purpose was to determine if QEEG can detect brain activity abnormalities earlier after blast exposure and to develop a QEEG data analysis protocol.

Methods: Six swines were used in this study. Swine were anesthetized using ketamine and propofol, and exposed to 410-460 kPa blast overpressure. EEG recordings were performed at 15 min before blast, and 15 min, 30 min and 2 hours, and 1, 2, 3 days post-blast using Biopac data acquisition system. Non-invasive surface recording electrodes were placed on the skin over both central (C3, C4) and parietal (P3, P4) areas of the skull. Acknowledge software was used for off-line EEG data analysis. qEEG parameters including frequency, Spectral edge frequency (SEF-90),

and power (V^2/Hz/Min) of delta, theta, alpha, and beta bands were analyzed and compared between pre-blast and post-blast and different recording locations. Other qEEG parameters including alpha-delta ratio (ADR). Statistical analysis was performed using SPSS software (Repaeted Measures of ANOVA, postHoc LSD).

Results: The EEG activity decreased fast frequency, and increased slower frequency after the blast. The EEG mean frequency have no statistic significant before and after blast at left parietal, left front and right front recording site. At the right parietal recording site, EEG mean frequency decreased from 6.78 ± 2.01 Hz before blast to 3.36 ± 0.28 Hz, 3.10 ± 0.19, 3.47 ± 0.21, 3.43 ± 0.11 at 15 min, 2h, 1d, 2d after blast ($P<0.05$), returned to 5.25 ± 1.96 Hz, 4.52 ± 1.26 Hz at 30 min, 3d after blast ($P>0.05$). The SEF-90 have no statistic significant before and after blast at left front recording site. At the left parietal recording site, SEF-90 decreased from 18.22 ± 3.51 Hz before blast to 10.27 ± 1.24 Hz, 10.84 ± 1.22 Hz at 15 min, 2d after blast ($P<0.05$), respectively, and returned to 14.25 ± 3.01 Hz, 17.27 ± 3.15, 14.94 ± 0.86 Hz, 11.03 ± 2.03 Hz at 30 min, 2h, 1d, 3d after blast ($P>0.05$), respectively. At the right parietal recording site, SEF-90 decreased from 20.46 ± 3.63 Hz before blast to 10.43 ± 1.26, 10.74 ± 1.18, 11.98 ± 1.15, 11.44 ± 0.72 at 15 min, 2h, 1d, 2d after blast ($P<0.05$), respectively, and returned to 13.84 ± 3.97, 13.21 ± 4.49 at 30 min, 3d after blast ($P>0.05$), respectively. At the right front recording site, SEF-90 decreased from 16.55 ± 4.14 Hz before blast to 9.31 ± 1.01 after blast ($P<0.05$), and returned to 16.10 ± 3.37, 15.09 ± 2.07, 12.52 ± 1.68, 10.10 ± 0.64, 13.29 ± 1.76 at 30 min, 2h, 1d, 2d, 3d after blast ($P>0.05$), respectively.

The Lower Alpha band power (8-10 Hz) have no statistic significant before and after blast at right parietal, left front, right front recording site. At the left parietal recording site, Alpha power decreased from $5\times10^{-3}\pm4\times10^{-3}$ V^2/Hz before blast to $4.9\times10^{-4}\pm4\times10^{-4}$ V^2/Hz, $8.8\times10^{-4}\pm4\times10^{-4}$ V^2/Hz, $1.7\times10^{-4}\pm3\times10^{-5}$ V^2/Hz, $2.5\times10^{-4}\pm8\times10^{-5}$ V^2/Hz at 15 min, 2h, 1d, 2d after blast ($P<0.05$), respectively, and returned to $1.2\times10^{-3}\pm5\times10^{-4}$ V^2/Hz , $7.6\times10^{-4}\pm2\times10^{-4}$ V^2/Hz at 30 min, 3d after blast ($P>0.05$), respectively. The Beta band power and theta band power, Delta band power, and Alpha-Delta power ratio (ADR) have no statistic significant before and after blast at all recording sites

Conclusions: The EEG activity lost fast frequency, and increased slower frequency after the blast. The EEG power significantly decreased in fast frequency band, and increased in slower frequency band. QEEG is sensitive for cerebral injury and can predict outcome in a swine model of brain injury. This study demonstrated the changes of QEEG after blast indicative of the potential of utilization of multiple parameters of QEEG for diagnosis of blast-induced brain injury. Further studies are necessary to investigate the effectiveness of QEEG in chronic brain injury and recovery.

AUTOBIOGRAPHICAL STATEMENT

Chengpeng Zhou

Department of Biomedical engineering

Wayne State University, College of Engineering,

Detroit, MI 48201

TEL: 313‐265‐8516

E‐mail: fl6928@wayne.edu

EDUCATION

Master Candidate of Biomedical Engineering, August 2015 (expected)

● **Wayne State University**, Department of Biomedical engineering, Detroit, MI 48201

Master of Orthopedics, July 2013-

● **Chongqing Medical University**, College of Clinical Medicine, Chongqing, P.R.China.

Bachelor of Clinical Medicine, July 2010-

● **North Sichuan Medical University,** College of Clinical Medicine, Nanchong, P.R.China.